



**SYSTEMS CONTROL TECHNOLOGY, INC.**

1801 PAGE MILL RD. □ PO. BOX 10180 □ PALO ALTO, CALIFORNIA 94303 □ (415) 494-2233

September 1982

EVALUATION OF TDOP TEST DATA  
Draft Final Report

Project No. 5381  
Task 9

Prepared for:  
Federal Railroad Administration  
Analysis and Evaluation Division  
Office of Rail Safety Research  
Washington, DC 20590

## ABSTRACT

Samples from the test data collected in Phase II of the railroad freight car Truck Design Optimization Project (TDOP) are reviewed to determine their suitability for use in assessing the safety performance of radial trucks. Omissions in the TDOP documentation are identified and corrected where possible to provide guidance for possible future users of the TDOP data tapes. The data reduction procedures which must be followed to extract information of engineering interest from the data tapes are described, and sample results from tests of one radial truck are shown. Analysis of these results identifies potential difficulties associated with the use of the TDOP data. On the basis of this analysis, recommendations are developed regarding future use of the TDOP data and the design of future rail vehicle test programs to build upon the experience gained from TDOP.

## ACKNOWLEDGMENTS

This work was conducted under the technical supervision of Dr. N. Thomas Tsai and Mr. Donald E. Gray of the Analysis and Evaluation Division, Office of Research and Development, Federal Railroad Administration. The guidance and assistance which they and Mr. Philip Olekszyk have offered are much appreciated.

Much of the information needed to conduct the work reported here was provided through the cooperation of people who were associated with the TDOP project. These include Robert L. Bullock of Standard Car Truck Co., Albert E. Martin of Dresser Industries, Gordon Bakken and Everett Bates of Wyle Laboratories and the following former employees of Wyle Laboratories: Robert Glaser, Arnold Gilchrist, Richard Peacock, Charles Bush and David Gibson. Special thanks are due to Mr. Glaser for his participation in several extensive telephone consultations about fine points of the TDOP data reduction procedures.

TABLE OF CONTENTS

	Page
1. INTRODUCTION .....	1
2. REVIEW OF TDOP PHASE II DATA AND DOCUMENTATION .....	3
3. DATA REDUCTION PROCEDURES .....	15
4. EXAMINATION OF TEST DATA .....	35
5. RECOMMENDATIONS FOR FURTHER WORK .....	91
APPENDIX .....	101

## 1. INTRODUCTION

The Truck Design Optimization Project (TDOP) was a multi-year, two-phase project which the FRA sponsored to develop an improved understanding of the dynamic performance, economics and safety of the diverse types of trucks which have been developed for use on North American railroad freight cars. The extensive test program incorporated in TDOP resulted in the production of a large library of test data for ~~seven~~ different trucks under a variety of operating conditions. Although considerable analysis of this data base was performed in the TDOP project, some aspects of truck performance could not be evaluated within the time and resource constraints of that project. The work reported here was performed in an attempt to use the TDOP test data to develop insights into the safety performance of radial trucks, in particular as affected by the forces imposed on the bearing adapters.

It was necessary to invest substantial effort in decoding the TDOP data tapes before attention could be directed to the safety assessment of radial trucks. Some of this effort was attributable to deficiencies in the TDOP documentation, some was a consequence of the great volume of the test data (up to 35 megabytes per tape), and some was associated with important shortcomings of the test results. The procedures which had to be followed are documented in this report so that any possible future users of the data will be able to avoid much of this effort. Once the sample tapes were decoded and the test results were examined carefully, some significant doubts about the accuracy and consistency of the results were raised. These doubts were judged to be serious enough that the contemplated assessment of bearing adapter forces could not be pursued with sufficient confidence in the validity of the results. The remainder of this report documents the basis for this conclusion, as part of a general evaluation of the applicability of the TDOP test data for evaluations of freight truck dynamic performance.

Chapter 2 contains a review of the test data and documentation available from the TDOP project, with general identification of problem areas and missing information. Chapter 3 explains the procedures which had to be followed to process the test data so that they could be studied in engineering units which have physical significance for truck dynamics (such as forces rather than strain gauge voltages). A detailed examination of some of the test data for one radial truck, with an extensive set of computer plots of results, is presented in Chapter 4. This is followed by the Chapter 5 recommendations regarding the applicability of the TDOP test data and the design of new test programs to supplement the data available from TDOP.

## 2. REVIEW OF TDOP PHASE II DATA AND DOCUMENTATION

This investigation is based on the use of the extensive truck test data collected by Wyle Laboratories as part of Phase II of the FRA-sponsored Truck Design Optimization Project (TDOP). TDOP Phase II included a series of sixteen separate test conditions for one standard (Type I) truck and six premium (Type II) trucks plus a subset of eight test conditions on an additional premium truck (the Alusuisse truck). These trucks were instrumented for recording 92 to 96 channels of response measurements at 200 samples per second. Some of the test runs lasted as long as 15 minutes, generating as much as 35 megabytes of data. This large volume of data must be processed selectively to obtain the results of interest in an efficient manner.

The TDOP Phase II test program is documented in an extensive set of Test Results Reports [1, 2] and Test Events Reports (such as [3, 4]). The Results Reports include lengthy appendices containing calibration data, data reduction equations and their derivations, diagrams of instrumentation locations and the test plans and procedures. The Test Events Reports reproduce the header files from the data tapes, including calibration information, and the handwritten daily Test Events Log maintained by the Test Director. This information is supplemented by the NTIS format information supplied with each of the test data tapes, describing the contents of each of the records on the tape.

SCT attempted to reduce the data on the tapes using only the information contained in these publicly-available sources, but found it necessary to request additional information from the FRA, Wyle Laboratories and several former Wyle employees who worked on specific parts of the TDOP project. For the benefit of possible future users of the TDOP data, the necessary information which was missing from the TDOP documentation is reviewed here.

## 2.1 Definition of Tape Records

Although the NTIS tape documentation was generally complete and correct, there was no indication in it or in the reports about how to use the calibration records. The maximum and minimum values for each channel in the calibration record are equivalent to the maximum and minimum values listed for those channels in the channel description record. These are not the maximum or minimum allowable values, but simply the ranges selected to use for the calibration. Some additional programming effort was required because of the incompatibility between the binary format of the calibration record and the ASCII of the channel descriptions. Also, word 8 of each data record is the accumulated distance divided by 10 feet, not multiplied by 10 feet (as indicated by the documentation).

## 2.2 Engineering Units

The engineering units described in the channel description record do not invariably correspond to the relevant physical units. The torque measurements T1 and T3 are described as kips, which is a force rather than a torque measurement. This may have corresponded to kips force applied in the calibration procedure. The data reduction equations summarized in Appendix D of the Type II Truck Test Results Report have no units associated with them, although pounds and inches appear to be the standard units for force and distance. The angle of attack equations produce results in terms of arc minutes (hardly an obvious choice!), and moments are all in terms of inch-pounds.

## 2.3 Biases (DC offsets)

The accelerometer and axle strain gauge channels (A and G prefixes in labels) have biases which in some cases are larger



than the variations in the measurements, even though these should be zero mean in most cases. The axle strain gauges must have the biases removed before they can be used to estimate wheel/rail forces. This requires an extra pre-processing step to calculate the mean value for each of these channels for a homogeneous segment of the test (such as negotiation of an individual curve) and to then subtract the mean from each sample value. A similar process must be followed for accelerometer channels, to remove biases which on the data tape would imply that bearing adapters are accelerating both vertically and laterally at several g's. The bias removal will also be needed for suspension deflections, especially the longitudinal axle deflections of the radial trucks.

The presence of substantial biases on the data tapes makes it impossible to use the TDOP data to derive confident estimates of some important steady state values, such as accelerations and suspension deflections during steady curving. The differences in these values for different curve negotiations in the same test run can be estimated roughly from the differences in the computed mean values for the different segments of the same tape. However, differences from one test run to another (different instrumentation calibrations, temperature effects, etc.) cannot be accounted for in this way. The bias problem also makes it impossible to use the wheel/rail force calibration data to estimate the real bias components on all the lateral forces which are attributable to wheel/rail contact geometry even when no external lateral forces are present (F1 in the derivation of Appendix C of the Type I Test Results Report). Biases on the axle longitudinal displacement measurements make it impossible to use these to calculate the extent to which the wheelsets of the radial trucks align themselves with curved track, although it may still be possible to make comparisons among curves on a single test run.

## 2.4 Bearing Adapter Strain Gauges

The procedures to be used for converting the bearing adapter strain gauge voltage outputs into estimates of the vertical forces and their lines of action at the bearing adapters were not documented as part of the TDOP project. Discussions with the Wyle Laboratories staff members who worked on that part of the project revealed that a combination of linearized equations and table look-up procedures was used to interpret the bearing adapter data. Neither the derivations nor the software associated with this could be located for re-use in the current work. Consequently, it was necessary to go back to the raw bearing adapter calibration data presented in the Appendices B of both the TDOP Type I and Type II Test Results Reports and use that to develop a new data reduction procedure.

The bearing adapter calibration data are presented as a series of curves of strain gauge voltage plotted as a function of the load applied to the adapter, for five different points of load application (centered above the adapter and at locations 1 and 2 inches to the left and right of center). The DR-1 adapters were also calibrated separately for three different levels of lateral force, but since the results did not appear to be very sensitive to the changes in lateral force, this effect was not considered further in developing the data reduction procedure. The instrumented adapters each produce three channels of strain data, two of which are used to identify the line of action of the vertical force (referred to as the inner and outer gauges) and the third of which is used to determine the magnitude of the force. The line of action must be defined properly for two reasons:

- (a) to determine the moment arm at which the force acts, as part of the calculation of the lateral wheel/rail forces
- (b) to select the right calibration curve to use with the third strain gauge channel.

The second of these is in practice the more important, because the calibration curves for vertical force on the third channel are highly sensitive to the line of action. Incorrect determination of the line of action could produce estimates of the vertical force which are wrong by factors as large as five or ten.

Because of the limited resources available for recreating the bearing adapter analysis procedure, the simplest feasible approach was adopted, recognizing that it will limit the accuracy of the results which can be obtained. The calibration curves were linearized about two different operating points, one corresponding to the nominal weight of the empty test car (8500 lb per adapter) and the other to the nominal weight of the fully loaded test car (30,000 lb per adapter). Separate sets of data reduction logic were developed for the loaded and empty cars and for the two different sets of adapters (Type I or DR-1). The TDOP documentation was confusing and ambiguous about the choice of adapters on each truck, making it appear that the Barber-Scheffel was tested using the DR-1 adapters, although this was denied by the Wyle Laboratories personnel most directly involved in the testing.

The relationship between the readings on the inner and outer strain gauges must be used to distinguish the line of action of the vertical force. Unfortunately, the calibration data do not permit this to be determined unambiguously for all of the adapters and loading conditions. Figure 1 is an example of a well-behaved bearing adapter calibration relationship, in which the line of action of the load can be readily determined (by interpolation) for any combination of measurements on the channels F21 and F22. The numbers assigned to the five radial lines on this figure correspond to lines of action at the center and 1 and 2 inches from the center of the adapter. By contrast, Figure 2 is a typical example of an ambiguous calibration result. If measurements of F11 and F12 corresponding to the

*this is just shows that there are other parameters involved*

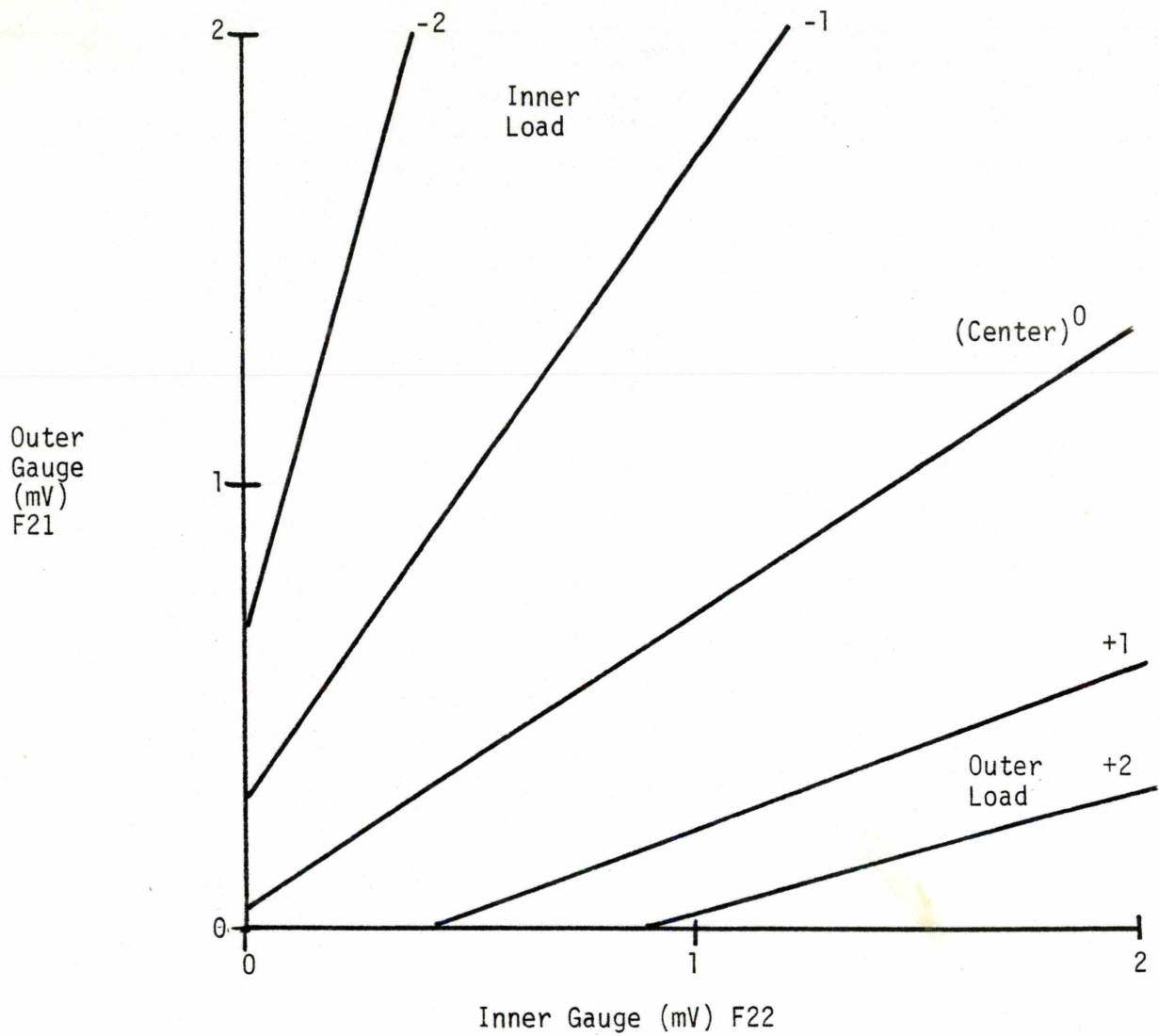


Figure 2.1 Calibration of Inner and Outer Strain Gauges for DR-1 Adapter BR-1 Under Fully Loaded Car

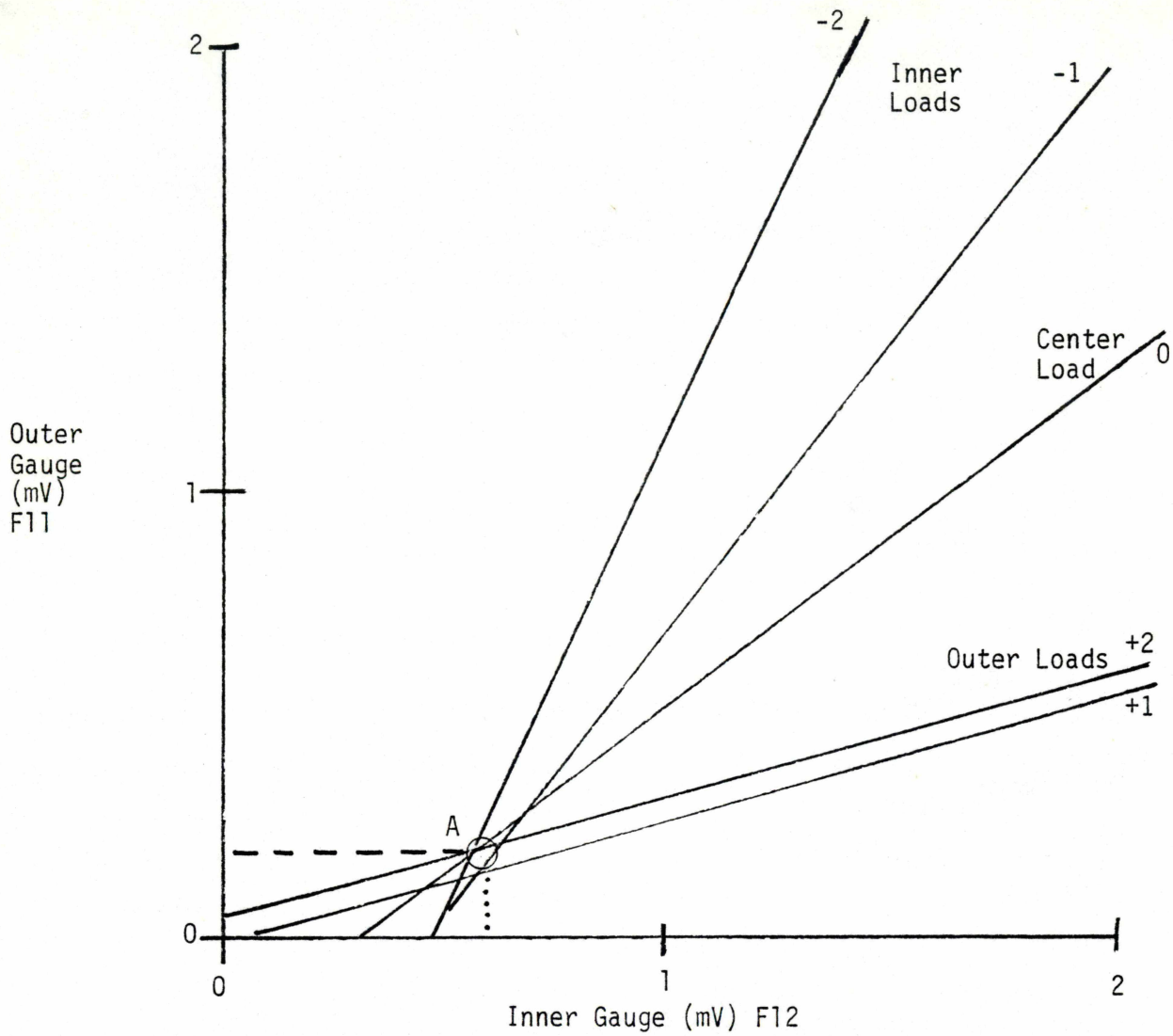


Figure 2.2 Calibration of Inner and Outer Strain Gauges for DR-1 Adapter BL-1 Under Fully Loaded Car

*for 2.1 / 2.2  
of same test run?*

*head  
of  
refraction  
analysis*

point labeled "A" are obtained, it is impossible to tell what the line of action was. Furthermore, the calibration curve for loads at the +2 location is between the curves for the 0 and +1 locations, making it impossible to do meaningful interpolations.

Results such as the example shown in Figure 2 sometimes make it impossible to identify the actual line of action from the TDOP test data. This in turn makes it impossible to choose the correct calibration curve to use to determine the magnitude of the vertical force on the bearing adapter, leading to potentially very large errors in the determination of this force. This problem is a direct outgrowth of the bearing adapter strain gauge force measurement system as implemented in the TDOP project.

## 2.5 Steering Arm Strain Gauges

The forces in the steering arms of the DR-1 truck and the cross arms and cross-struts of the Barber-Scheffel truck were measured using strain gauges. However, these measurements were not very clearly documented and indeed the Barber-Scheffel gauges were not calibrated. As a result, strain gauge voltages can be observed for one Barber-Scheffel arm and one strut, but these cannot be translated into estimates of forces.

The DR-1 steering arms were calibrated, although the procedure is not clearly described in the TDOP reports. The location of the strain gauges was not reported, although discussions with some of the people involved in the testing have revealed that they were mounted near the center of the steering arm assembly, on the piece which connects the two C-shaped arms inside the truck bolster. These gauges can measure the bending of that piece as a way of estimating the forces transmitted from the one arm to the other. The calibration was apparently conducted using lateral forces applied to one bearing adapter, with the opposite wheelset rigidly restrained. However, this is not documented. There is also a question about the excitation

voltage level used during the TDOP tests, which may not have been the same as the 10 volts used for the calibrations. If it was different, as one of the former Wyle employees suspected, the gain factors would need to be adjusted further.

## 2.6 Angle of Attack Measurements

The angle of attack and lateral displacements between wheels and rails were measured using a set of four eddy current transducers per wheelset. These detect the distances between a special test fixture mounted on the truck sideframe and the wheel and rail. The measurements relative to the rail were found to have sharp spikes at intervals corresponding to rail joints, which were phase shifted for the transducers mounted fore and aft of the axle. In order to use these measurements to indicate the actual wheel-rail angles of attack, it is necessary to shift one of the channels by the amount of time it takes for the train to travel the distance by which the two transducers are separated. This requires an additional step in the data reduction process. With only this phase shift, it will still not be possible to obtain an accurate and unbiased measurement of the lateral wheel-rail displacement. An inherent bias is built into the measurement system because the transducers are not mounted at the same distances from the wheel and rail. Furthermore, deviations in the upper or outer rail surface observed by the transducer may not be good representations of the deviations in the gauge (inner) surface, which are of greater importance to vehicle dynamic response.

The measurements relative to the wheel are dominated by a sinusoidal component at the wheel rotation frequency, representing a slight wheel wobble (about 5 arc minutes on Barber-Scheffel test BS-002A). This wheel wobble component, which appears to be so repeatable from cycle to cycle that it must be measuring wheel face irregularities, has to be filtered

out in order to observe the true angle of the wheel relative to the test fixture, which is needed for the angle of attack calculation.

## 2.7 TDOP Data Reduction Procedures

The axle-bending force measurement technique involves use of some complicated data analysis and reduction procedures which are not easy to derive. The derivation of these procedures in Appendix C of the TDOP Type I Test Results Report has a variety of problems which make it very difficult to follow. It is plagued with numerous typographical errors, illegible labels on the figure which defines the variables, at least one missing page (after page 8) and the reversal of two pages (11 and 12). The sources of the numerical values which need to be inserted in the equations were not apparent, and some were not defined in any of the TDOP documentation. The most important of these omissions was the failure to define the spacing between the left and right sets of axle-mounted strain gauges, which was found to be 30 inches.

The equations which were reported in Appendix D of the Type II Test Results Report were not consistent with the derivation in the earlier report. One important simplification was the assumption that lateral forces acting at the bearing adapter would be applied to the wheelset along its centerline rather than at the upper axle surface. Furthermore, the lateral force equations in the two different reports disagree in the choice of left or right axle bending moment terms and in the polarities of these terms.

The data reduction equations for the axle bending measurements in Appendix D of the Type II Results Report contain RMS terms used for normalization, but these were not documented at all.



The rationale for this choice of equations was not made clear, and indeed these equations would not appear to be suitable for producing the desired estimates of axle bending moments. For use in the present work, the mean value for each axle bending channel was calculated using the largest possible sequence of data gathered under uniform operating conditions, to try to ensure that the mean value estimates are not unduly degraded by including a non-integral number of cycles. These mean values were then subtracted from the instantaneous measurements in the quadrature equations in order to remove biases in the raw data.

Most of the TDOP documentation refers to filtering of the axle bending strain gauge channels at 500 Hz, except for the Type I Truck Test Plan, which referred to a frequency response of 50 Hz. This was apparently superseded at a later stage by the 500 Hz filtering, with the resulting problem of aliasing of signals above 100 Hz (to be discussed more thoroughly later).

## 2.8 Custom Software Development

Substantial software development efforts are needed before one can make use of the data for any analysis, as one would expect for any work involving data tapes containing many records. The NTIS tape documentation provides most of the information needed to decode the information on the tapes, but the exact procedures which a programmer must implement will be highly machine dependent. For example, on the SCT VAX 11/780 computer it was necessary to swap the bytes of the two-byte integer words containing the data because of the differences between this computer and the computer which was originally used to write the tapes.

In order for an analyst to be able to efficiently study the data, data management and plotting interface software must be developed. A properly designed interactive data handling software system enables the analyst to select the subset of

channels he needs for the time interval or track segment (by milepost) of interest. He should be able to filter or resample the data as desired and plot any channels or combination of channels he needs, as well as computing basic statistics on these channels. The data handling software development requires a substantial front-end effort, but it remains the only practical way of extracting information from data tapes as extensive as the TDOP tapes.

### 3. DATA REDUCTION PROCEDURES

The 96 channels of data recorded in the TDOP Phase II test program do not all correspond directly to the quantities of engineering interest. It is necessary to use combinations of multiple channels to develop estimates of many of the important quantities, especially the wheel-rail forces. Wherever possible, the equations and definitions presented in the TDOP reports (Figure 3.1) were used, but in some cases these had to be modified and supplemented with additional equations.

#### 3.1 Axle Bending

The axle bending moment calculations shown under the heading "Wheel/Rail Forces" were modified substantially for the current work. The axle bending strain gauge channels, the 24 channels with the prefix G, were generally found to have substantial biases (DC offsets), which would seriously distort any results derived from the equations of Figure 3.1. Therefore, those equations were modified by the removal of the RMS terms and the insertion of a bias removal term on each channel (subtraction of the mean value calculated over an extended steady-state period). This change leads to equations of the form:

$$(A-V) = [(G116-M116)^2 + (G112-M112)^2]^{1/2},$$

where the M terms are the mean values. The three separate equations for (A-V), (B-V) and (C-V) represent the calculations of axle bending from three different quadrature pairs of strain gauges, which are then averaged together in the equation for (R1-V). The quadrature pairs are strain gauges located 90° apart on the axle, and can be identified by numbers which are separated from each other by 4.

## APPENDIX D - DATA REDUCTION EQUATIONS

### WHEEL/RAIL FORCES

Typical Vertical Axle Bending Moment Calculations:

$$(A-V) = \left\{ \left[ \left( \frac{\text{RMS}_{R1}}{\text{RMS}_{G116}} \right) G116 \right]^2 + \left[ \left( \frac{\text{RMS}_{R1}}{\text{RMS}_{G112}} \right) G112 \right]^2 \right\}^{\frac{1}{2}}$$

$$(B-V) = \left\{ \left[ \left( \frac{\text{RMS}_{R1}}{\text{RMS}_{G115}} \right) G115 \right]^2 + \left[ \left( \frac{\text{RMS}_{R1}}{\text{RMS}_{G111}} \right) G111 \right]^2 \right\}^{\frac{1}{2}}$$

$$(C-V) = \left\{ \left[ \left( \frac{\text{RMS}_{R1}}{\text{RMS}_{G113}} \right) G113 \right]^2 + \left[ \left( \frac{\text{RMS}_{R1}}{\text{RMS}_{G109}} \right) G109 \right]^2 \right\}^{\frac{1}{2}}$$

$$(R1-V) = [(A-V) + (B-V) + (C-V)] / 3$$

Similar calculations were made for (L1-V), (R2-V), and (L2-V).

### PRIMARY SPRING VERTICAL DISPLACEMENTS (MAXIRIDE)

$$X_{R1} = 0.8333 D15 + .0834 (D15 + D17)$$

$$X_{L1} = 0.8333 D17 + .0834 (D15 + D17)$$

$$X_{R2} = 0.8333 D16 + .0834 (D16 + D18)$$

$$X_{L2} = 0.8333 D18 + .0834 (D16 + D18)$$

Using these displacements vertical forces and moments were calculated using nonlinear spring constants provided by the manufacturer.

### LATERAL AND VERTICAL FORCE CALCULATIONS

$$FVR1 = 1500. + .03333 [(R1 - V) - (L1 - V)] + VLA1$$

$$FVL1 = 1500. - .03333 [(R1 - V) - (L1 - V)] + VLA2$$

$$FLR1 = 156.45 - .05556 \times BMA1 + .05556 \times (L1 - V) + 0.081944 [(R1 - V) - (L1 - V)]$$

$$FLL1 = 156.45 - .05556 \times BMA2 + .05556 \times (R1 - V) - 0.081944 [(R1 - V) - (L1 - V)]$$

$$QUR1 = FLR1/FVR1$$

Figure 3.1 - Data Reduction Equations from TDOP Phase II, Type II Truck Test Results Report

$$QUL1 = FLL1/FVL1$$

$$AXL1 = FLR1 - FLL1$$

$$AXV1 = FVR1 + FVL1$$

Same calculations are repeated for axle 2.

#### WHEEL UNLOADING INDEX

$$FVT = FVR1 + FVL1 + FVR2 + FVL2$$

$$MINV = \text{Minimum of } (FVR1, FVL1, FVR2, FVL2)$$

$$WUI = 1 - 3 \times [MINV / (FVT - MINV)]$$

#### ANGLE OF ATTACK

$$LRS1 = .5 (P2 + P4)$$

$$LWS1 = .5 (P1 + P3)$$

$$LWR1 = LWS1 - LRS1$$

$$LRS2 = .5 (P6 + P8)$$

$$LWS2 = .5 (P5 + P7)$$

$$LWR2 = LWS2 - LRS2$$

$$ARS1 = C1 \times (P2 - P4)$$

$$AWS1 = C2 \times (P1 - P3)$$

$$AWR1 = AWS1 - ARS1$$

$$ARS2 = C1 \times (P6 - P8)$$

$$AWS2 = C2 \times (P5 - P7)$$

$$AWR2 = AWS2 - ARS2$$

See Table E-1 for values for C1 & C2.

Figure 3.1 (Cont'd)

### TRUCK AND TRUCK/CARBODY MOTIONS

SWIV	=	C3 (D13 - D14)
TRAM	=	C4 (D6 - D5)
SGVD	=	(D1 + D2 + D3 + D4)/4.
SGRL	=	C5 (D1 + D2 - D3 - D4) or C5 (D15 + D16 - D17 - D18)
CBBL	=	C6 (D11 - D12)
CBSF	=	SGRL + CBBL

### CARBODY MOTIONS

Prior to using accelerometer data to calculate carbody motions, it was necessary to adjust the scale factors and polarities of some channels. These adjustments were made in the ADARS data base to data base parameters GAIN and C1. The data are divided by GAIN. C1 is the conversion factor from volts to engineering units. Table E-2 shows the changes made to GAIN and C1. Polarities of some accelerometers were found to be in error and were corrected in the ADARS data bases. Two techniques were used to determine accelerometer polarities. First, the polarity of the lateral accelerometers was determined by examining the lateral accelerometers during curve negotiation at off-balance speed. Second, the polarity of some of the vertical accelerometers was determined from roll motions of the vehicle at relatively low speed for the Blue Diamond test runs. Table E-3 shows the polarities that were determined using the above techniques.

PTCH	=	C7 (A1 - A2)
VERT	=	0.5 (A1 + A2)
AROL	=	C8 (A2 - A4)
BROL	=	C9 (A7 - A3)
ROLL	=	0.5 (AROL + BROL)
TWST	=	BROL - AROL
ARLL	=	C10 x (A16 - A6) + C11 x YAW

Figure 3.1 (Cont'd)

$$\begin{aligned}
\text{BRL} &= \text{C12} \times (\text{A5} - \text{A6}) - \text{C13} \times \text{YAW} \\
\text{RLL} &= 0.5 (\text{ARLL} + \text{BRL}) \\
\text{LAT (EMPTY)} &= \text{C14} \times (\text{A5} + \text{A6}) + \text{C15} \times (\text{A15} + \text{A16}) \\
\text{LAT (LOADED)} &= \text{C16} \times (\text{A5} + \text{A6}) + \text{C17} \times (\text{A15} + \text{A16}) \\
\text{YAWB} &= \text{C18} \times (\text{A5} - \text{A6}) \\
\text{YAWT} &= \text{C19} \times (\text{A15} - \text{A16}) \\
\text{YAW} &= 0.5 (\text{YAWB} + \text{YAWT})
\end{aligned}$$

Table E-4 gives the coefficients for carbody motions.

**NOMENCLATURE**

- SWIV - Truck swivel rotation (carbody to bolster)
- TRAM - Truck tram rotation (bolster to side frame)
- SGVD - Spring group vertical displacement
- SGRL - Spring group roll angle
- CBBL - Carbody - bolster roll angle
- CBSF - Carbody - side frame roll angle
- A-V - Vertical axle bending moment from the first pair of quadrature gages
- B-V - Vertical axle bending moment from the second pair of quadrature gages.
- C-V - Same as A-V except third pair of gages
- R1-V - Vertical axle bending moment for the gages near the right wheel of axle 1
- L1-V - Same as R1-V except left wheel
- R2-V - Same as R1-V except axle 2
- L2-V - Same as L1-V except axle 2

Figure 3.1 (Cont'd)

VLA1	-	Vertical load on bearing adapter #1 (R1)
VLA2	-	Vertical load on bearing adapter #2 (L1)
VLA3	-	Vertical load on bearing adapter #3 (R2)
VLA4	-	Vertical load on bearing adapter #4 (L2)
BMA1	-	Bending moment due to VLA1
BMA2	-	Bending moment due to VLA2
BMA3	-	Bending moment due to VLA3
BMA4	-	Bending moment due to VLA4
FVR1	-	Vertical wheel/rail force - R1
FVL1	-	Vertical wheel/rail force - L1
FVR2	-	Vertical wheel/rail force - R2
FVL2	-	Vertical wheel/rail force - L2
FLR1	-	Lateral wheel/rail force - R1
FLL1	-	Lateral wheel/rail force - L1
FLR2	-	Lateral wheel/rail force - R2
FLL2	-	Lateral wheel/rail force - L2
QUR1	-	L/V ratio - R1
QUL1	-	L/V ratio - L1
QUR2	-	L/V ratio - R2
QUR2	-	L/V ratio - L2
AXL1	-	Total lateral wheel/rail force on axle 1
AXL2	-	Total lateral wheel/rail force on axle 2
AXV1	-	Total vertical wheel/rail force on axle 1
AXV2	-	Total vertical wheel/rail force on axle 2
X <sub>R1</sub>	-	Primary spring displacement, R1 spring group

Figure 3.1 (Cont'd)



$X_{L1}$	-	Primary spring displacement, L1 spring group
$X_{R2}$	-	Primary spring displacement, R2 spring group
$X_{L2}$	-	Primary spring displacement, L2 spring group
FTV	-	Total vertical wheel/rail force for B-end truck
MINV	-	Minimum vertical wheel/rail force for four wheels of B-end truck
WUI	-	Wheel unloading index, equal to zero implies all four wheels have equal load, equal to one implies one wheel has no load
LRSi	-	Lateral displacement of rail relative to side frame for axle i, i = 1,2
LWSi	-	Lateral displacement of wheel relative to side frame for axle i, i = 1,2
LWRi	-	Lateral displacement of wheel relative to rail for axle i, i = 1,2
ARSi	-	Angular displacement of rail relative to side frame for axle i, i = 1,2
AWSi	-	Angular displacement of wheel relative to side frame for axle i, i = 1,2
AWRi	-	Angular displacement of wheel relative to rail for axle i, i = 1,2
PTCH	-	Carbody pitch acceleration
VERT	-	Carbody vertical acceleration
AROL	-	Carbody A-end roll acceleration (from vertical accelerometers)
BROL	-	Carbody B-end roll acceleration (from vertical accelerometers)
ROLL	-	Carbody roll acceleration (from vertical accelerometers)
TWST	-	Carbody twist acceleration (from vertical accelerometers)
ARLL	-	Carbody A-end roll acceleration (from lateral accelerometers)
BRLL	-	Carbody B-end roll acceleration (from lateral accelerometers)
RLLL	-	Carbody roll acceleration (from lateral accelerometers)
LAT	-	Carbody lateral acceleration at CG
YAWB	-	Carbody yaw acceleration near bottom of carbody
YAWT	-	Carbody yaw acceleration near top of carbody
YAW -	-	Carbody yaw acceleration near center of carbody

Figure 3.1 (Cont'd)

The quadrature pairs which were used to calculate the four axle bending moment estimates were:

	<u>Left Side</u>	<u>Right Side</u>
<u>Axle 1</u>	G101 and G105	G112 and G116
	G102 and G106	G111 and G115
	G103 and G107	G109 and G113
<u>Axle 2</u>	G209 and G213	G201 and G205
	G212 and G216	G204 and G208
	(G210 and G214)	

There were only two quadrature pairs available on the right side of axle 2, and the third pair for the left side of that axle is in parentheses because channel G214 was giving extremely low readings on the sample Barber-Scheffel test runs. For further data analysis work, its quadrature equation should be removed to avoid distorting the results.

### 3.2 Bearing Adapter Vertical Forces and Moments

The lateral and vertical force calculations at the bottom of the first page of Figure 3.1 rely on the use of measurements of four vertical bearing adapter forces,  $VLA_i$  and the bending moments produced by these forces,  $BMA_i$ . Those quantities must be extracted from the twelve bearing adapter strain gauge channels,  $F_i$ ,  $F_{i1}$  and  $F_{i2}$ , for  $i=1,2,3$  and 4. The specific definitions of these channels are found in the channel description files, such as Figure 3.2. Two different sets of instrumented bearing adapters were used in TDOP Phase II, one for the Dresser DR-1 truck and the other for the remaining trucks. The adapters were calibrated in static tests at TTC, and the complete sets of calibration curves are reproduced in Appendices B of the TDOP Type I (109 plots) and Type II (220 plots for DR-1) Test Results Reports.

TABLE 3-4. CHANNEL DESCRIPTION FILE FOR BARBER-SCHEFFEL TRUCK

PHIIBLU  
 TYPE= 30 RATE= 200 NCHN= 96 DATE= 7/13/80  
 START MP= 314,979

1	S1	SPEED	MPH	0.0	50.0
2	S2	AUTOMATIC LOCATION DETECTOR	DETECTION	0.0	5.0
3	S3	BRAKE CYLINDER PRESSURE	PSID	0.0	90.0
4	S4	THROTTLE SETTING	POSITION	0.0	5.0
5	A1	B END CNTR CARBODY VERT ACCEL	G'S	0.0	0.937
6	A2	A END CNTR CARBODY VERT ACCEL	G'S	0.0	1.316
7	A3	B END RT(BL) CARBODY VERT ACCEL	G'S	0.0	1.566
8	A4	A END RT(AL) CARBODY VERT ACCEL	G'S	0.0	1.548
9	A5	B END RT(BL) CARBODY LAT ACCEL	G'S	0.0	0.984
10	A6	A END RT(AL) CARBODY LAT ACCEL	G'S	0.0	0.966
11	A7	B END LF(BR) CARBODY VERT ACCEL	G'S	0.0	1.573
12	A8	B END CNTR CARBODY LONG ACCEL	G'S	0.0	1.000
13	A9	BL-1 (RT FT) BRG ADPT VERT ACCEL	G'S	0.0	5.874
14	A10	BL-1 (RT FT) BRG ADPT LAT ACCEL	G'S	0.0	5.977
15	A11	BL-2 (RT RR) BRG ADPT LAT ACCEL	G'S	0.0	5.531
16	A12	BR-1 (LF FT) BRG ADPT VERT ACCEL	G'S	0.0	6.424
17	A13	AL-3 (RT FT) BRG ADPT LAT ACCEL	G'S	0.0	5.599
18	A14	AL-4 (RT RR) BRG ADPT LAT ACCEL	G'S	0.0	3.779
19	A15	B-END CNTR CARBODY TOP LAT ACCEL	G'S	0.0	1.538
20	A16	A-END CNTR CARBODY TOP LAT ACCEL	G'S	0.0	1.587
21	A17	CARBODY BOTTOM CNTR LAT ACCEL	G'S	0.0	1.570
22	F1	BL-1 BEAR ADPT VERT STRAIN	MILLIVOLTS	0.0	1.0
23	F11	BL-1 REAR ADPT OUT VERT STRAIN	MILLIVOLTS	0.0	-1.0
24	F12	BL-1 BEAR ADPT IN VERT STRAIN	MILLIVOLTS	0.0	-1.0
25	F2	BR-1 BEAR ADPT VERT STRAIN	MILLIVOLTS	0.0	1.0
26	F21	BR-1 BEAR ADPT OUT VERT STRAIN	MILLIVOLTS	0.0	-1.0
27	F22	BR-1 BEAR ADPT IN VERT STRAIN	MILLIVOLTS	0.0	-1.0
28	F3	BL-2 BEAR ADPT VERT STRAIN	MILLIVOLTS	0.0	1.0
29	F31	BL-2 BEAR ADPT OUT VERT STRAIN	MILLIVOLTS	0.0	-1.0
30	F32	BL-2 BEAR ADPT IN VERT STRAIN	MILLIVOLTS	0.0	-1.0
31	F4	BR-2 BEAR ADPT VERT STRAIN	MILLIVOLTS	0.0	1.0
32	F42	BR-2 BEAR ADPT OUT VERT STRAIN	MILLIVOLTS	0.0	-1.0
33	F41	BR-2 BEAR ADPT IN VERT STRAIN	MILLIVOLTS	0.0	-1.0
34	P1	BL-1 WHEEL/SIDEFAME POS "A"	INCHES	0.0	1.0
35	P2	BL-1 RAIL/SIDEFAME POS "B"	INCHES	0.0	1.0
36	P3	BL-1 WHEEL/SIDEFAME POS "C"	INCHES	0.0	1.0
37	P4	BL-1 RAIL/SIDEFAME POS "D"	INCHES	0.0	1.0
38	P5	BL-2 WHEEL/SIDEFAME POS "A"	INCHES	0.0	1.0
39	P6	BL-2 RAIL/SIDEFAME POS "B"	INCHES	0.0	1.0
40	P7	BL-2 WHEEL/SIDEFAME POS "C"	INCHES	0.0	1.0
41	P8	BL-2 RAIL/SIDEFAME POS "D"	INCHES	0.0	1.0
42	G1	B-1 AXLE ROTARY PULSE GEN	POSITION	0.0	6.263
43	G2	B-2 AXLE ROTARY PULSE GEN	POSITION	0.0	6.263
44	H1	CROSS ARM STRAIN	MILLIVOLTS	0.0	1.0
45	H2	CROSS STRUT STRAIN	MILLIVOLTS	0.0	1.0
46	T1	B-1 AXLE TORQUE (GAGE 1A)	KIPS	0.0	1010.2
47	T3	B-2 AXLE TORQUE (GAGE 1A)	KIPS	0.0	968.7
48	G201	AXLE #2 STRAIN GAUGE 1	IN-LBS	0.0	1117000.
49	G202	AXLE #2 STRAIN GAUGE 2	IN-LBS	0.0	1149000.
50	G203	AXLE #2 STRAIN GAUGE 3	IN-LBS	0.0	1157000.

Size	Code Ident No.	C-901-0012-A
A	2B360	
Scale	Rev	Sheet 44

Figure 3.2 - Sample Channel Description File from TDOP Phase II, Type II Truck Test Results Report (Typical of file included on each data tape)

TABLE 3-4 (CONT'D). CHANNEL DESCRIPTION FILE FOR BARBER-SCHEFFEL TRUCK

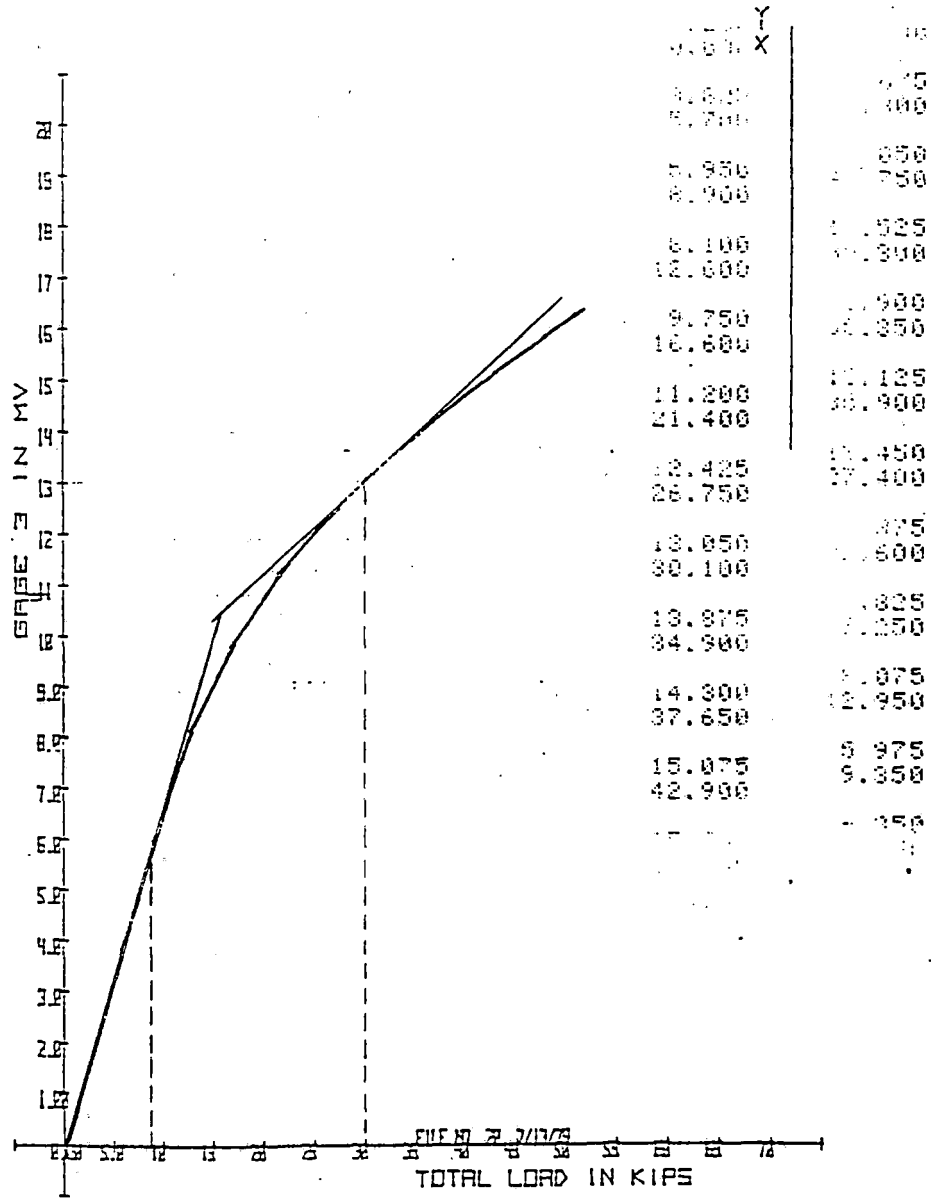
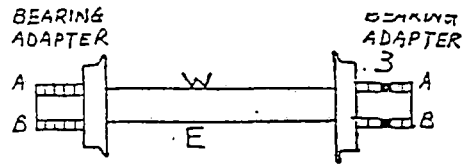
PHIBLU						
TYPE= 31		RATE= 200	NCHN= 96	DATE= 7/13/80		
START MP= 314.979						
51	G204	AXLE #2 STRAIN GAUGE 4	IN-LBS	0.0	1157000.	
52	G205	AXLE #2 STRAIN GAUGE 5	IN-LBS	0.0	1152000.	
53	G208	AXLE #2 STRAIN GAUGE 8	IN-LBS	0.0	1119000.	
54	G209	AXLE #2 STRAIN GAUGE 9	IN-LBS	0.0	1174000.	
55	G210	AXLE #2 STRAIN GAUGE 10	IN-LBS	0.0	1174000.	
56	G212	AXLE #2 STRAIN GAUGE 12	IN-LBS	0.0	1157000.	
57	G213	AXLE #2 STRAIN GAUGE 13	IN-LBS	0.0	1174000.	
58	G214	AXLE #2 STRAIN GAUGE 14	IN-LBS	0.0	1175000.	
59	G216	AXLE #2 STRAIN GAUGE 16	IN-LBS	0.0	1157000.	
60	D5	BL-1(RT FT) BOLST/SIDE FR LAT DISP	INCHES	0.0	1.000	
61	D6	BL-2(RT RR) BOLST/SIDE FR LAT DISP	INCHES	0.0	1.000	
62	D7	BL-2(RT) BOLST/SIDE FR ROTATION	INCHES	0.0	1.000	
63	D8	BR-1(LF FT) BOLST/SIDE FR LAT DISP	INCHES	0.0	1.000	
64	D9	BR-2(RT RR) BOLST/SIDE FR LAT DISP	INCHES	0.0	1.000	
65	D10	BR-2(RT) BOLST/SIDE FR ROTATION	INCHES	0.0	1.000	
66	D1	BL-1(RT FT) SPG GP VERT DISP	INCHES	0.0	1.000	
67	D2	BL-2(RT RR) SPG GP VERT DISP	INCHES	0.0	1.000	
68	D3	BR-1(LF FT) SPG GP VERT DISP	INCHES	0.0	1.000	
69	D4	BR-2(LF RR) SPG GP VERT DISP	INCHES	0.0	1.000	
70	D11	BL(RT) CARBODY/BOLST REL VERT DISP	INCHES	0.0	1.000	
71	D12	BR(LF) CARBODY/BOLST REL VERT DISP	INCHES	0.0	1.000	
72	D13	B END FWD CARBODY/TRUCK LAT DISP	INCHES	0.0	1.000	
73	D14	B END REAR CARBODY/TRUCK LAT DISP	INCHES	0.0	1.000	
74	D19	BL-1(RT FR) SIDE FR/AXLE LONG DISP	INCHES	0.0	-1.0	
75	D20	BL-2(RT RR) SIDE FR/AXLE LONG DISP	INCHES	0.0	1.0	
76	D21	BR-1(LF FR) SIDE FR/AXLE LONG DISP	INCHES	0.0	1.0	
77	D22	BR-2(LF RR) SIDE FR/AXLE LONG DISP	INCHES	0.0	1.0	
78	C1	B END COUPLER FORCE	POUNDS	0.0	3000.0	
79	C2	B END COUPLER ANGLE	DEGREES	0.0	5.0	
80	C3	A END COUPLER FORCE	POUNDS	0.0	3000.0	
81	C4	A END COUPLER ANGLE	DEGREES	0.0	5.0	
82	GR	FILTERED LONGITUDINAL ACCEL	% GRADE	0.0	6.73	
83	G116	AXLE #1 STRAIN GAUGE 16	IN-LBS	0.0	1183000.	
84	G115	AXLE #1 STRAIN GAUGE 15	IN-LBS	0.0	1180000.	
85	G113	AXLE #1 STRAIN GAUGE 13	IN-LBS	0.0	1183000.	
86	G112	AXLE #1 STRAIN GAUGE 12	IN-LBS	0.0	1186000.	
87	G111	AXLE #1 STRAIN GAUGE 11	IN-LBS	0.0	1189000.	
88	G109	AXLE #1 STRAIN GAUGE 9	IN-LBS	0.0	1184000.	
89	G107	AXLE #1 STRAIN GAUGE 7	IN-LBS	0.0	1171000.	
90	G106	AXLE #1 STRAIN GAUGE 6	IN-LBS	0.0	1175000.	
91	G105	AXLE #1 STRAIN GAUGE 5	IN-LBS	0.0	1164000.	
92	G103	AXLE #1 STRAIN GAUGE 3	IN-LBS	0.0	1174000.	
93	G102	AXLE #1 STRAIN GAUGE 2	IN-LBS	0.0	1171000.	
94	G101	AXLE #1 STRAIN GAUGE 1	IN-LBS	0.0	1172000.	
95	G3	RESET PULSE B-1 RPG	VOLTS	0.0	5.0	
96	G4	RESET PULSE B-2 RPG	VOLTS	0.0	5.0	

Size	Code Ident No.	C-901-0012-A
A	2B360	
Scale	Rev	Sheet 45

Figure 3.2 (Cont'd)

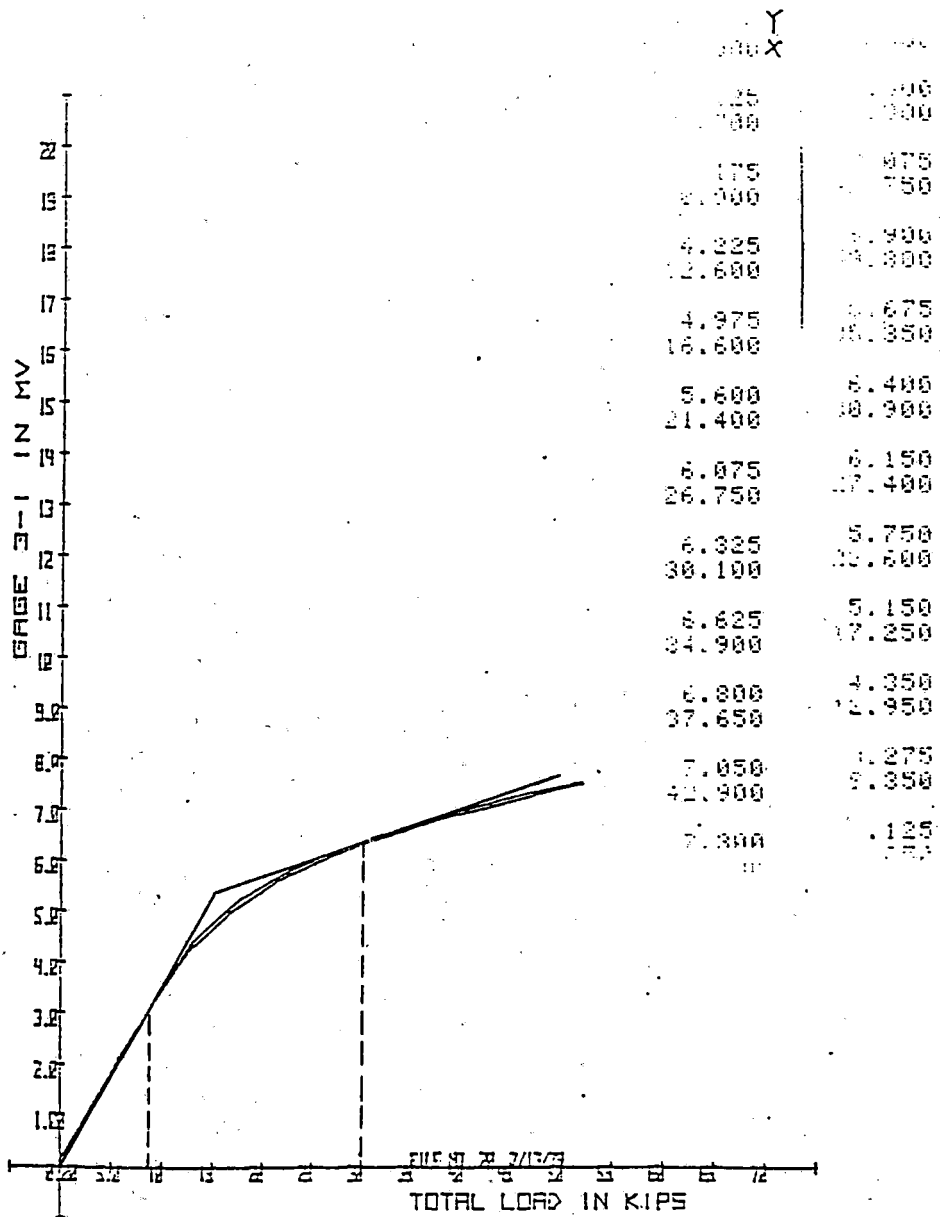
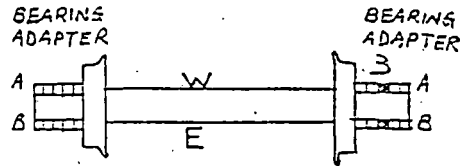
A typical set of calibration curves for a Type I bearing adapter loaded at its center line is reproduced in Figures 3.3-3.5. The darkening in the middle square on the right side of the wheelset schematic (upper right corner of each figure) indicates that the vertical load was centered above adapter 3. Figure 3.3 is the calibration for the center strain gauge (identification of total load) while Figures 3.4 and 3.5 are the calibrations for the inner and outer strain gauges, which are used to identify the line of action of the load. For use in the current work, these calibration curves were linearized about two nominal load levels, 8500 lb for the empty car and 30,000 lb for the loaded car. The linear approximations, shown on the figures, are quite close to the nonlinear calibrations over a substantial range of values. The one situation in which these would produce serious errors is the unloading of an adapter on a fully loaded car (such as a near wheel-lift), for which the linear approximation would estimate a substantial negative vertical force. That caution should be borne in mind when the linearization is used, and the data reduction program should switch to the separate linearization for the empty car when the signal level drops into its range.

Linear equations of the form  $y = ax + b$  were developed to describe each of the approximations, where  $y$  represents the measured voltage and  $x$  represents the vertical load on the bearing adapter. Five sets of data comparable to Figures 3.3-3.5 were used to characterize each adapter. The DR-1 adapter had separate calibrations for three different levels of lateral force, but because these did not differ much only the set for no lateral force was used. When analyzing the test data, there is no way to tell a priori what the line of action of the bearing adapter force was. The relationship between the readings on the inner and outer strain gauges must be used to identify the line of action. For the empty car linearizations, which all pass through the origin, this can be described simply as the ratio



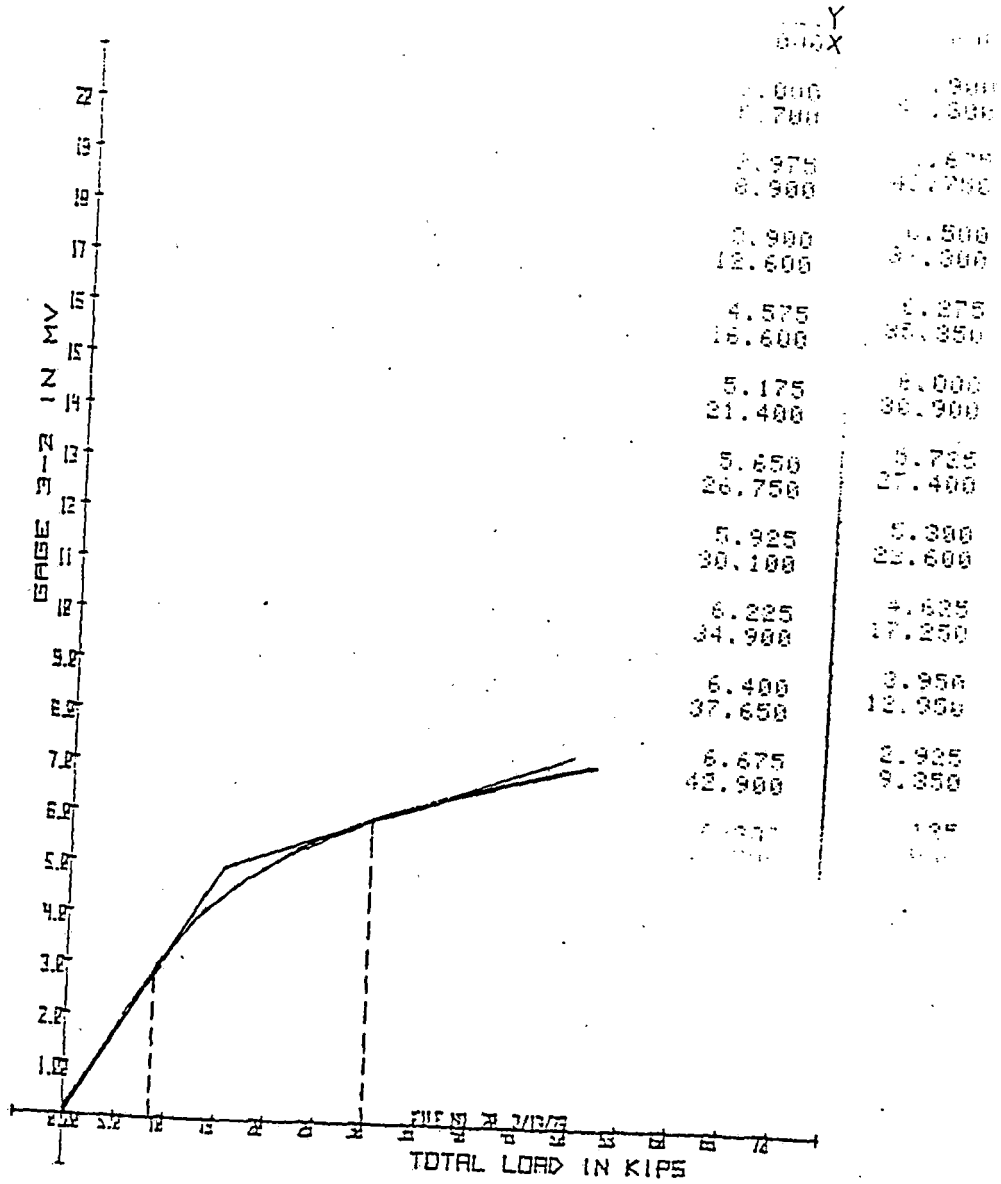
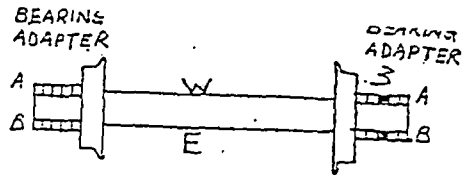
BEARING ADAPTER RE-CALIBRATION  
FIGURE 68

Figure 3.3 - Calibration Curve for Bearing Adapter Strain Gauge (Center Gauge) from TDOP Phase II, Type II Truck Test Results Report, Appendix B



BEARING ADAPTER RE-CALIBRATION  
FIGURE 69

Figure 3.4 - Calibration Curve for Bearing Adapter Strain Gauge (Outer Gauge) from TDOP Phase II, Type II Truck Test Results Report, Appendix B



BEARING ADAPTER RE-CALIBRATION  
FIGURE 70

Figure 3.5 - Calibration Curve for Bearing Adapter Strain Gauge (Inner Gauge) from TDOP Phase II, Type II Truck Test Results Report, Appendix B



between the two gauge readings. For the loaded car linearizations, this requires plotting the relationship between the two calibration curves in a form like that of Figs. 2.1 and 2.2. Each line in each of those figures describes a pair of loaded-car linearizations similar to those shown in Figs. 3.4 and 3.5. The ambiguous cases, such as the example of Figure 2.2, must be treated with great care to retain as much information as possible and eliminate that which seems most physically unreasonable. In some cases the calibrations were so ambiguous (scattered results, with no clear trends with line of action) that the line of action could not be distinguished. For these cases, the line of action was assumed to be at the adapter centerline and an average gain was chosen for the vertical force estimate. The quality of the calibration data for each adapter under each of the two loading conditions is described in Table 3.1. The important aspects of the calibrations are the certainty with which they can be used to identify the line of action of the vertical force and the sensitivity of the estimated vertical force level to possible errors in the identification of that line of action.

The calibration data were used to derive a set of equations and associated logic to convert the strain gauge voltages on the data tapes into estimates of vertical force and line of action. The computer code which implements this procedure is shown in the Appendix. A two-dimensional interpolation procedure (subroutine TWODIM) is used to blend the answers produced by the calibration curves for different lines of action when the actual line of action falls between two of the calibration cases. The data reduction program calculates the forces  $VLA_i$  and moments  $BMA_i$  at each time interval by:

- 1) Using the inner and outer strain gauge measurements  $F_{i1}$  and  $F_{i2}$  to identify the line of action of the vertical force (if possible).

Table 3.1 - Summary of Bearing Adapter Calibration Quality

TYPE I ADAPTER

Adapter Number	Empty	Loaded
1 (BL-1) Front, Right	Consistent calibration, Insensitive to line of action	Small region of ambiguous calibration
2 (BR-1) Front, Left	Cannot resolve line of action, but results are relatively insensitive to that	Small region of ambiguous calibration
3 (BL-2) Rear, Right	Cannot resolve line of action, but results are not too sensitive to that	One anomalous calibration curve deleted
4 (BR-2) Rear, Left	Calibration ambiguous at very low force level, but results are not too sensitive to that	Many ambiguities in line of action, but force trend is consistent

DRESSER DR-1 ADAPTER

Adapter Number	Empty	Loaded
1 (BL-1) Front, Right	Impossible to resolve line of action, and results are extremely sensitive to that	Significant ambiguity in line of action, so one calibration was deleted. Results are sensitive to the ambiguity
2 (BR-1) Front, Left	Good resolution of line of action, with results somewhat sensitive to that	Good resolution of line of action
3 (BL-2) Rear, Right	Serious ambiguities in line of action, and results are extremely sensitive to that	Good resolution of line of action
4 (BR-2) Rear, Left	Fair resolution of line of action, and results are quite sensitive to that	Small region of ambiguous calibration, results quite sensitive to that

- 2) Using the identified line of action to select the appropriate vertical force calibration (or blending of calibrations) to apply to the center strain gauge measurement,  $F_i$ , to calculate the vertical force  $VLA_i$ .
- 3) Multiplying the force  $VLA_i$  by the moment arm of the identified line of action relative to the intersection of the axle centerline with the vertical plane of the wheel/rail contact to calculate the moment  $VMA_i$ . For a line of action centered on the adapter, this moment arm is ten inches.

### 3.3 Vertical and Lateral Wheel/Rail Forces

The axle bending and bearing adapter calculations described in Sections 3.1 and 3.2 are needed to estimate the wheel/rail contact forces from the TDOP data. The discrepancies between the wheel/rail force equations as derived in Appendix C of the TODP Type I Test Results Report and as reported in Appendix D of the Type II Test Results Report were already discussed in Section 2.7. The simplified form of the latter reference (Figure 3.1) was adopted for use here, with cross-checks to the derivation.

The source of the 1500 lb constant added in the two equations for vertical forces was not identified, although it probably corresponds to half of the weight of the wheelset. That weight would contribute to the vertical wheel/rail force, but not to the bearing adapter force. The second "=" sign in the equation for  $FVL1$  is a typographical error, and should actually be a negative sign ("-").

The source of the 156.45 lb constant added in the two lateral force equations was also undocumented, but it could correspond to the lateral force component imposed on each rail by the wheelset as a function of the wheel/rail contact angle. The remaining terms in the lateral force equations differ somewhat in

the two TDOP source documents. Proceeding from the derivation in the Type I documentation, it would appear that the lateral force equations in Figure 3.1 should be:

$$\begin{aligned} FLL1 = 156.45 - .05556 \cdot BMA2 - .05556(L1-V) \\ - .081944 [(R1-V) - (L1-V)] \end{aligned}$$

$$\begin{aligned} FLR1 = 156.45 - .05556 \cdot BMA1 - .05556(R1-V) \\ + .081944 [(R1-V) - (L1-V)] \end{aligned}$$

The third term in each equation differs from Figure 3.1 in sign and in the side of the axle used to obtain the bending moment estimate. This discrepancy remains unexplained.

#### 3.4 Additional Data Reduction Equations

The data reduction procedures specified in the TDOP project reports were supplemented with some additional procedures for cross-checking results and deriving additional measures of truck performance.

Two different methods of calculating the angle formed by the two axles on the instrumented truck were implemented. These are intended to show the extent to which the wheelsets of a radial truck align themselves in negotiating a curve. The first method simply uses the difference between the angles of attack of the two wheelsets relative to the rail:

$$XNG1 = AWR1 - AWR2$$

This relies on the assumption that the rail is essentially tangent for the length of the truck, which is obviously not true in a curve. However, if the local radius of curvature of the track is known, the angle subtended by a chord of the length of

the truck wheelbase can be subtracted from XNG1 to define the angle formed by the two axles. The second method, which is valid for the DR-1 truck but not for the Barber-Scheffel, uses the four measurements of axle longitudinal displacement relative to the truck side frame:

$$XNG2 = 43.52(D21+D22-D19-D20).$$

This method cannot be applied to the Barber Scheffel because the D19-D22 measurements are of displacement relative to the special shear pad housings, which can in turn align themselves relative to the side frames. Even for the DR-1 truck, XNG2 must be regarded as an approximation because the side frames and bolster are not rigidly connected, but are subject to a lozenging or parallelogramming type of distortion.

The wheel/rail force equations were supplemented with some new equations designed to provide additional physical insights and to serve as cross-checks on the lateral and vertical force estimates. These include the wheelset net lateral forces:

$$\begin{aligned} FL1 &= FLR1 - FLL1 \\ FL2 &= FLR2 - FLL2, \end{aligned}$$

the net vertical and lateral forces on the truck:

$$\begin{aligned} FVNT &= FVR1 + FVL1 + FVR2 + FVL2 \\ FLNT &= FLR1 + FLR2 - FLL1 - FLL2, \end{aligned}$$

and the truck side lateral/vertical force ratios:

$$\begin{aligned} QLFT &= (FLL1 + FLL2)/(FVL1 + FVL2) \\ QRG1 &= (FLR1 + FLR2)/(FVR1 + FVR2). \end{aligned}$$

The net vertical truck force should have a long-term mean value comparable to half the tare weight of the car (steady-state load on the truck). The truck side L/V force ratios can be used to evaluate the potential for rail-rollover derailments.

The cross-checks on the data reduction procedures were implemented using alternate derivations for one of the lateral wheel/rail forces and for the net lateral force on the bearing adapters. The calculations of the lateral forces on the bearing adapters (net per wheelset) were derived from corrected versions of the equations in Appendix C of the Type I Test Results Report, yielding

$$\begin{aligned} \text{FNL1} &= 0.0437 (-1.95 ((R1-V)-(L1-V))-BMA1+BMA2) \\ \text{FNL2} &= 0.0437 (-1.95 ((R2-V)-(L2-V))-BMA3+BMA4). \end{aligned}$$

The difference between the two lateral forces calculated using the equations in the Type II Results Report is:

$$\text{FLR1-FLL1} = 0.05556(1.95((R1-V)-(L1-V))-BMA1+BMA2).$$

The coefficient is different because this method assumed the lateral force at the bearing adapter to be acting along the axle centerline rather than at the axle radius. The different sign on the axle bending moment term appears to be a discrepancy between the two derivations, perhaps attributable to inconsistent sign conventions.

#### 4. EXAMINATION OF TEST DATA

The TDOP Phase II test data were reviewed carefully to establish their suitability for use in evaluating the force environment experienced by the bearing adapters. This involved examination of the truck instrumentation channels, but generally not of the carbody channels. It was necessary to go through this process to gain a complete understanding of the significance of each channel and to identify any problems with particular channels. It also helped in the evaluation of the confidence with which the measured data could be used to estimate the important measures of truck performance. In this chapter, the test data in several major categories are reviewed and assessed:

1. Wheel/rail displacement and angle of attack
2. Strains in radial truck cross arm and strut  
(Barber-Scheffel)
3. Dynamic forces in suspension springs
4. Axle longitudinal displacements
5. Axle bending moments
6. Bearing adapter forces
7. Net wheel/rail forces
8. L/V force ratios

Unless otherwise noted the test data to be illustrated were from the start of curve negotiation test case BS002A on the Barber-Scheffel truck. This was on tangent track (prior to the

*transient*

first curve) at a speed of 26 mph. The abscissas of the time-history plots are labelled by number of samples at 200 Hz. Therefore, a label of 200 corresponds to one second.

#### 4.1 Wheel/Rail Displacement and Angle of Attack

The lateral displacements and angles of attack of the two wheelsets relative to the rail are determined from eight eddy current transducers, on channels P1-P8. These measure the distances to the wheel rim and the outer rail face fore and aft of each axle centerline. The individual data channels are not very revealing by themselves, although they can be more interesting when plotted in combinations. An example of this is Figure 4.1, which shows the distances measured to the rail by the transducers fore and aft of axle 1.

Figure 4.1 provides a convincing illustration that the majority of the signal observed on these channels is produced by track geometry variations. The two curves are phase shifted by a time interval equivalent to the time it took for the test car to travel the distance separating transducers P2 and P4. The shapes of the curves are nearly identical, indicating that they are measuring the same thing at different times. Finally, the major dips in each curve are separated by one second, corresponding very closely to the 39-foot interval between rail joints. The phase shift apparent in Fig. 4.1 means that the data reduction equations which were listed in Fig. 3.1 for the wheel/rail displacement and angle of attack should not be used directly on the raw test data. Rather, the data channels for the transducers mounted ahead of the axles (P2 and P6) should be delayed by a time interval equal to the phase shift relative to the behind-axle channels (P4 and P8) before applying the data reduction equations.

The suggested shifting of the two channels will lead to improved estimates of angle of attack, but will still leave the



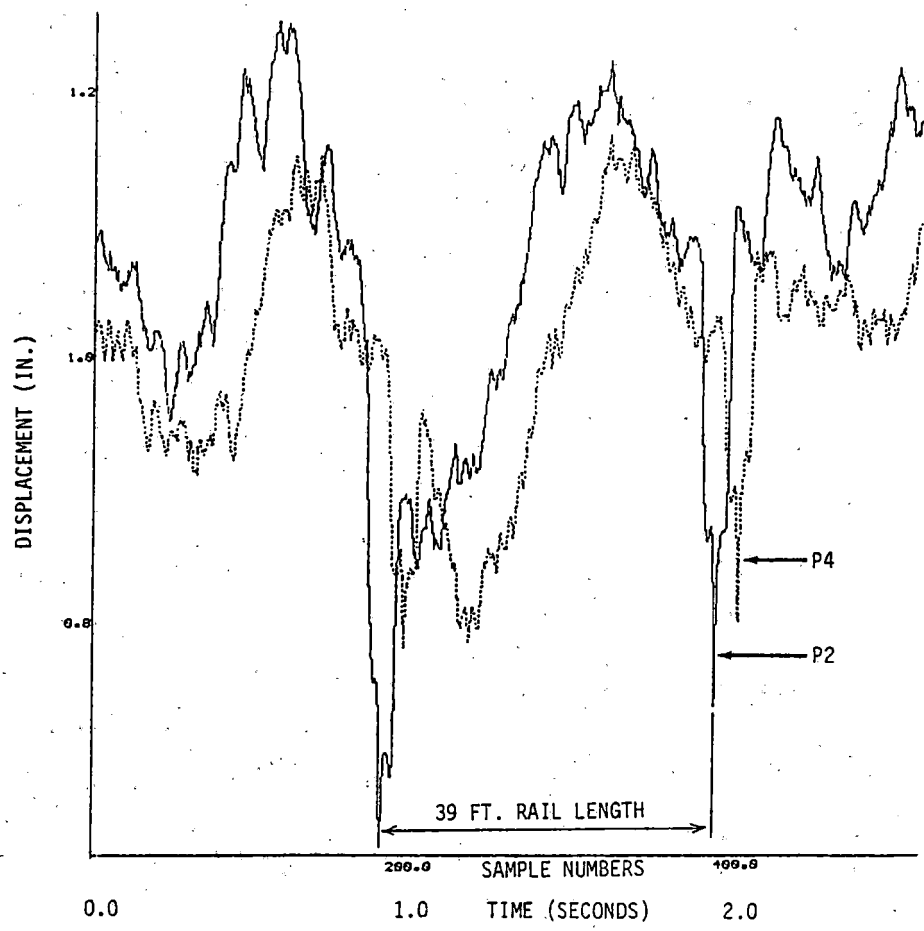


Figure 4.1 - Rail Displacement Fore and Aft of Lead Axle (P2 and P4)

lateral displacement estimates with two problems. The first is that the lateral displacement of the wheel relative to the rail will appear to change abruptly at each rail joint (or other track perturbation) regardless of whether or not it really changes. This can be avoided by low-pass filtering of the data to eliminate the fast transients and to restrict attention to the slow, quasi-steady changes in wheel/rail lateral displacement. The second problem with the lateral displacement estimates is the lack of suitable calibration data to tell what values of the differences between the measurements to the wheel rim and to the rail correspond to zero lateral displacement. Appendix E of the TDOP Type II Test Results Report contains one set of static test data for test run BS-012 on the Barber-Scheffel truck, showing the distance from each transducer to the wheel or rail. Unfortunately, all of these distances proved to be significantly larger than the mean values observed on the tape for test BS-002A at the start (tangent track) or in either curve #2 or #3 (respectively left-hand and right-hand curves of greater than  $6^\circ$ ). Indeed the static test distances exceeded the maxima observed in these two sharp curves in all but two cases (channels P6 and P8 in curve #2). The minimum values of displacement relative to the rail were negative for all transducers in curve #3, which would appear to be difficult to achieve physically and may imply the existence of a calibration problem. Based on these observations, it is doubtful that the true lateral displacement of the wheelsets can be identified from the test data, although the relative lateral displacements for different curves in the same test run should be identifiable.

Proceeding with this caution in mind, it is still interesting to observe the intermediate quantities which are calculated in order to estimate wheelset lateral displacements using the TDOP data reduction equations without the suggested corrections. Figures 4.2 and 4.3 show the distances to rail and wheel respectively at the lead axle for the first four seconds of

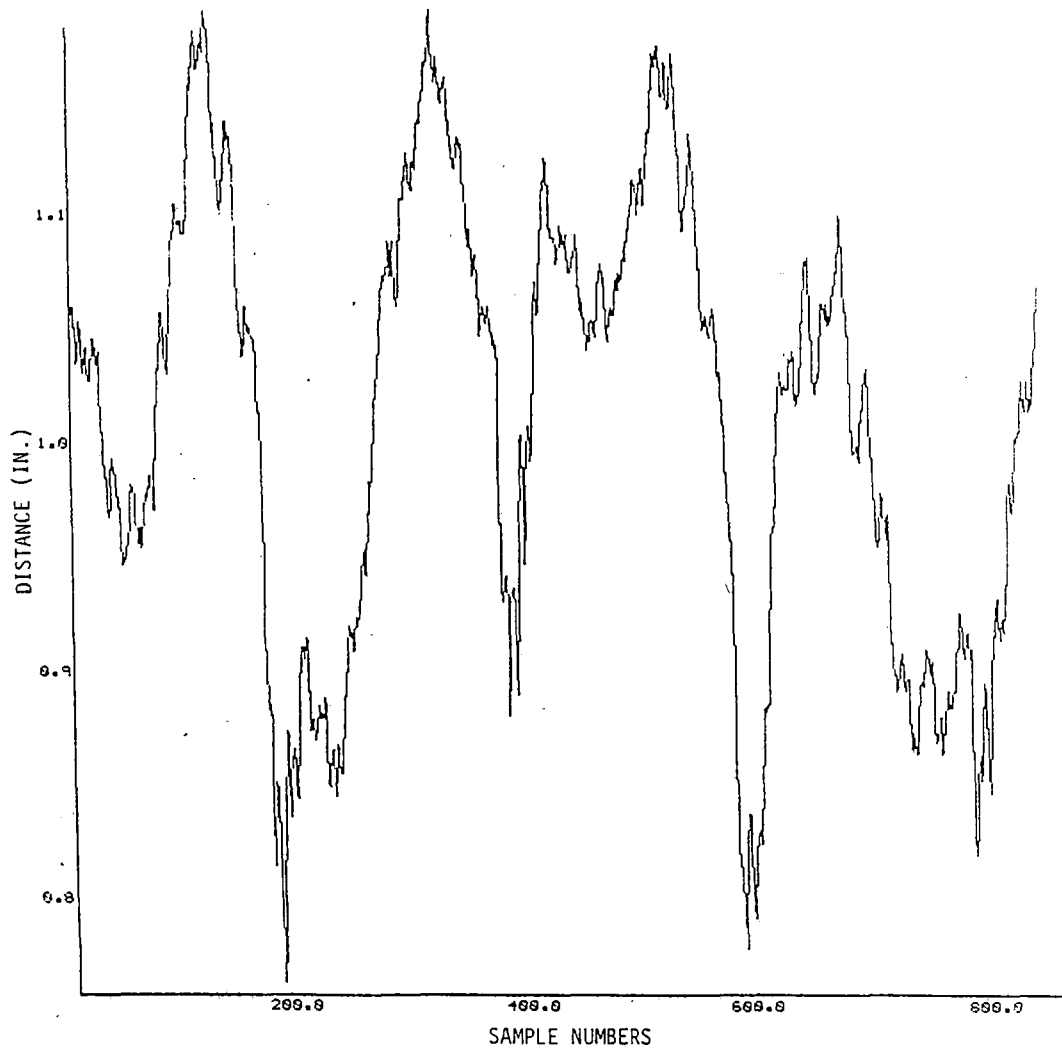


Figure 4.2 - Computed Distance to Rail at Lead Axle (LRS1)

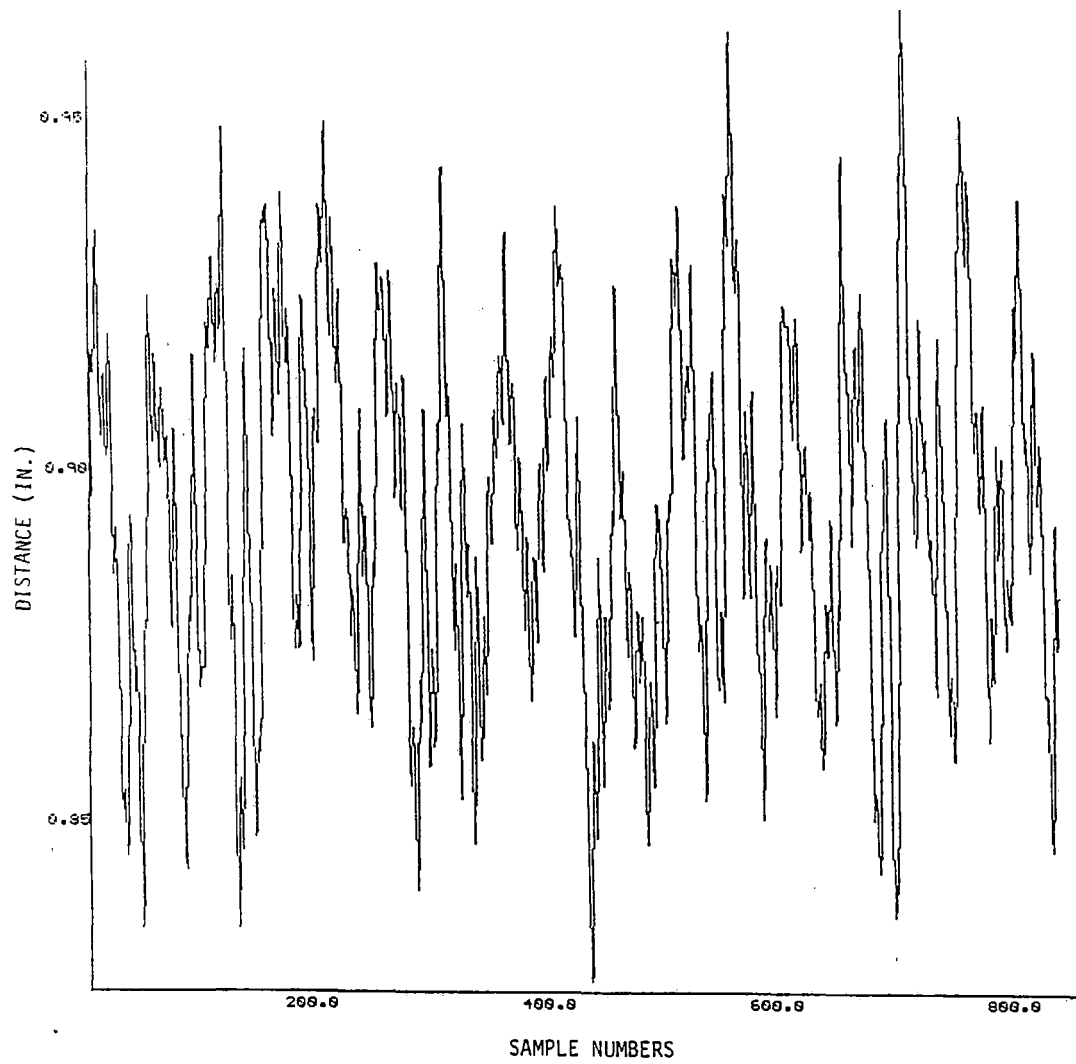


Figure 4.3 - Computed Distance to Wheel at Lead Axle (LWS1)

test BS-002A. While the rail measurement is dominated by the relatively low frequency associated with large track geometry variations, the wheel measurement is dominated by smaller amplitude variations at a higher frequency, associated with individual wheel rotations. This is illustrated very dramatically in Figure 4.4, which shows the angle between the wheel and the bracket holding the transducers at axle 1, derived from the difference between P1 and P3. The large, nearly sinusoidal, waveform corresponds to wheel rotations, and the very repeatable perturbations near the peaks probably represent surface irregularities on the wheel rim. Figure 4.4 shows how a wheel wobble produced by a wheel-to-axle misalignment of about 6 arc minutes can contribute significantly to the angle-of-attack calculations. This should be removed in future attempts to apply the TDOP angle-of-attack data by appropriate compensation (subtraction of the wheel-wobble component).

The calculated values of the angles between the transducer brackets and the rail are, as expected, dominated by the track geometry and particularly the rail joints. Figure 4.5 shows an example for about 6.3 seconds of test data, with the sharp peaks caused by the successive passage of transducers P2 and P4 over the rail joint.

The final products of the measurements which have been described here are the estimates of wheel-rail lateral displacement and angle of attack. The lateral displacement estimates for the two instrumented wheelsets are shown in Figure 4.6. The dominant influence of track geometry is apparent from the phase shift corresponding to the truck wheelbase. The bias separating the two curves could represent a real difference between the two wheelsets or could be the result of different transducer mounting geometries or calibration conditions. Unfortunately, it is not possible to tell which explanation applies. The computed angles of attack of the two wheelsets for one second of test time are shown in Figure 4.7, where the

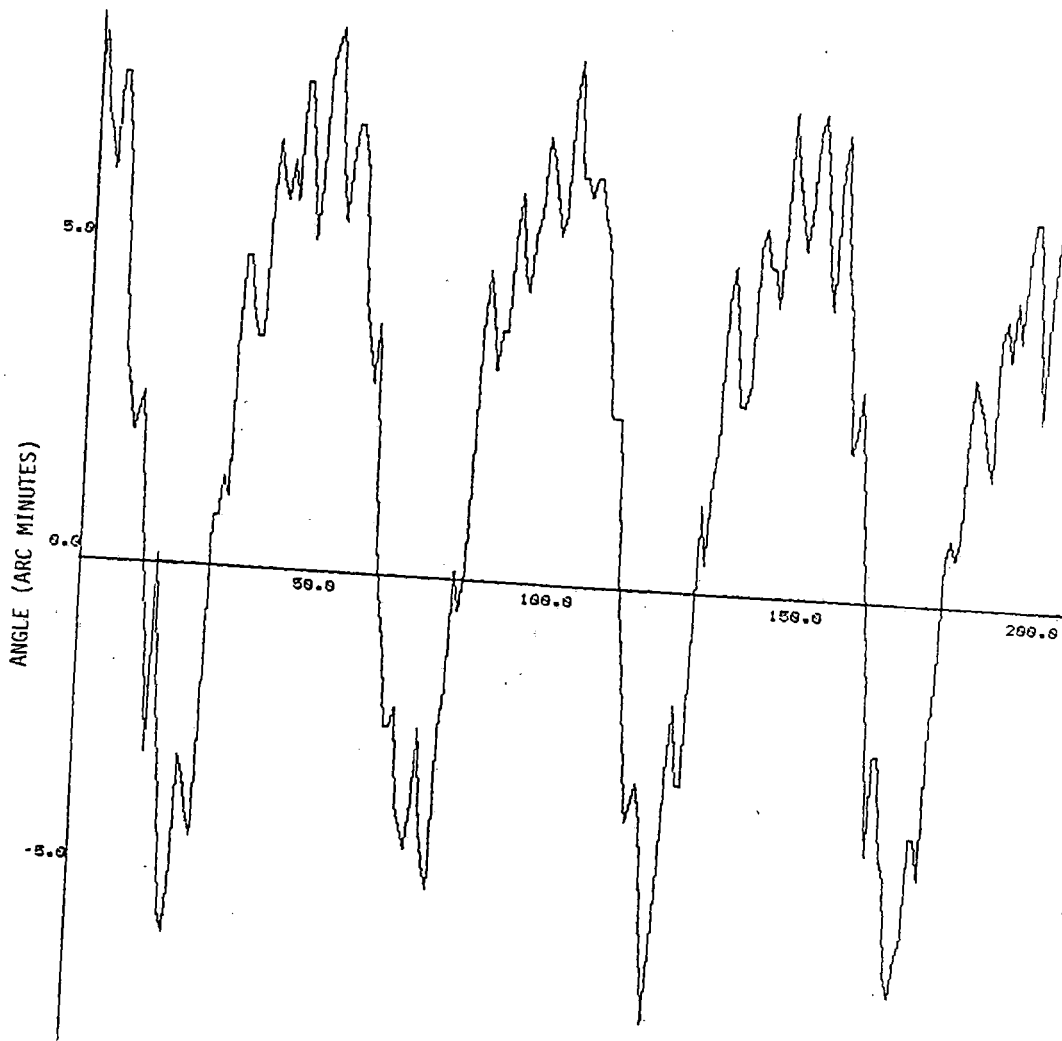


Figure 4.4 - Computed Angle to Wheel at Lead Axle (AWS1), Showing Wheel Wobble and Rim Surface Irregularities

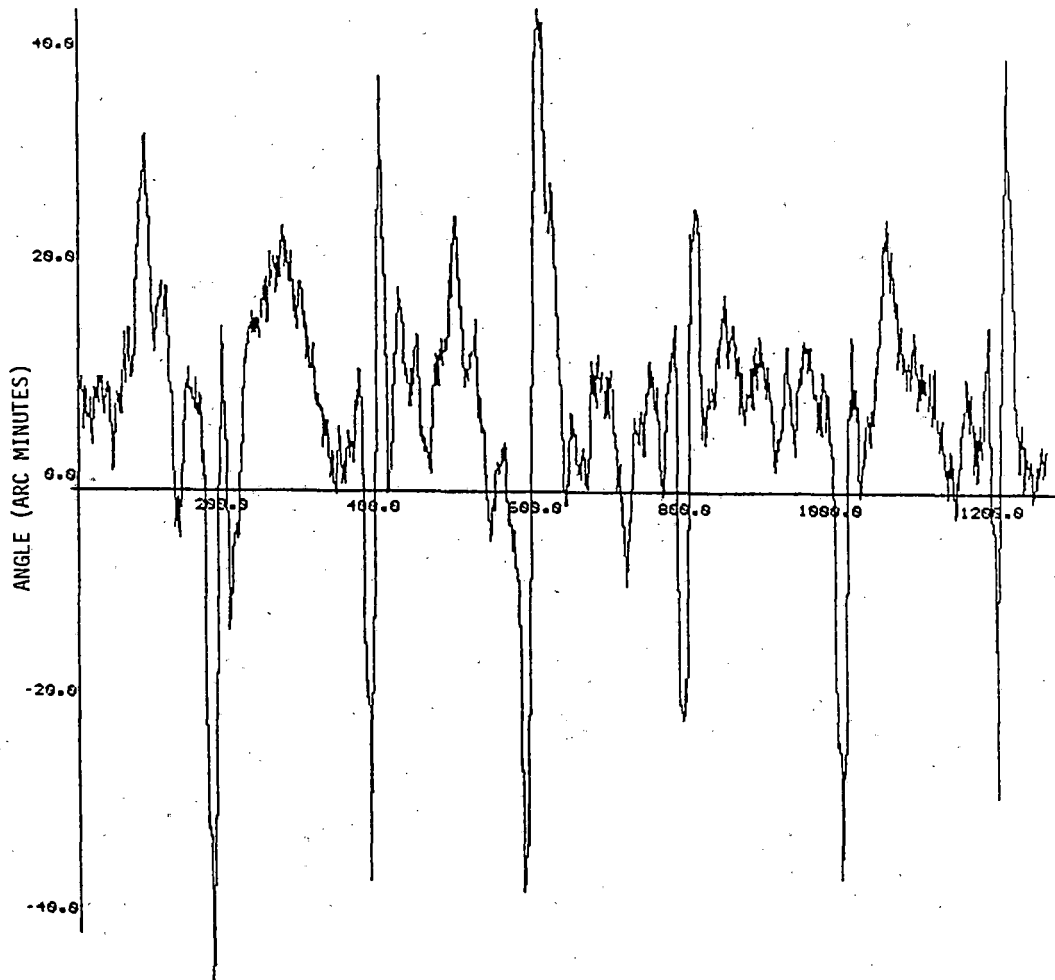


Figure 4.5 - Computed Angle to Rail at Lead Axle (ARS1), Showing Rail Joints

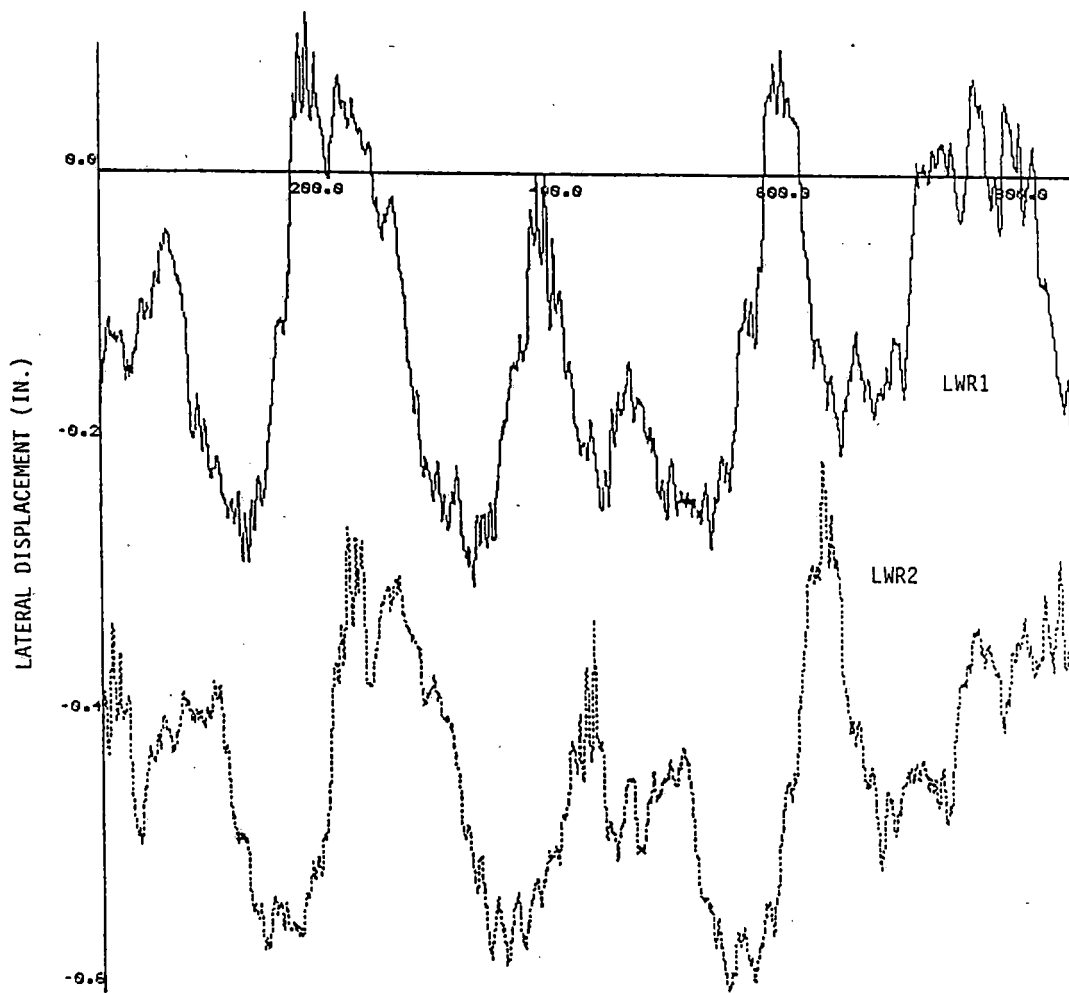


Figure 4.6 - Computed Mean Lateral Displacements of Wheelsets (LWR1 and LWR2), Showing Rail Joints



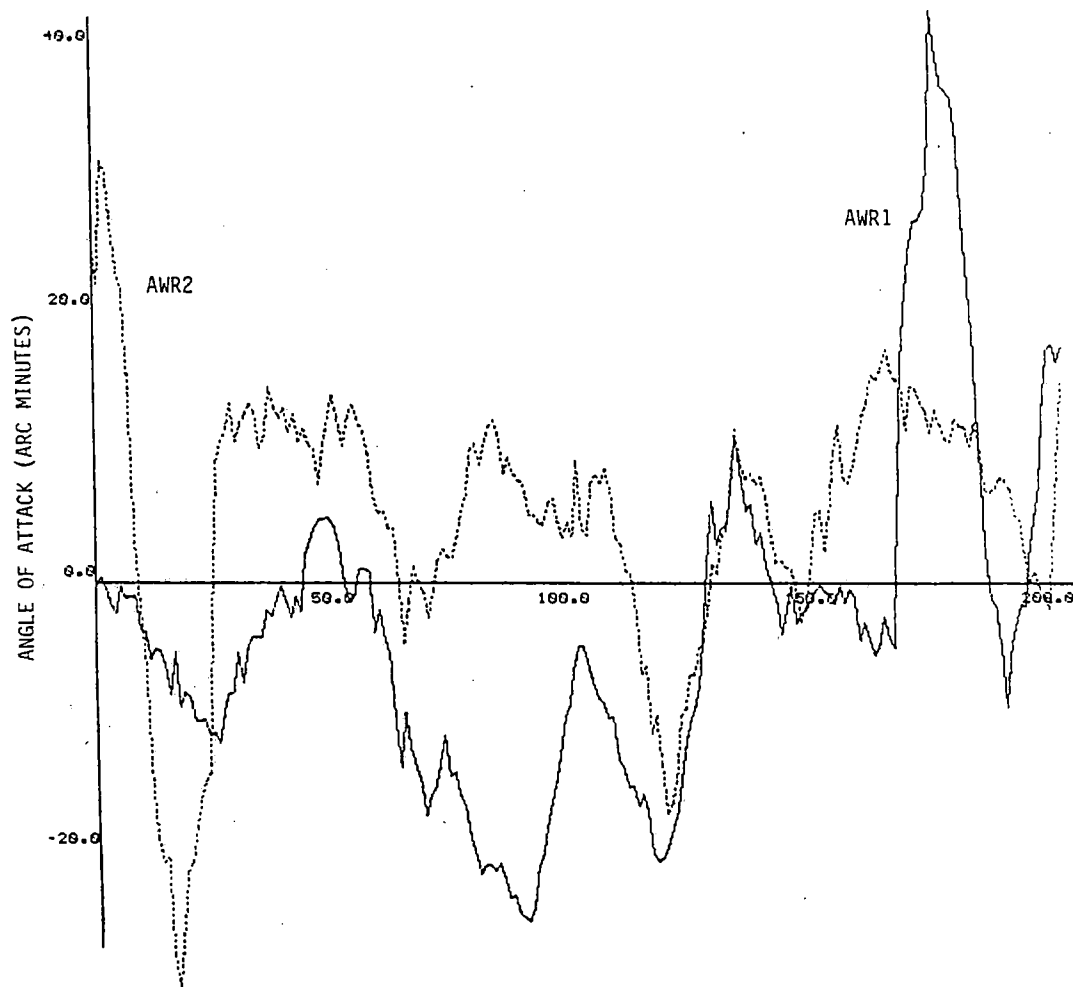


Figure 4.7 - Computed Wheel/Rail Angles of Attack, Leading and Trailing Axles (AWR1 and AWR2)

influence of track geometry is once again apparent. These results are virtually useless for evaluating vehicle dynamic response in their present condition because the true angle of attack is submerged below the much larger influence of track geometry variations. With appropriate phase shifting of channels and compensation for wheel wobble these measurements may be able to provide high-quality estimates of angle of attack.

The difference between the two angles of attack, XNG1, is plotted in Figure 4.8 as a crude estimate of the angle formed by the two wheelsets on tangent track. This estimate is of course corrupted by the same problems which plague the estimates of the individual angles of attack. An alternative calculation of the angle between the two wheelsets appropriate for a DR-1 truck is XNG2, shown in Figure 4.9. Because of the unusual construction of the Barber-Scheffel truck, this is not a valid representation of the aligning of its wheelsets. However, the XNG1 calculation can probably be of use after the angle of attack calculation procedures are refined in the suggested ways. Even using the procedures specified in the TDOP data reduction equations, the differences between negotiation of left and right hand curves can be distinguished. Figures 4.10 and 4.11 show XNG1 in "steady state" curving on two  $6^{\circ}$  curves, one left hand and the other right hand. The mean value of XNG1 was -28.01 arc minutes in the left hand curve and -8.61 arc minutes in the right hand curve.

#### 4.2 Strains in Radial Truck Cross Arm and Strut

Strain gauges were applied to one cross-arm and one cross-strut of the Barber-Scheffel truck, but they were not calibrated during the TDOP project. The results which are available are therefore in the form of voltages rather than forces, and can only be used to show relative trends rather than absolute magnitudes. As Figure 4.12 shows, the variations in strain for an empty car on tangent track were small enough that

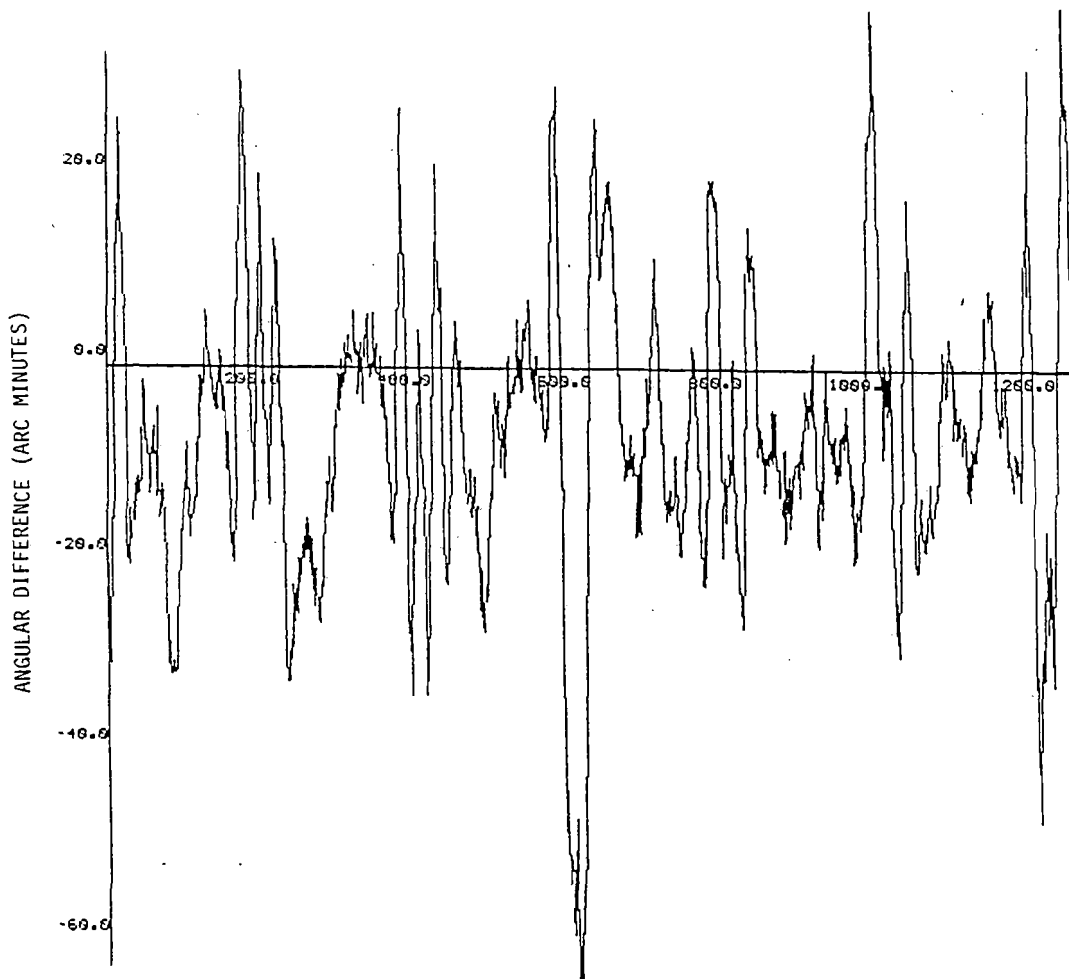


Figure 4.8 - Angular Difference Between Axles (XNGI), Calculated From Angles of Attack

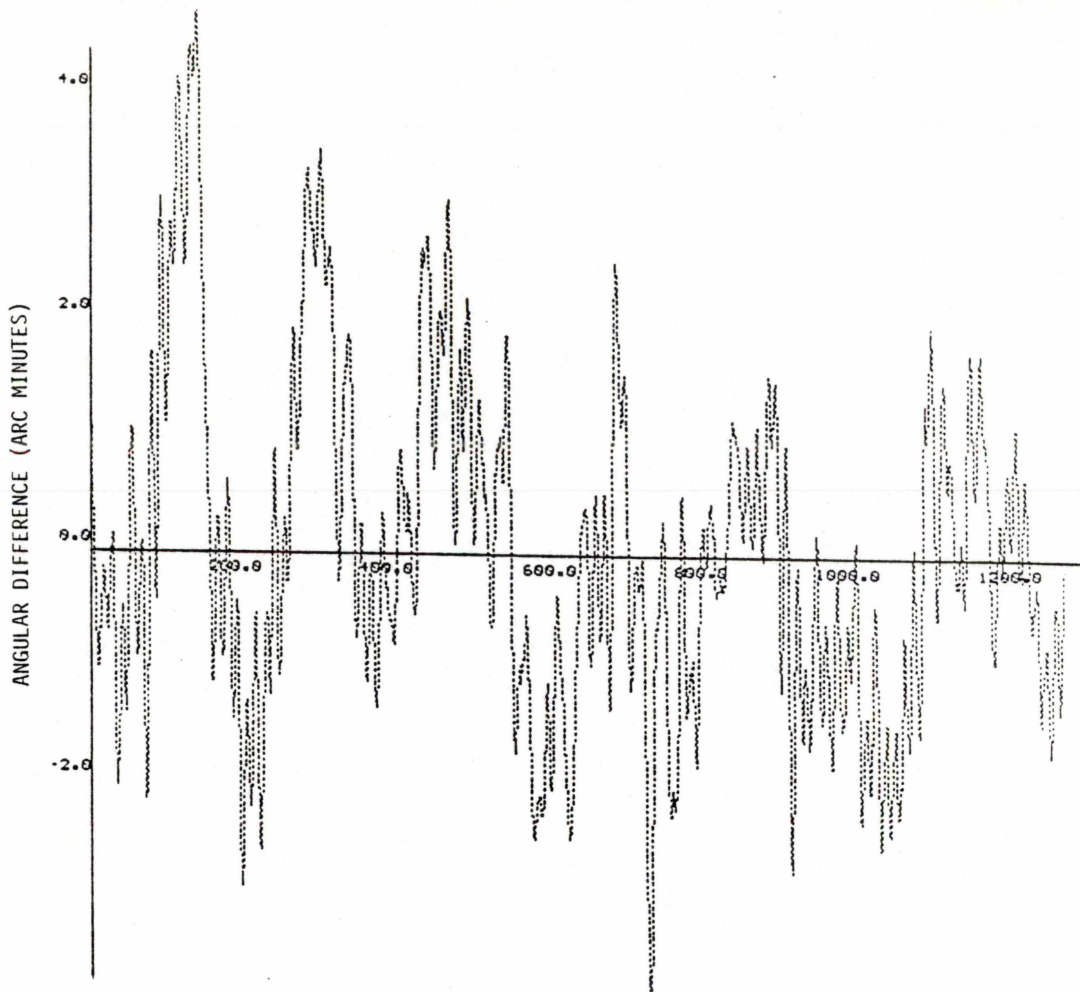


Figure 4.9 - Angular Difference Between Axles (XNG2), Calculated From Axle Longitudinal Displacements

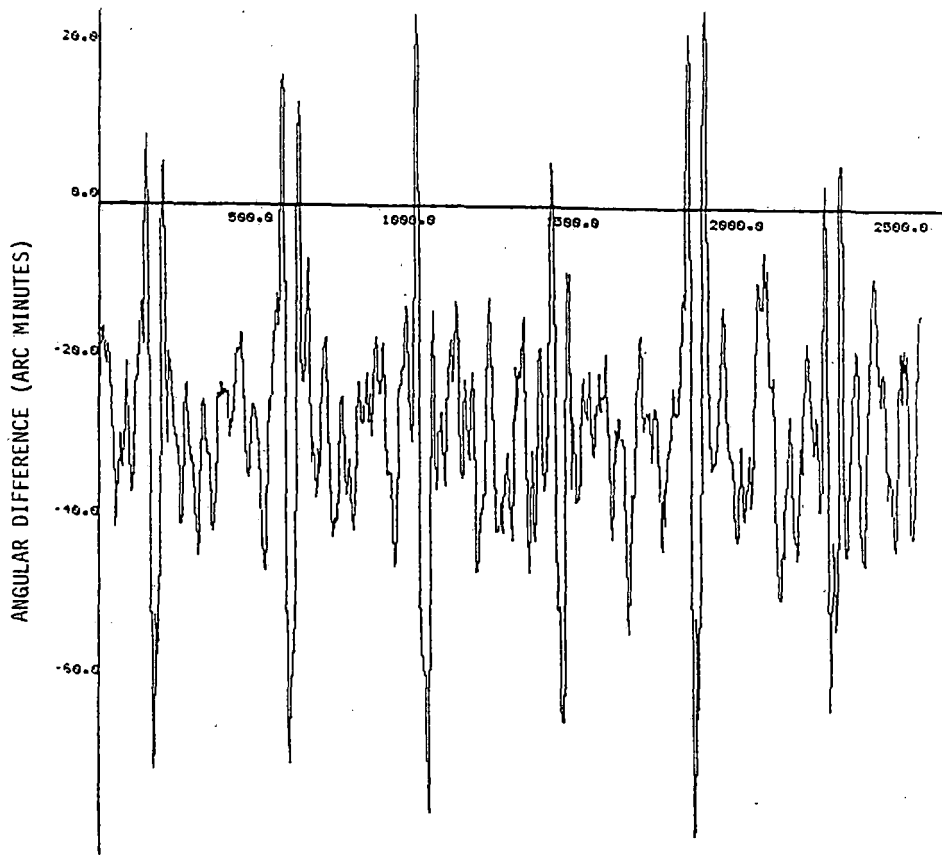


Figure 4.10 - Angular Difference Between Axles (XNG1) on Curve #2 (6.2° Left Hand Curve)

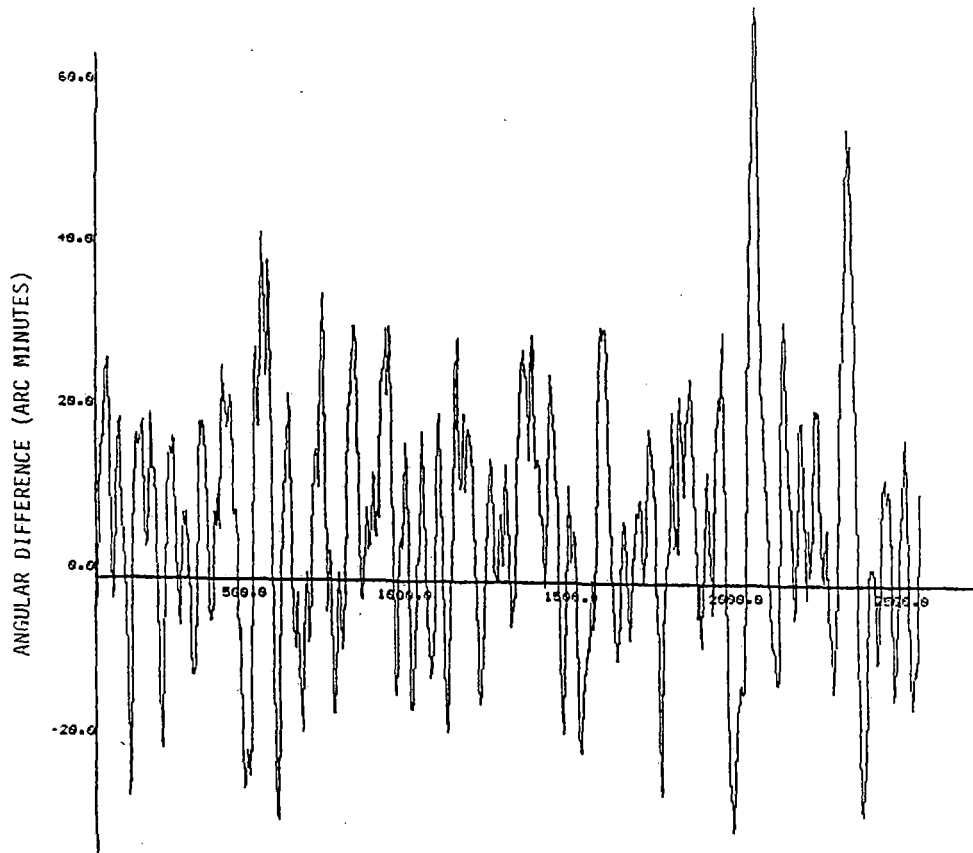


Figure 4.11 - Angular Difference Between Axles  
(XNG1) on Curve #3 (6.1° Right  
Hand Curve)

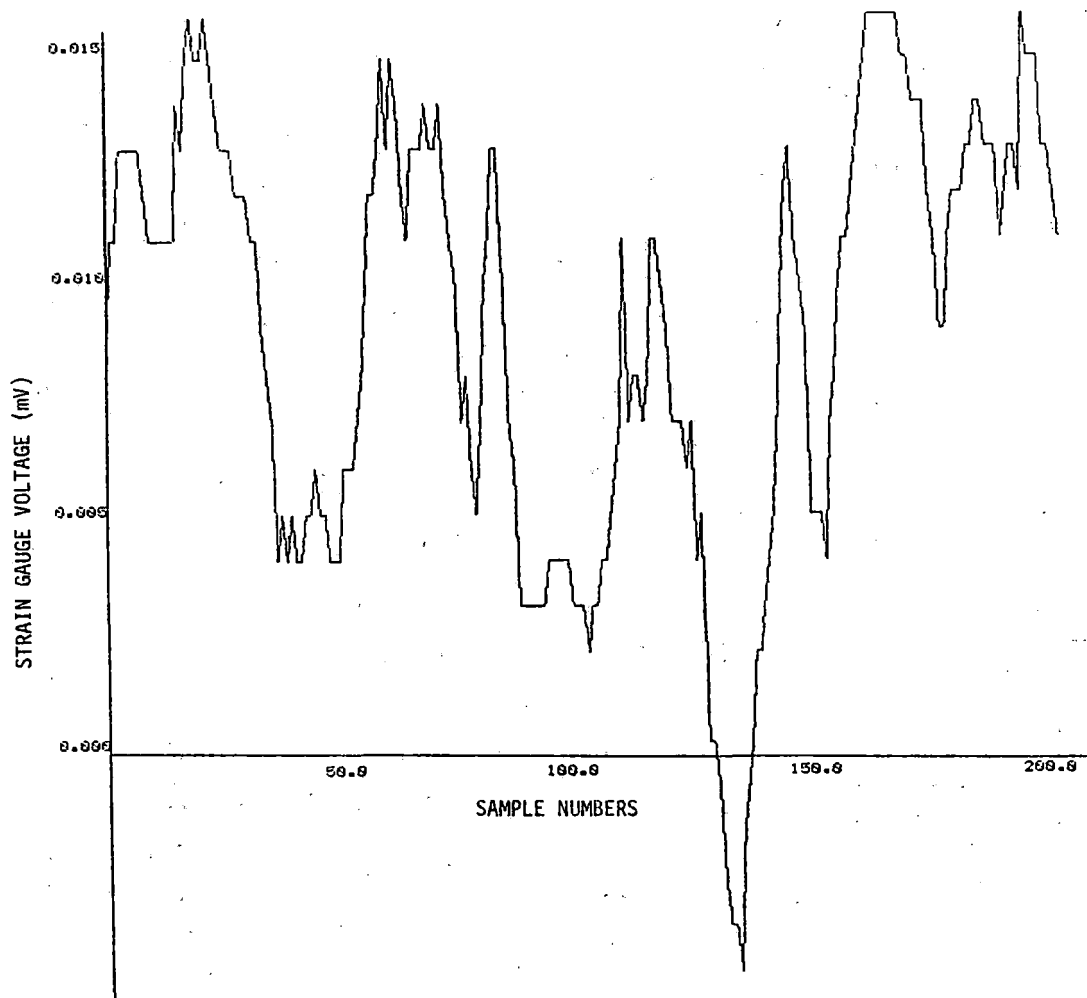


Figure 4.12 - Cross-Arm Strain Gauge Voltage on Tangent Track (B1), Unfiltered

the lower limit of the dynamic range of the instrumentation system was encountered ("jumpiness" of the curve). This could be smoothed by filtering at 50Hz (Figure 4.13) or 20Hz (Figure 4.14). The relationship between variations in the strain of the cross arm and the strut did not appear to be strong on tangent track (Figure 4.15).

Steady curve negotiation results for a fully loaded car on the Barber-Scheffel trucks (from test run BS010) provide additional information. For the left hand 6.2° curve, Figures 4.16 and 4.17 show little apparent relationship between the strains in the cross arm and strut (for time intervals of 1 second and 12.5 seconds respectively). On the 6.1° right hand curve, Figures 4.18 and 4.19 illustrate an apparent negative correlation between these strains. Also note the reversal of sign for the two strains on the opposing curves (Figures 4.17 and 4.19).

The raw calibration data for the DR-1 steering arm strain gauges (in Appendix B of the Type II Test Results Report) were used to develop relationships between the strain gauge voltages on the data tapes and the lateral forces imposed on a wheelset. This led to two force estimates, based on use of the two strain gauge channels:

$$\text{FSA1} = 7300 \text{ B1}$$

$$\text{FSA2} = 3470 \text{ B2}$$

The approximate factor of two difference may have been the consequence of only having a half bridge for B1 rather than a full bridge. The calibration for B2 appeared to be much more stable and linear, and fortunately it was B1 rather than B2 which was destroyed early in the test. Considerable uncertainty still surrounds these values because of the possibility that the excitation voltage used in the test program was half of that used for the calibrations and because of some doubts about the precise positioning of the strain gauges and about the calibration conditions (points of force application and restraints on



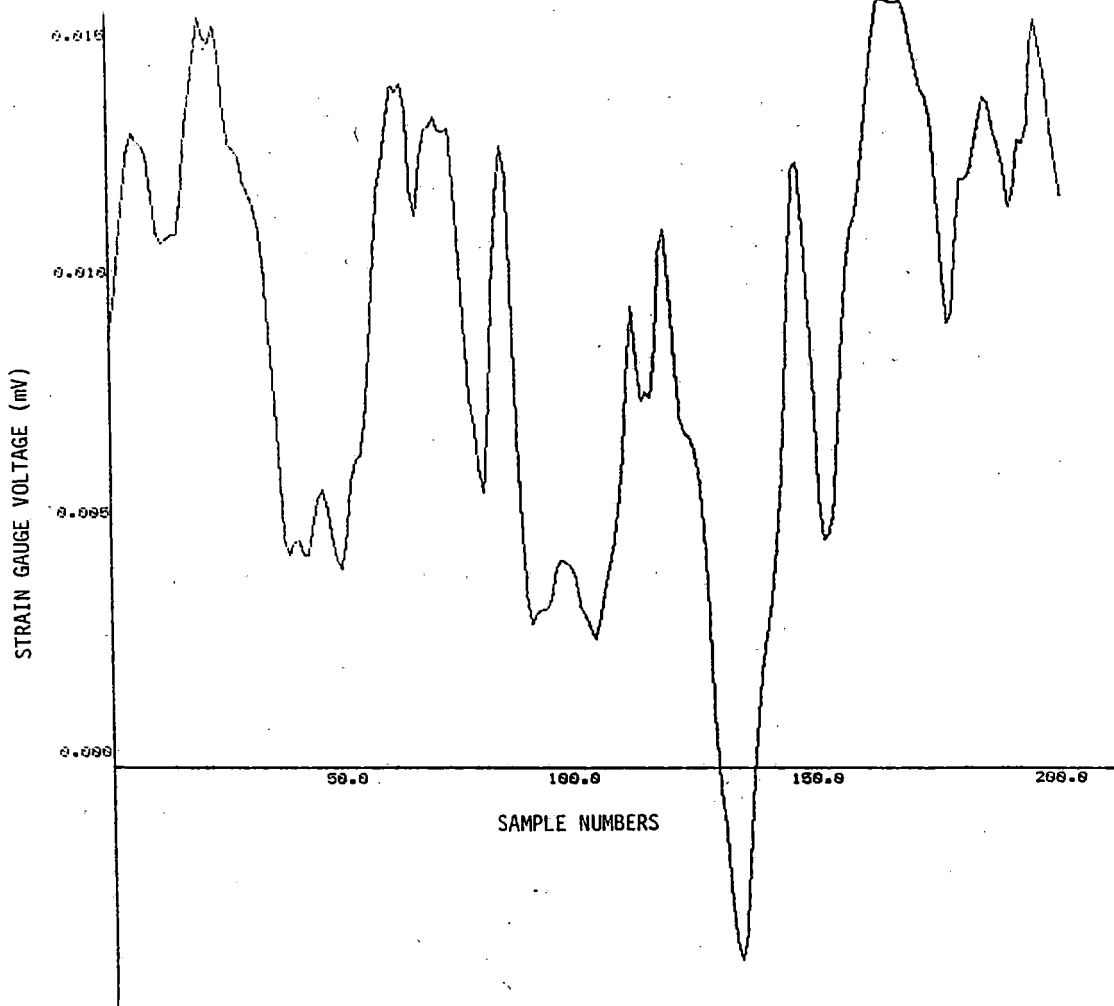


Figure 4.13 - Cross-Arm Strain Gauge Voltage on Tangent Track (B1), Filtered at 50Hz

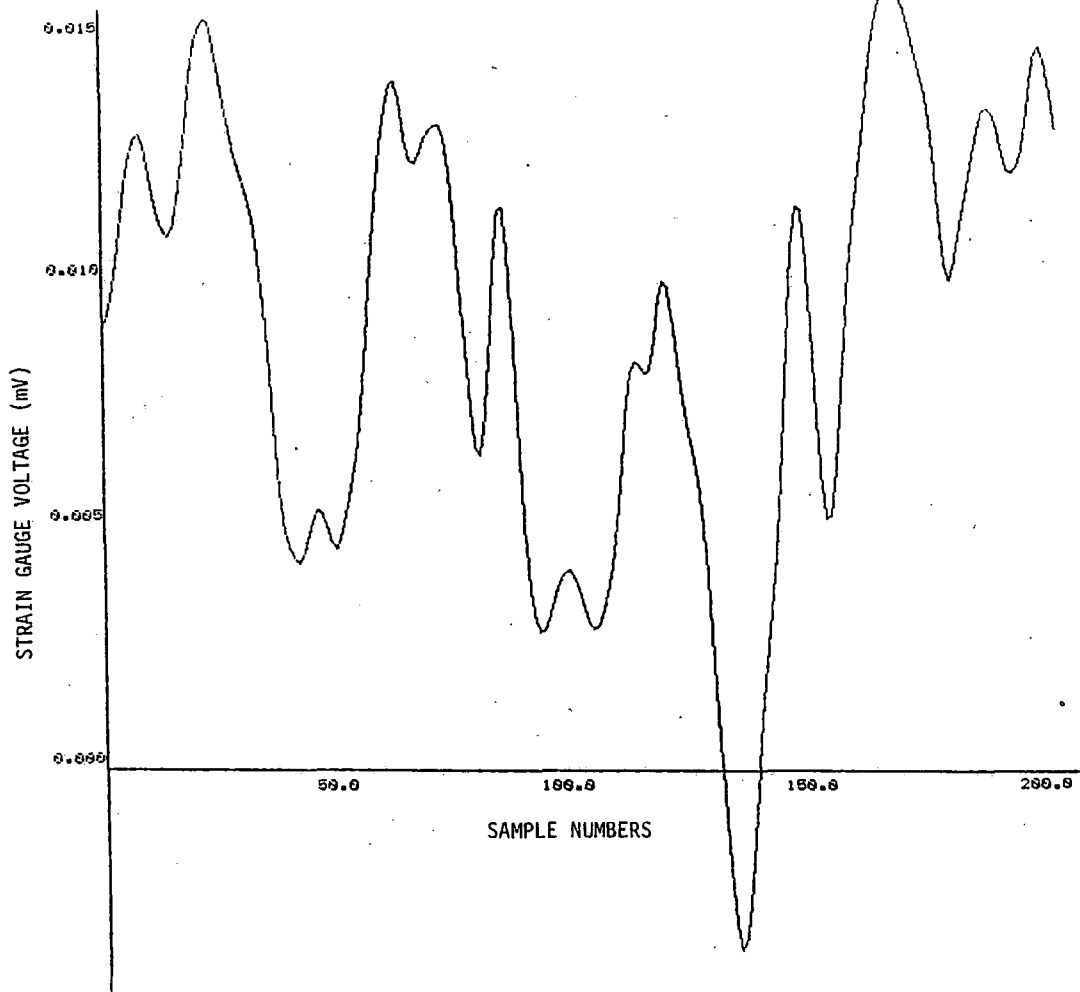


Figure 4.14 - Cross-Arm Strain Gauge Voltage on Tangent Track (B1), Filtered at 20Hz

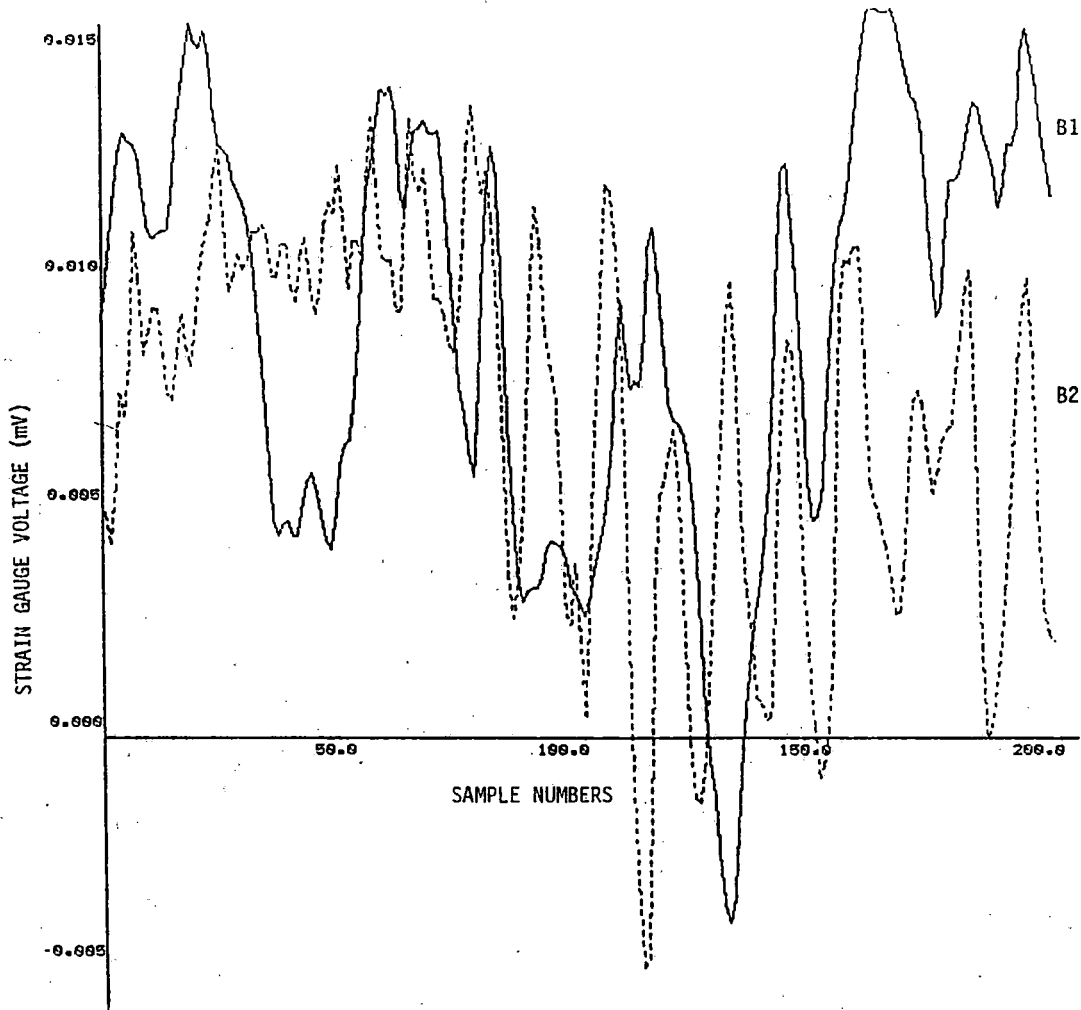


Figure 4.15 - Cross-Arm and Cross-Strut Strain Gauge Voltages on Tangent Track (B1 and B2), Filtered at 50Hz

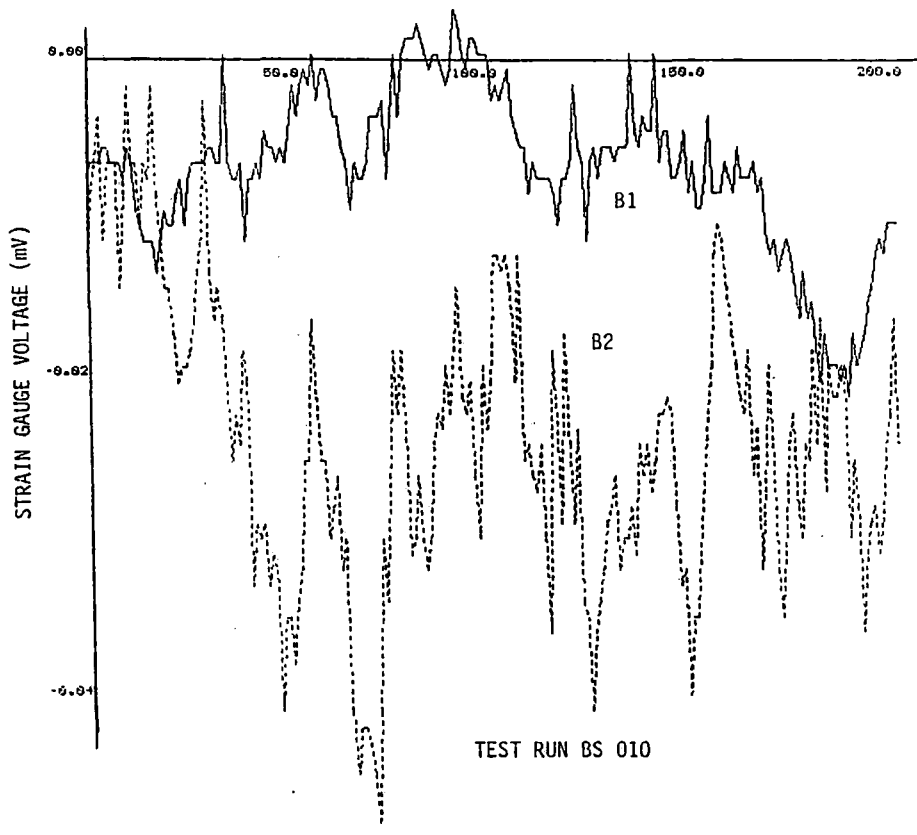


Figure 4.16 - Cross-Arm and Cross-Strut Strain Gauge Voltages in Curve #2 (6.2° Left Hand Curve), 1 Second Duration

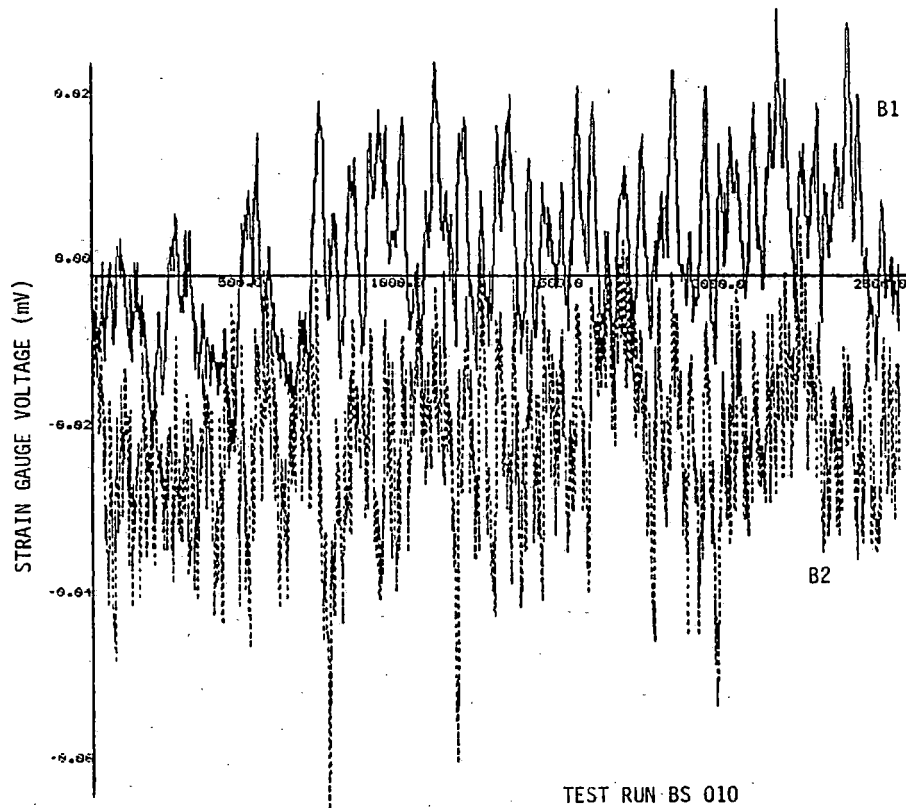


Figure 4.17 - Cross-Arm and Cross-Strut Stain Gauge Voltages in Curve #2 (6.2° Left Hand Curve), 13 Seconds Duration

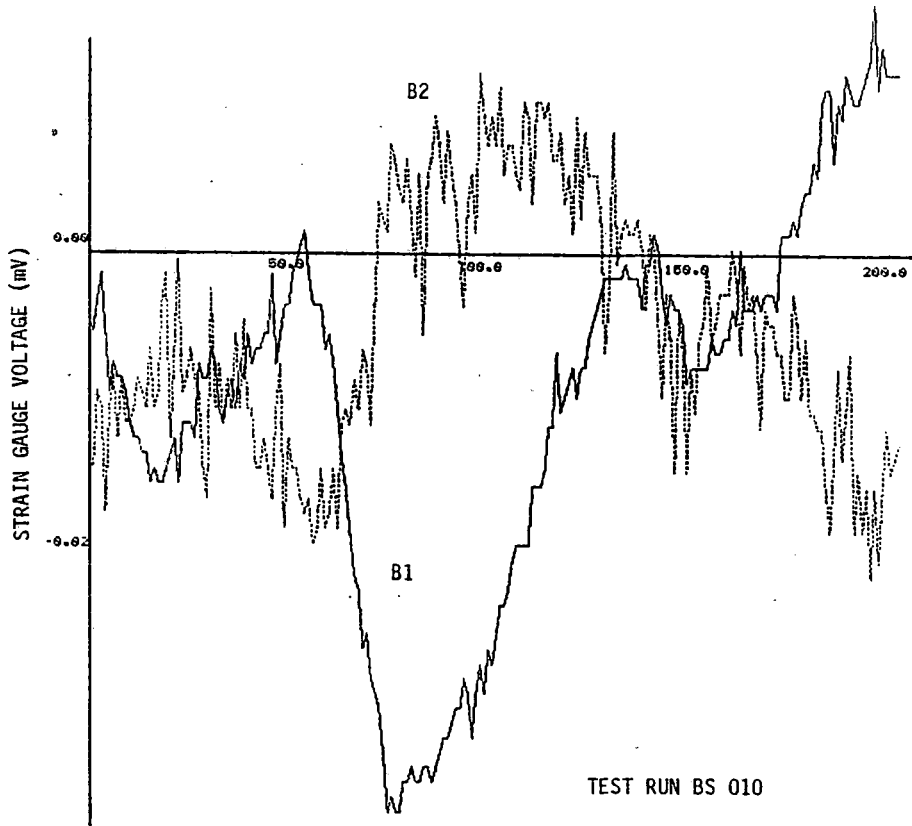


Figure 4.18 - Cross-Arm and Cross-Strut Stain Gauge Voltages in Curve #3 (6.1° Right Hand Curve), 1 Second Duration

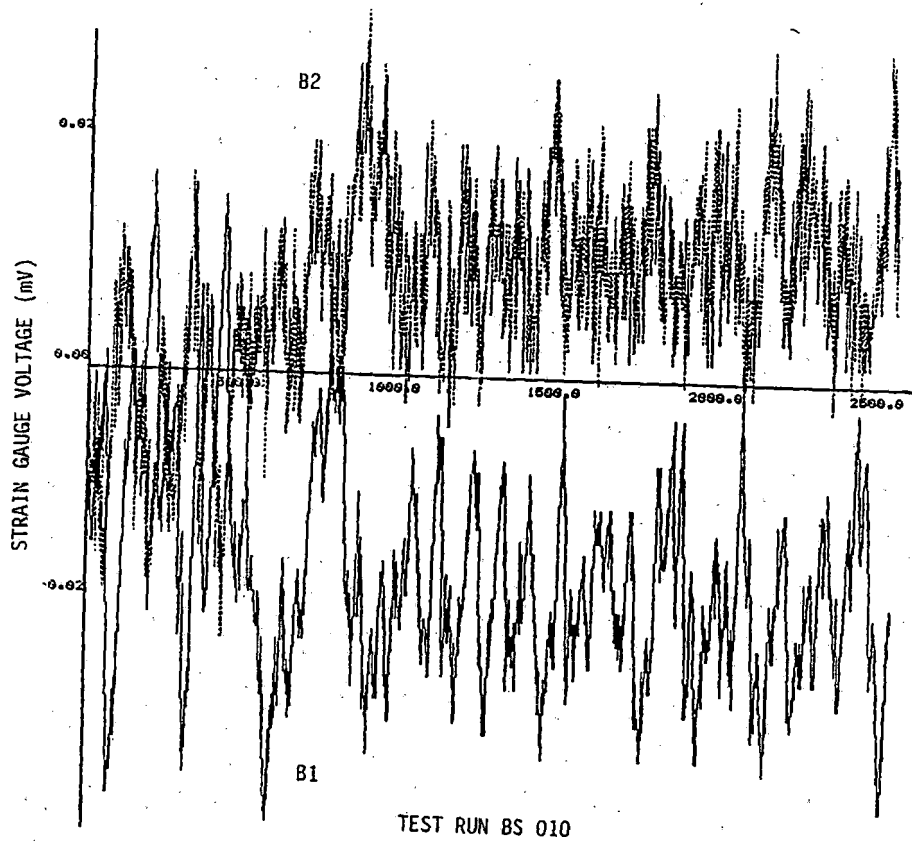


Figure 4.19 - Cross-Arm and Cross-Strut Stain Gauge Voltages in Curve #3 (6.10 Right Hand Curve), 13 Seconds Duration

wheelsets). Once again, the trends are likely to be of considerably more significance than the absolute magnitudes. In particular, because of the choice of calibration conditions, these strain gauge measurements cannot reveal the magnitude of the loads experienced by the steering arms, but may only indicate something of the lateral bearing adapter or wheel/rail forces which were imposed on the wheelset or truck.

#### 4.3 Vertical Spring Dynamic Forces

The vertical deflections of the coil springs were used to estimate the variations in the forces transmitted across these springs for comparison with the variations in the bearing adapter vertical forces. The comparison would not be expected to be especially close because of the forces transmitted through the friction snubbers. The steady-state spring deflection (from vehicle weight alone) cannot be readily identified because of unknown biases on the spring deflection channels (D1-D4). Therefore, only dynamic spring forces can be considered here.

The spring constants were not explicitly defined in any of the TDOP documentation, but were derived from the reported static vertical deflections of the loaded and unloaded cars. By equating the differences in these deflections with the weight differences of the cars, it was estimated that the Barber-Scheffel had a vertical stiffness of 27,500 lb./in. for each side (left or right) of the truck and the DR-1 had a stiffness of 25,900 lb./in. These stiffnesses were multiplied by the average spring deflections  $[(D1 + D2)/2$  on the right and  $(D3 + D4)/2$  on the left] to derive the estimates of dynamic vertical force variations on each side of the truck.

The front and rear spring deflections on the right side of the instrumented truck, D1 and D2, appear to be almost mirror images of each other on the basis of the plots of Figures 4.20 and 4.21. Similarly, D3 and D4 on the left side (Figures 4.22



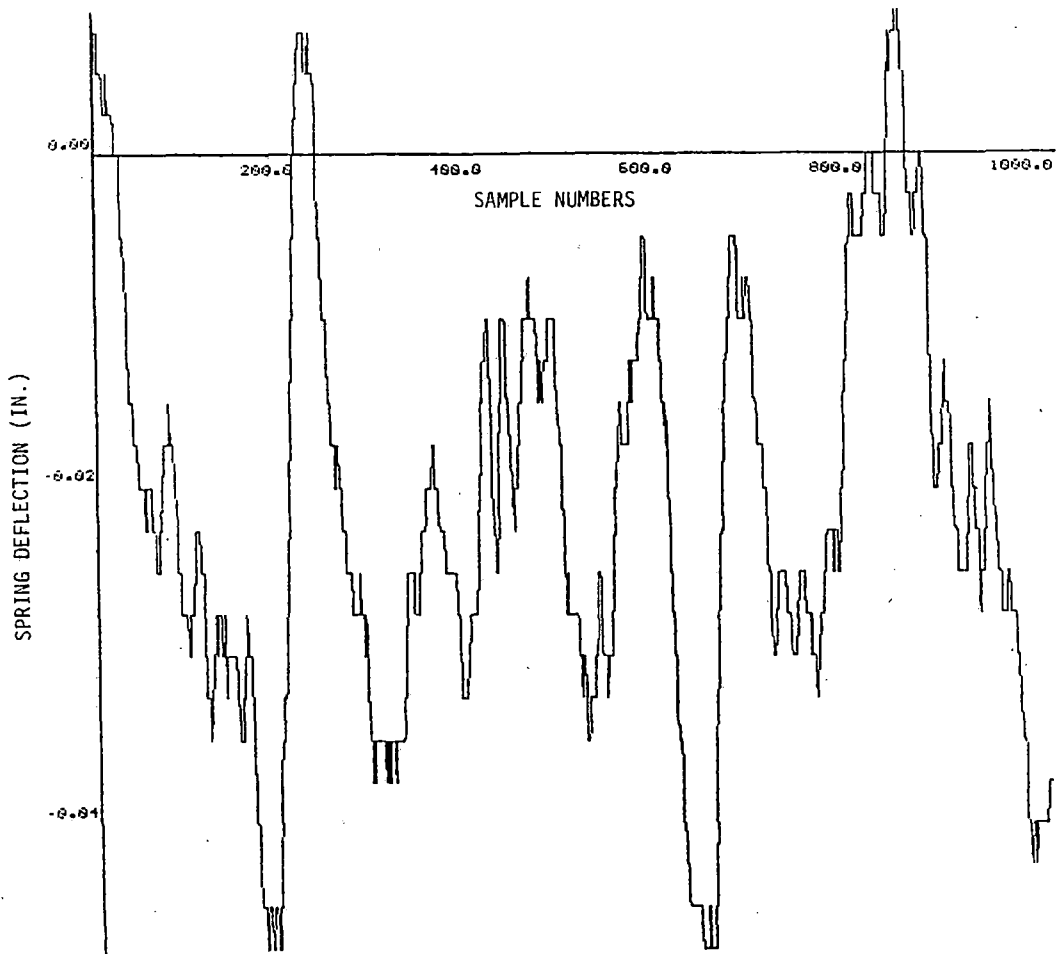


Figure 4.20 - Vertical Deflection of Right Front Suspension Spring (D1)

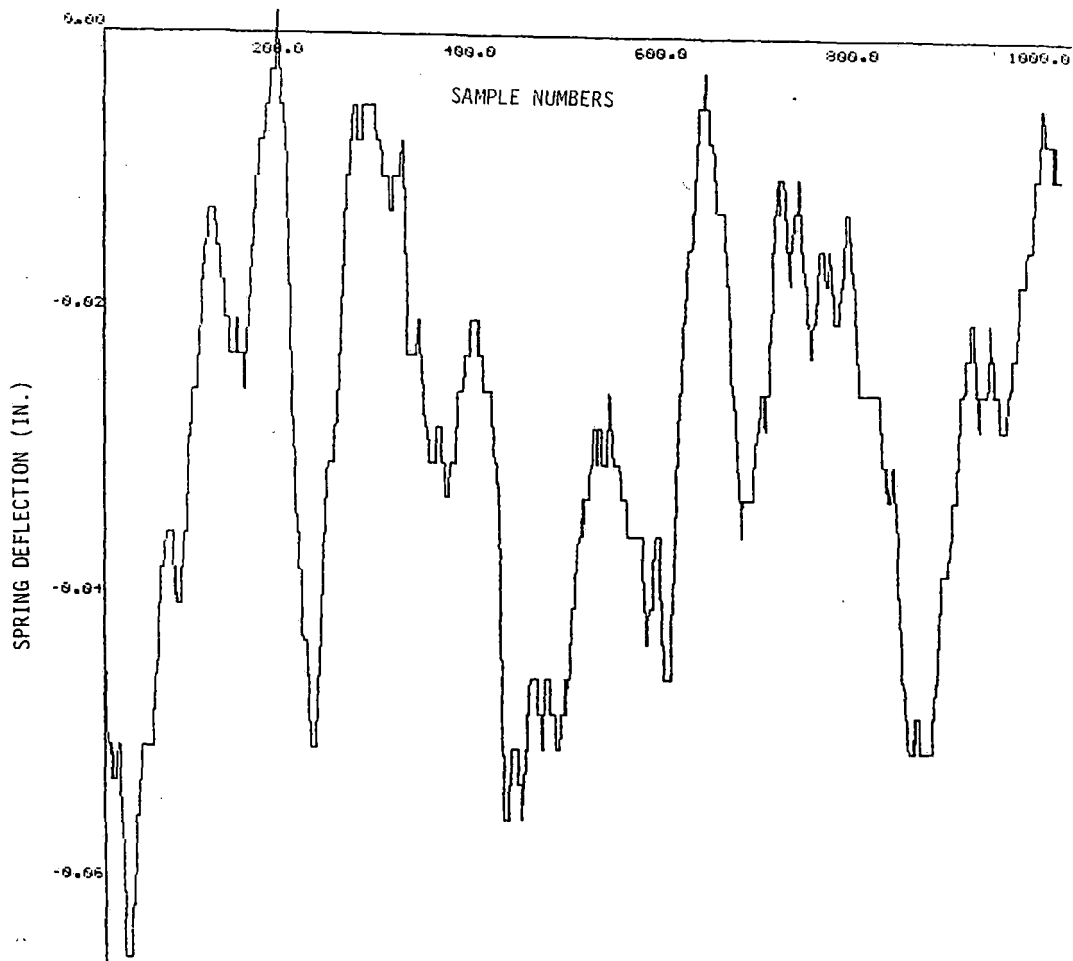


Figure 4.21 - Vertical Deflection of Right Rear Suspension Spring (D2)

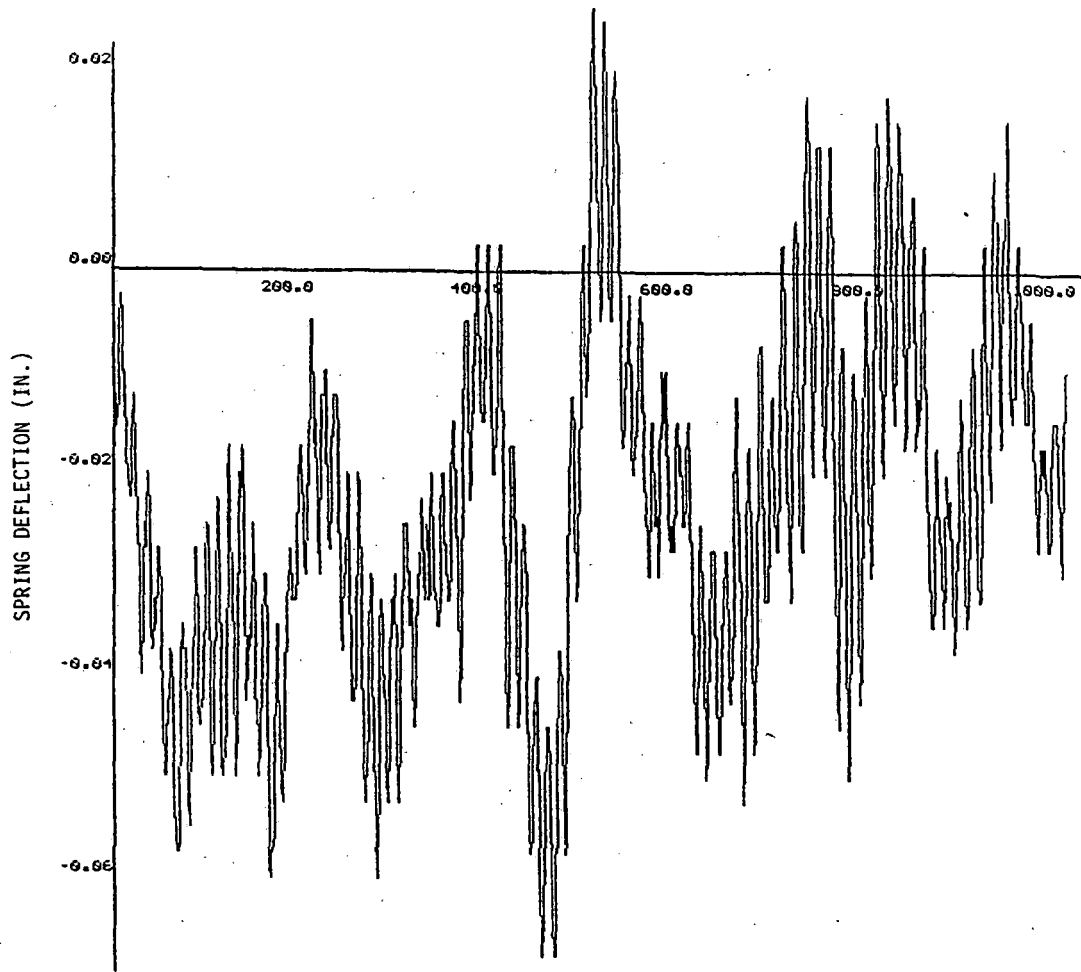


Figure 4.22 - Vertical Deflection of Left Front Suspension Spring (D3)

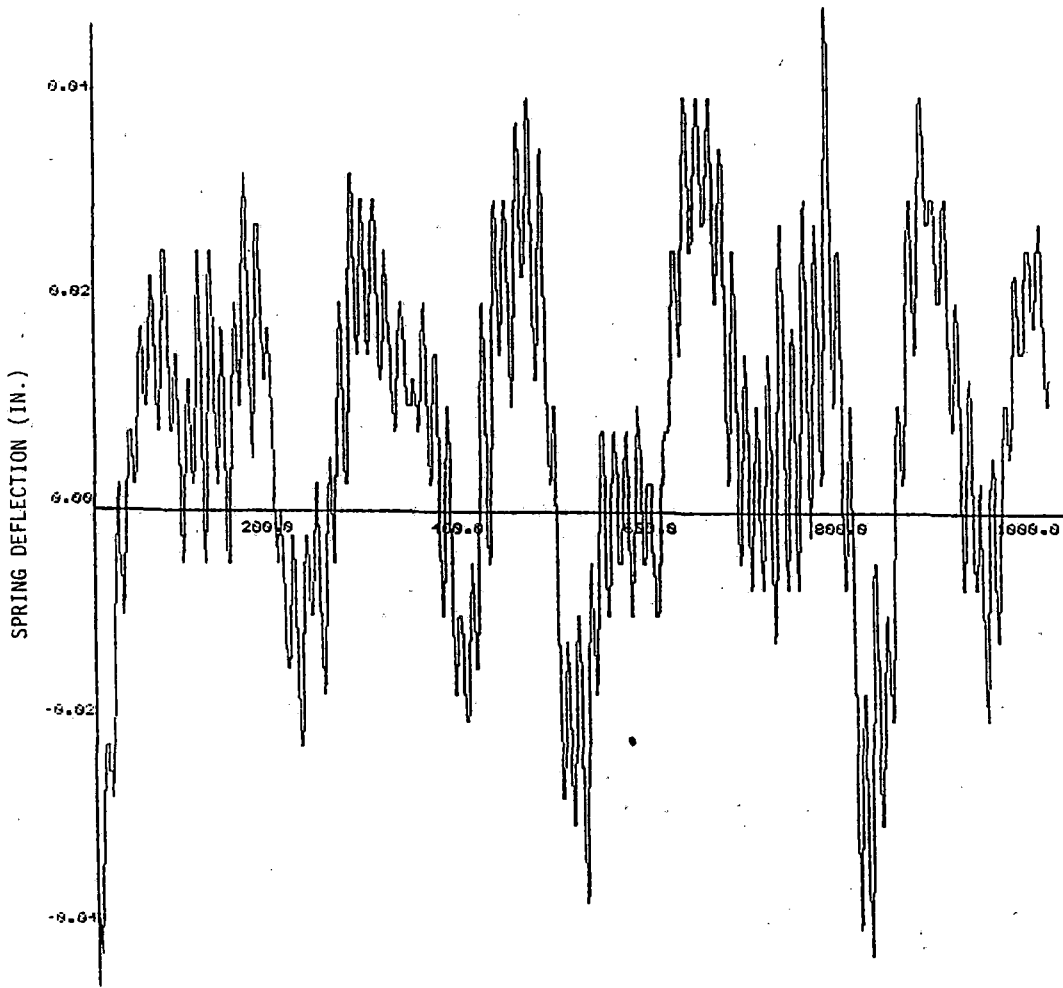


Figure 4.23 - Vertical Deflection of Left Rear Suspension Spring (D4)

and 4.23) are of opposite phase with each other, implying that truck pitch (or bolster pitch) is the dominant response mode. The magnitudes of the deflections are small enough to test the lower limit of the dynamic response range for all four of these channels. It seems odd that the left side is experiencing much higher frequency disturbances than the right side, even though the magnitudes are comparable. The net force variations associated with these spring deflections on the two sides of the truck are shown in Figures 4.24 and 4.25 for one and 6.5 seconds respectively. These force plots appear to bear little if any relationship to each other.

#### 4.4 Axle Longitudinal Displacements

The longitudinal displacements of the axle ends relative to the truck side frames (or the shear pad housings on the Barber Scheffel) were recorded on channels D19-D22. These measurements may have had some zero offsets (biases), based on results observed in unperturbed operations on tangent track. If this were the case, the true zero displacement values could not really be known and only the relative displacements could be investigated. Examples of these measurements for the Barber-Scheffel truck under an empty car are shown in Figures 4.26 - 4.28.

Figures 4.26 and 4.27 show the longitudinal displacements in inches of the left and right ends of the lead axle (without bias removal). Although these are almost perfectly in phase, the magnitudes are different by a factor of about 20, bringing the Figure 4.27 results down to such a low level that the quantization effect of the D/A conversion is painfully apparent. This could have been caused by an instrumentation problem or by some physical constraint on the truck which would keep the front left bearing adapter almost immobilized. Later segments of the same test run (BS-002A) in curves produced a much wider range of

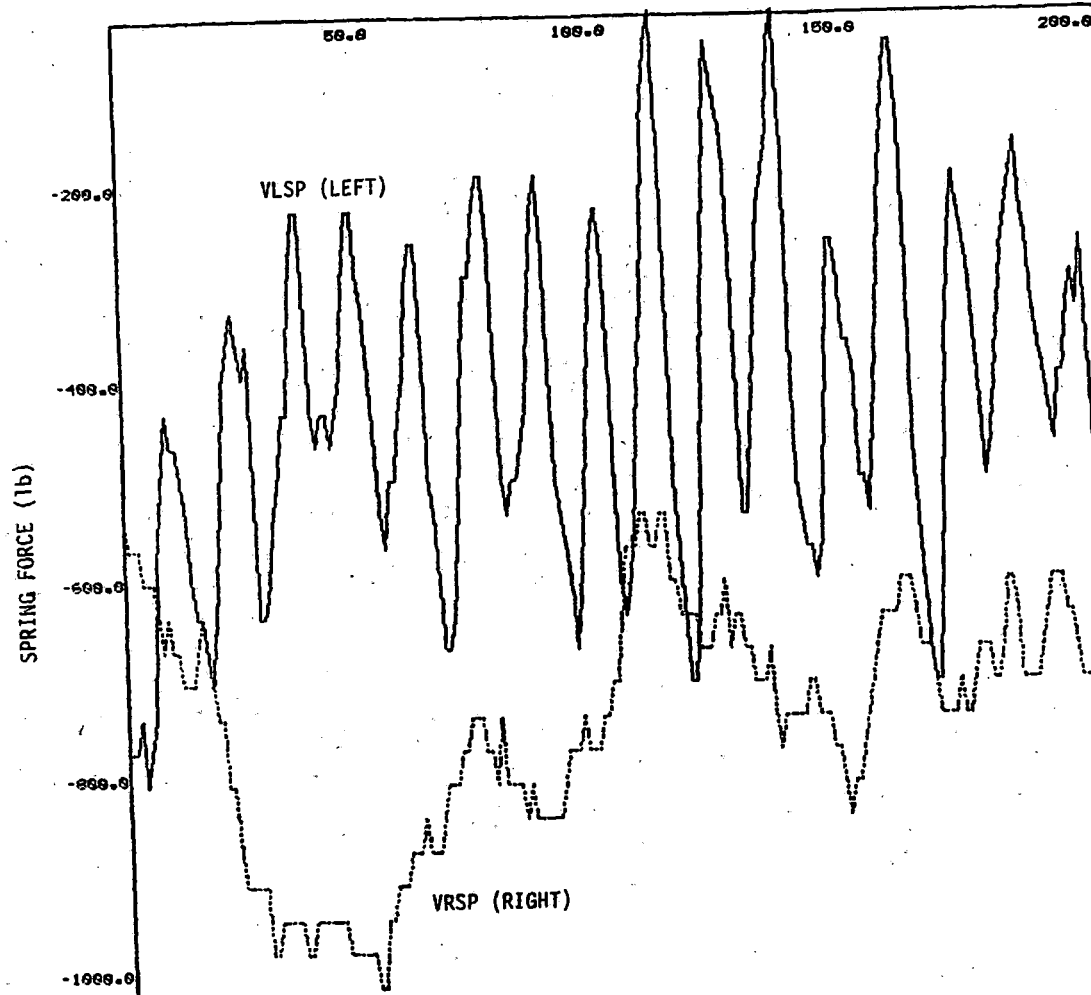


Figure 4.24 - Vertical Truck Side Spring Dynamic Forces (one second duration)

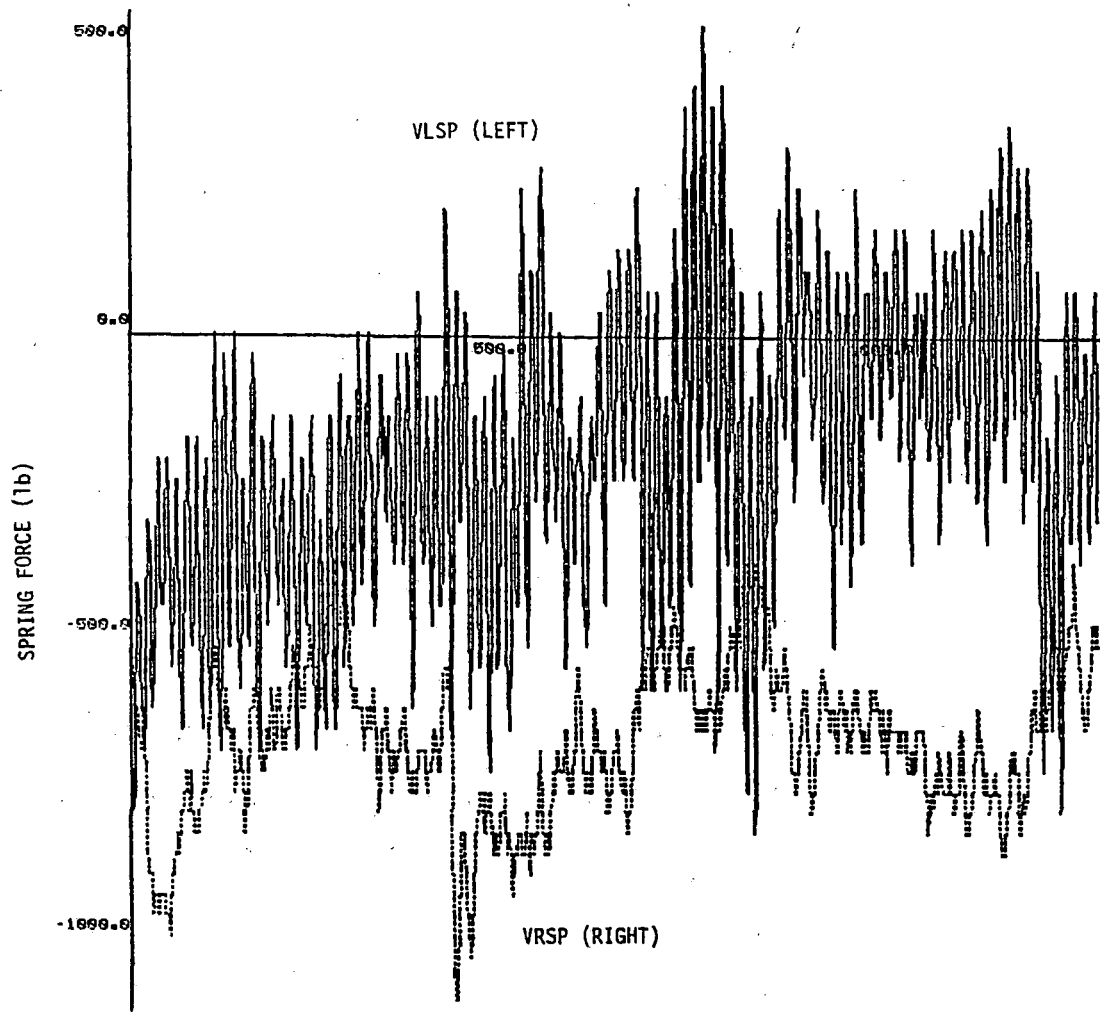


Figure 4.25 - Vertical Truck Side Spring Dynamic Forces (six second duration)

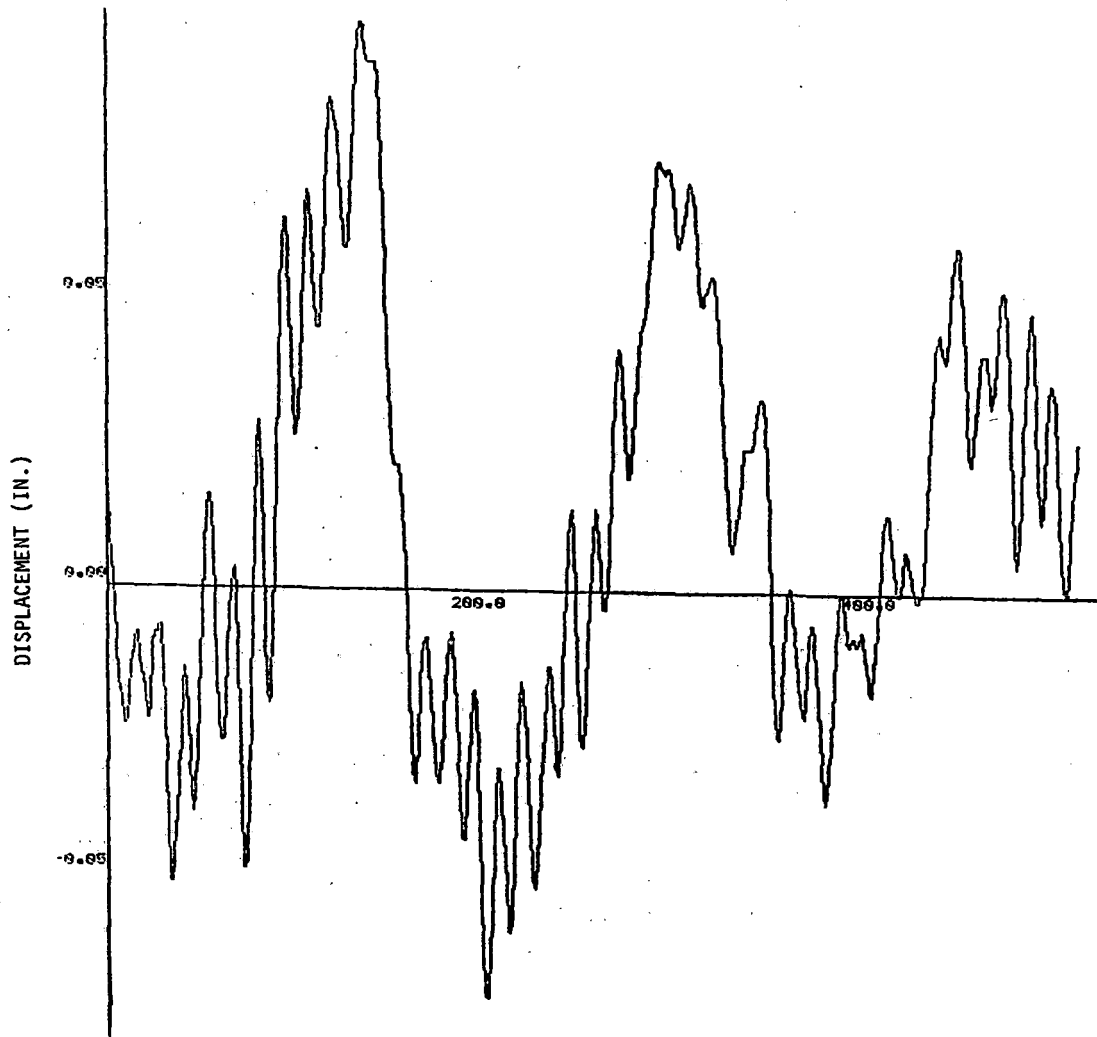


Figure 4.26 - Longitudinal Displacement of Left End of Front Axle (D21)



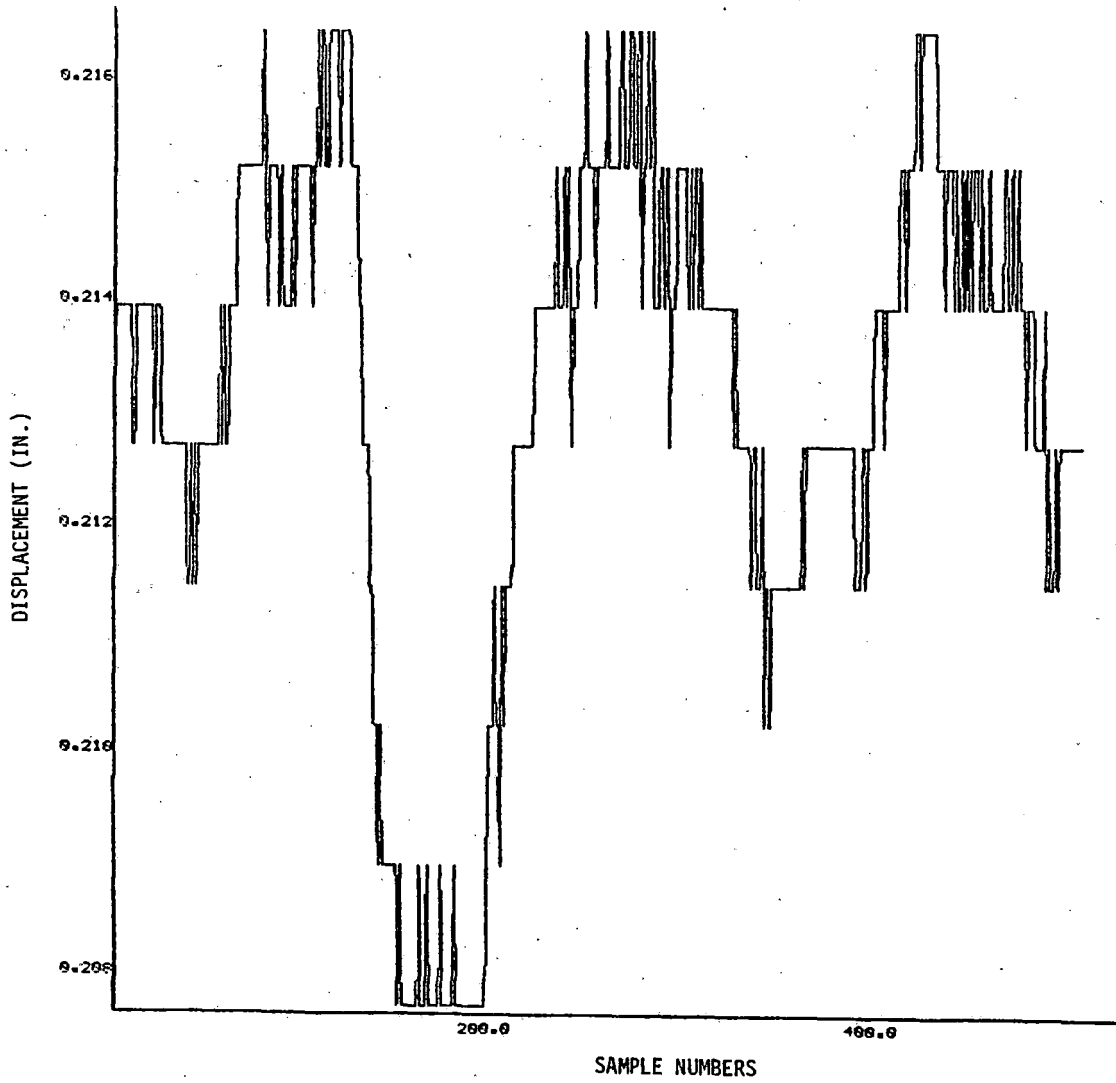


Figure 4.27 - Longitudinal Displacement of Right End of Front Axle (D19)

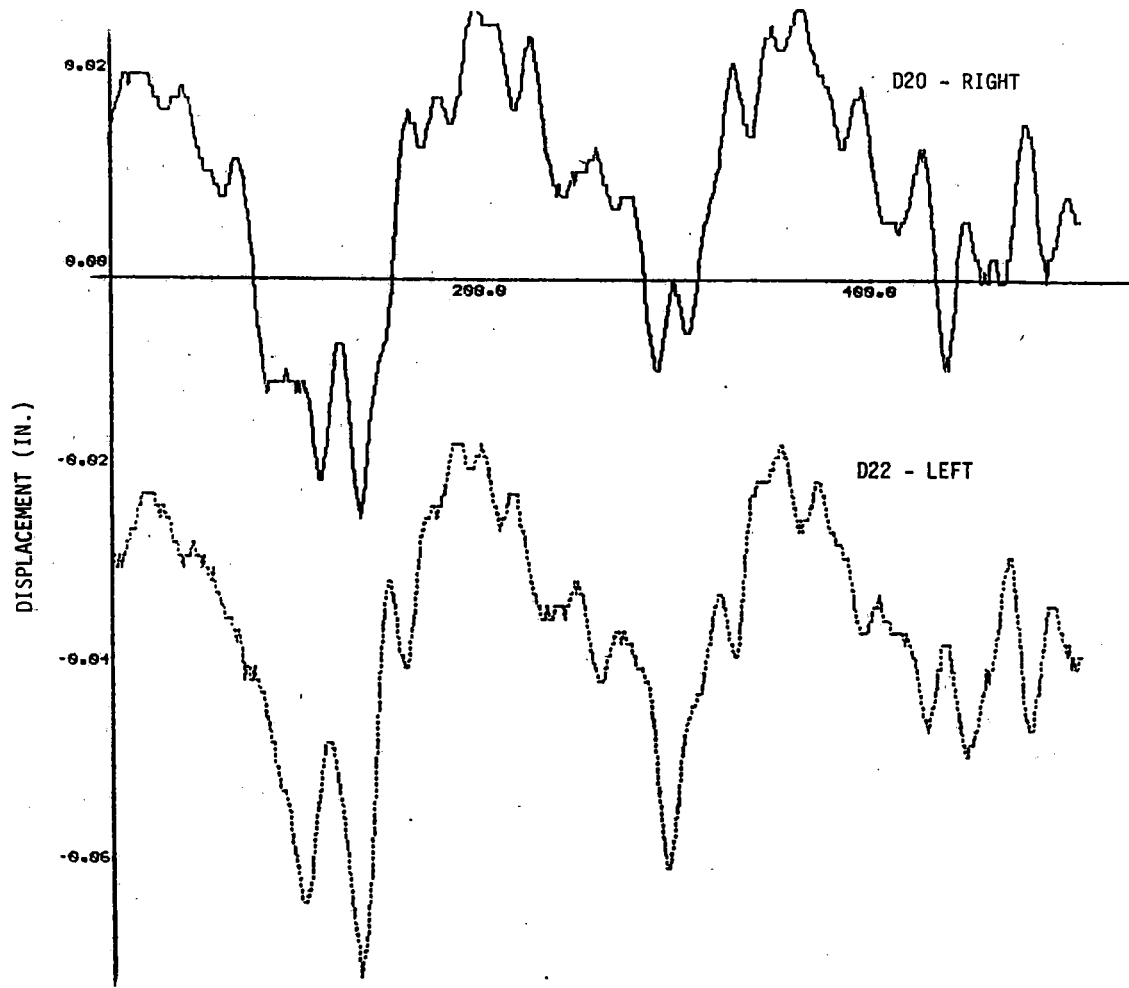


Figure 4.28 - Longitudinal Displacements of Both Ends of Rear Axle (D20, D22)

values on channel D19, so this was either the result of a temporary physical constraint or an intermittent instrumentation problem. Figure 4.28 shows the longitudinal displacements of both ends of the rear axle, which are almost identical in waveform but appear to have different biases. The results for both axles indicate that the axle displacements at low speed on tangent track are mainly longitudinal translations and not yawing. The changes in the mean values of D19-D22 for operations on different curves indicate the trends in wheelset alignment. For test runs BS-002A and BS-010, these mean values changed very substantially between curve #2 ( $6.2^{\circ}$  left) and curve #3 ( $6.2^{\circ}$  right), and in most cases they had opposite signs on these two curves. Because of the lingering uncertainty about the zero calibration points for these channels, this information should only be used to calculate steady state axle alignment estimates with caution.

#### 4.5 Axle Bending Moments

The TDOP Phase II testing of the Type I trucks generated 32 channels of axle bending strain gauge data, while the testing of the Type II trucks produced 24 channels of these data (6 channels for each side of each axle). The quadrature pairs of gauges at the same location (those located  $90^{\circ}$  apart around the axle) are used to estimate axle bending moments. The axle bending channels and their combinations in the data reduction process were scrutinized closely because of their significant influence on the estimates of lateral wheel/rail forces.

A sample plot of three of the strain gauge channels on the right side of the lead axle is shown in Figure 4.29. The large sinusoidal component corresponds to wheel rotations, and provides no information about force or moment variations. The three channels are phase shifted because of their differing locations around the periphery of the axle. The biases which are apparent

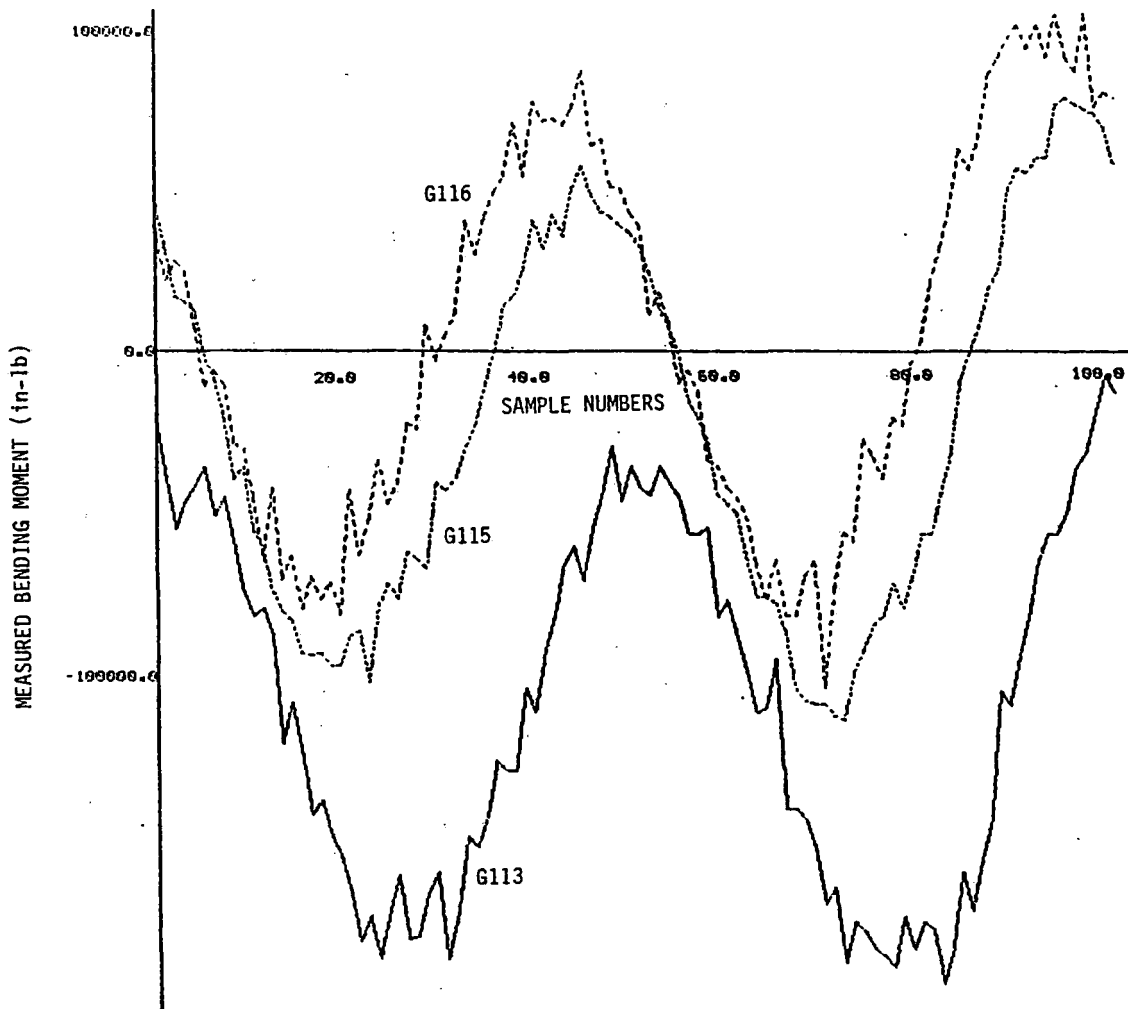


Figure 4.29 - Three Axle Bending Strain Gauge Channels, Front Axle, Right Side (G113, G115, G116)

in the Figure (non-zero mean values) must be removed before further use can be made of the data for estimating forces and moments.

The most serious problem apparent in the axle bending data is the roughness of the plots, indicating substantial changes in value from one sample to the next. This observation, coupled with the statements in several of the TDOP project reports about filtering of the axle bending data only at 500Hz, leads to a strong suspicion of aliasing on these data channels. Because these channels were sampled at 200Hz, any strains produced by structural vibrations or external inputs at frequencies between 100Hz and 500Hz would be expected to be aliased into the data, making them appear to be occurring at lower frequencies. It is very likely that several lightly damped structural modes of the wheelset occur within this frequency range and would therefore make appreciable contributions to the measured strains. Unfortunately, it is virtually impossible to remove the aliased components after the sampling (in the absence of continuous, analog data), so the axle bending channels must always be to some extent suspect.

A graphic visualization of the use of a quadrature pair of strain gauges to estimate an axle bending moment is shown in Figure 4.30, which is a cross-plot of channels G109 and G113. When the biases are removed from these channels, the circular pattern formed by the cross-plot will be centered at the origin. The radius of the "circle," such as it is, represents the net bending moment on the axle (most of which is attributable to vehicle weight). As Figure 4.30 illustrates, the jaggedness of the individual strain gauge channels produces very abrupt changes in the estimated bending moment. This effect can be countered by low pass filtering, but the filtering will still not be able to eliminate all of the distortions produced by aliasing.

Figures 4.31-4.33 show one second of the data on axle bending channel G109 unfiltered and then low-pass filtered at

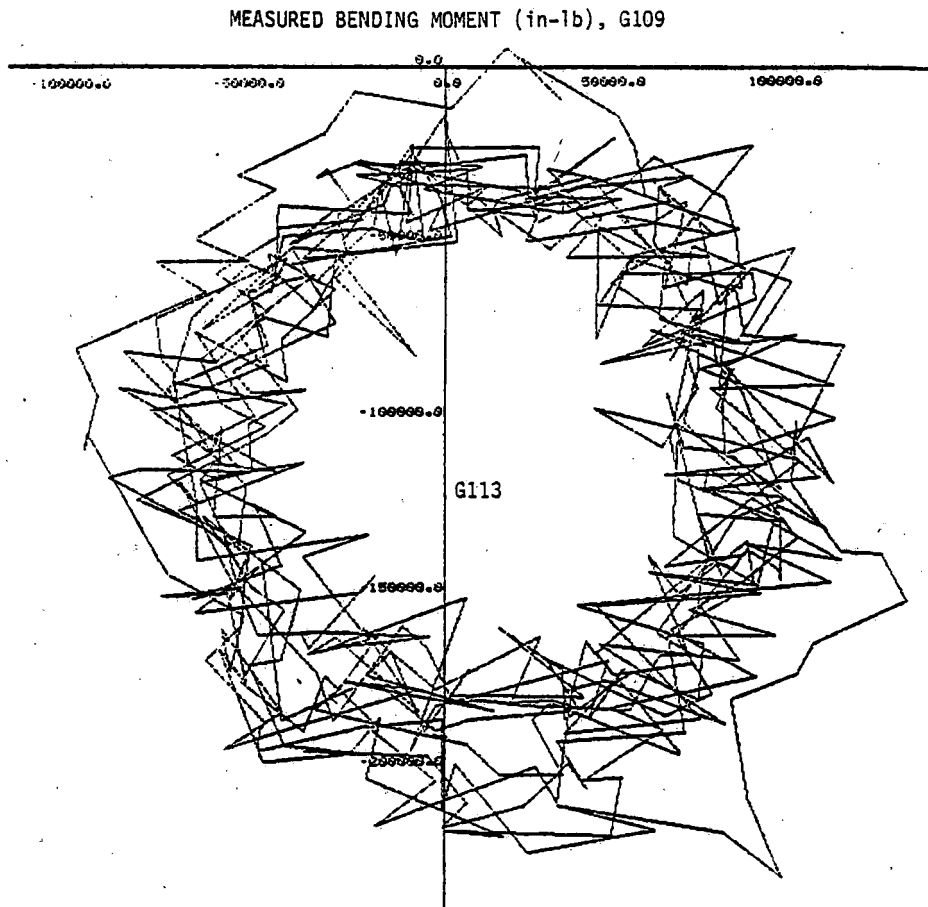


Figure 4.30 - Cross-Plot of Quadrature Pair of Axle Bending Strain Gauges, Front Axle, Right Side (G109, G113)

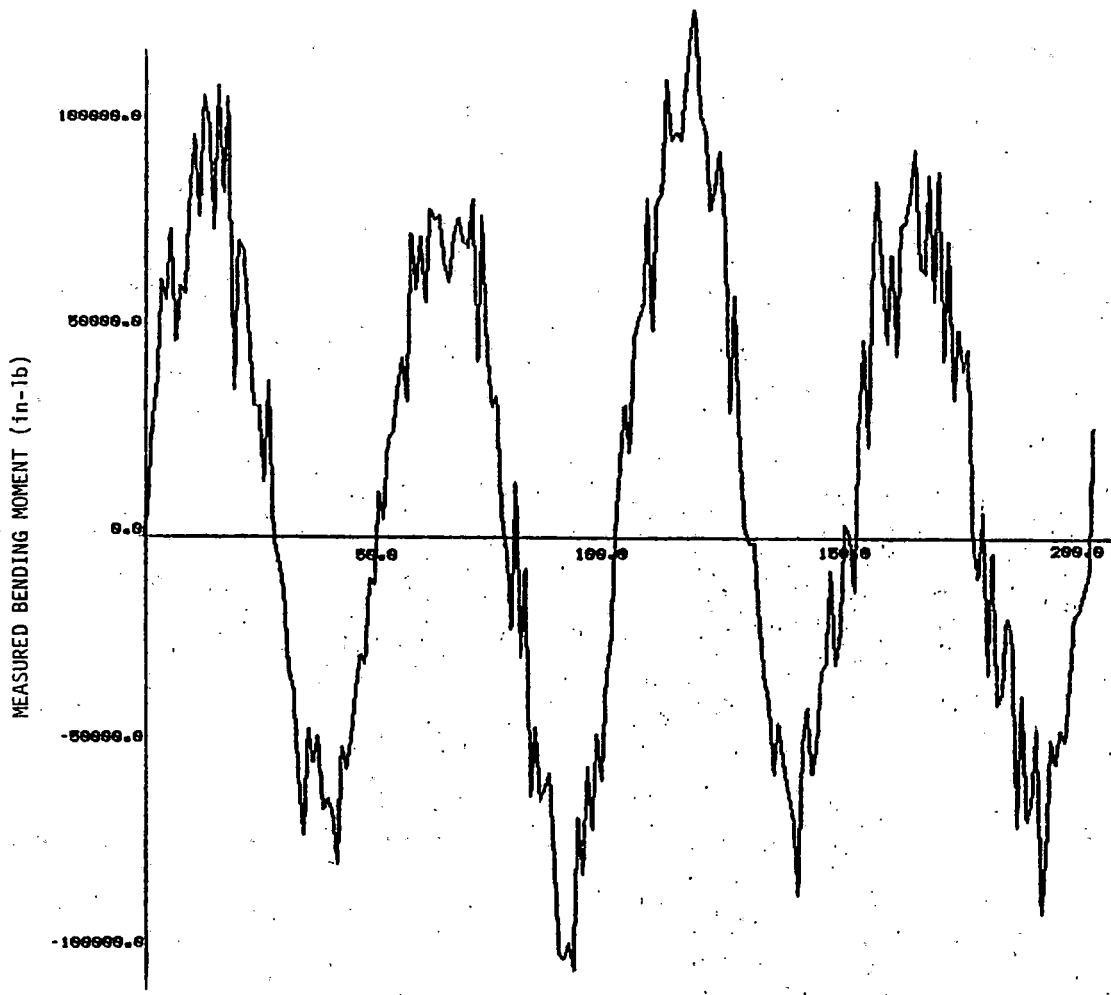


Figure 4.31 - Axle Bending Strain Gauge G109, Unfiltered, One Second Duration

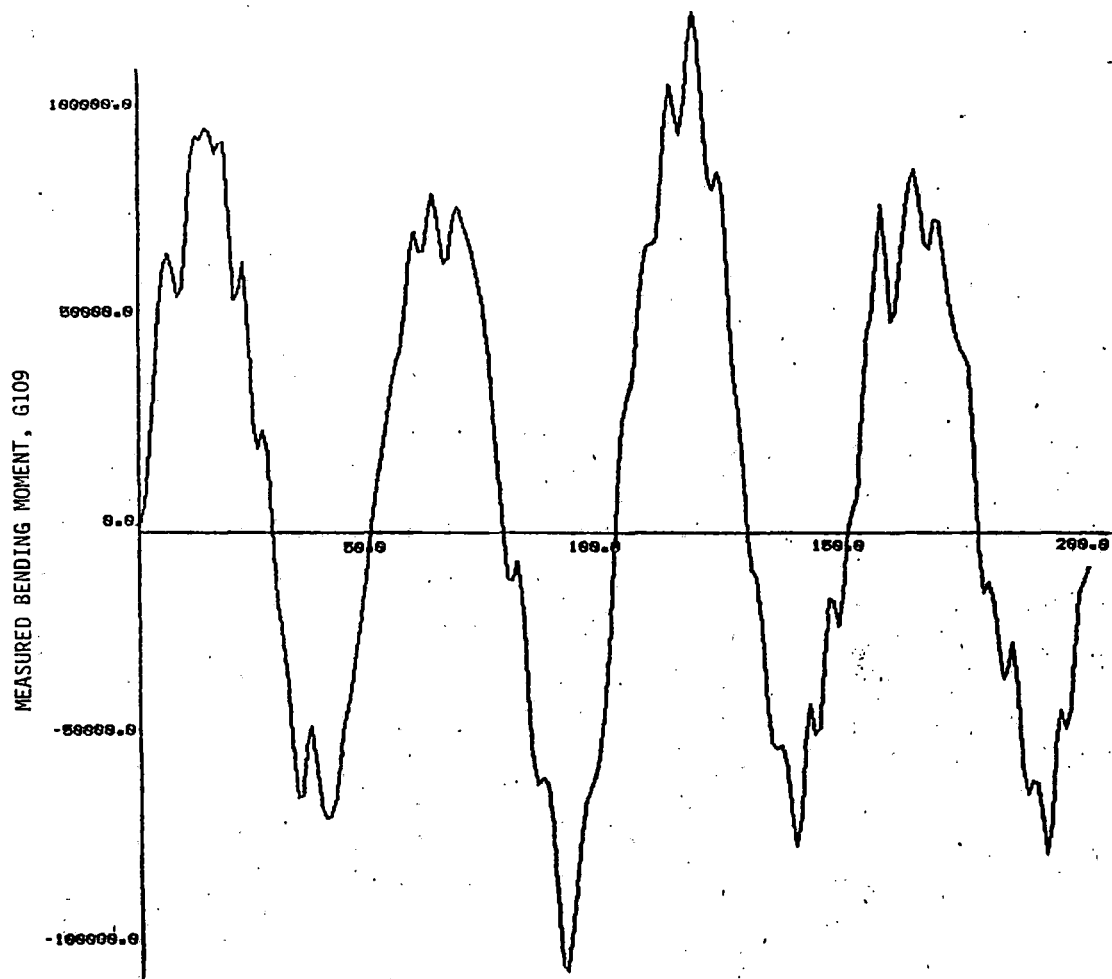


Figure 4.32 - Axle Bending Strain Gauge G109,  
Filtered at 50Hz, One Second  
Duration



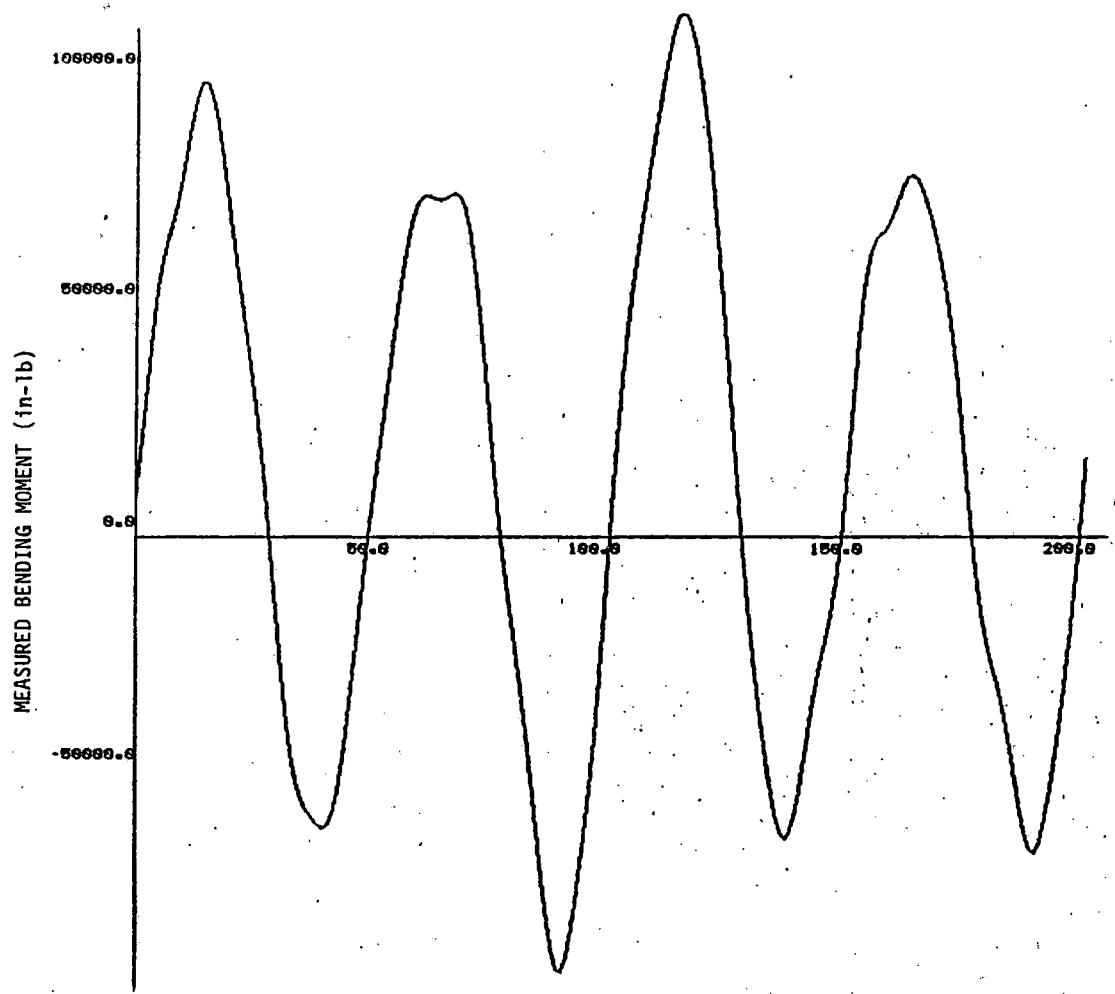


Figure 4.33 - Axle Bending Strain Gauge G109,  
Filtered at 20Hz, Once Second  
Duration

50Hz and 20Hz cutoff frequencies (4-pole Butterworth filters). Cross-plots of this channel with its quadrature pair G113 filtered at 50Hz and 20Hz are shown in Figures 4.34 and 4.35 for comparison with Figure 4.30. Much of the roughness has been removed by the filtering, although the comparison is not completely fair because Figure 4.30 was based on a longer segment of the test run. Cross-plots of longer stretches of data (5 seconds), filtered at 50Hz and 20Hz, are shown in Figures 4.36 and 4.37.

The data reduction equations discussed in Chapter 3 were used to derive axle bending moment estimates from the axle strain gauge channels. A sample time history for the intermediate variable CVR1 (one bending moment from a quadrature pair on the right side of axle 1) is shown in Figure 4.38. The many moderate size peaks in this curve do not match the peaks in the simultaneous curves for AVR1 and BVR1, which are the estimates of the same bending moments using the two other quadrature pairs at the same location. The one large peak at about 120 samples into the run does match (indicating that it must be a real physical phenomenon) but the other peaks are most likely artifacts of the aliased data. The three estimates of bending moments, AVR1, BVR1 and CVR1, are averaged together to get R1V, which is shown in Figure 4.39. The averaging process has not eliminated much of the roughness in this case.

Filtering (of the raw data channels) can greatly reduce the discrepancies among AVR1, BVR1 and CVR1, although it cannot entirely eliminate them. Figures 4.40 and 4.41 show the averaged estimates of the bending moment R1V when the data were low-pass filtered at 50Hz and 20Hz. In the latter case, the separate components of the estimated moment were sufficiently similar to each other that most of the peaks and valleys probably correspond to real variations in the bending moment.

Not all of the axle bending strain gauge channels were found to be working satisfactorily all of the time. In particular,

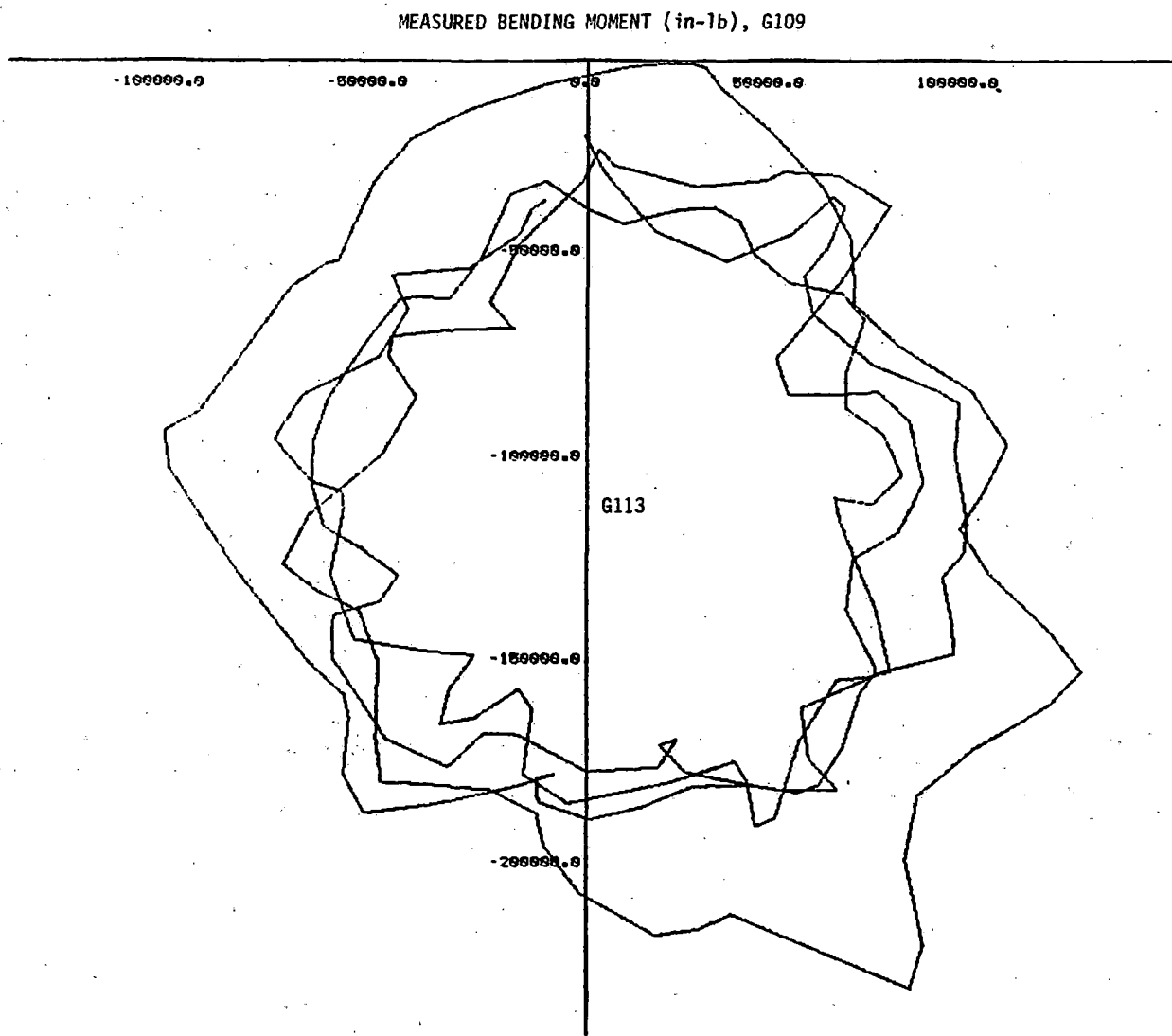


Figure 4.34 - Cross-Plot of Quadrature Pair of Axle Bending Strain Gauges (G109, G113) Filtered at 50Hz, Once Second Duration

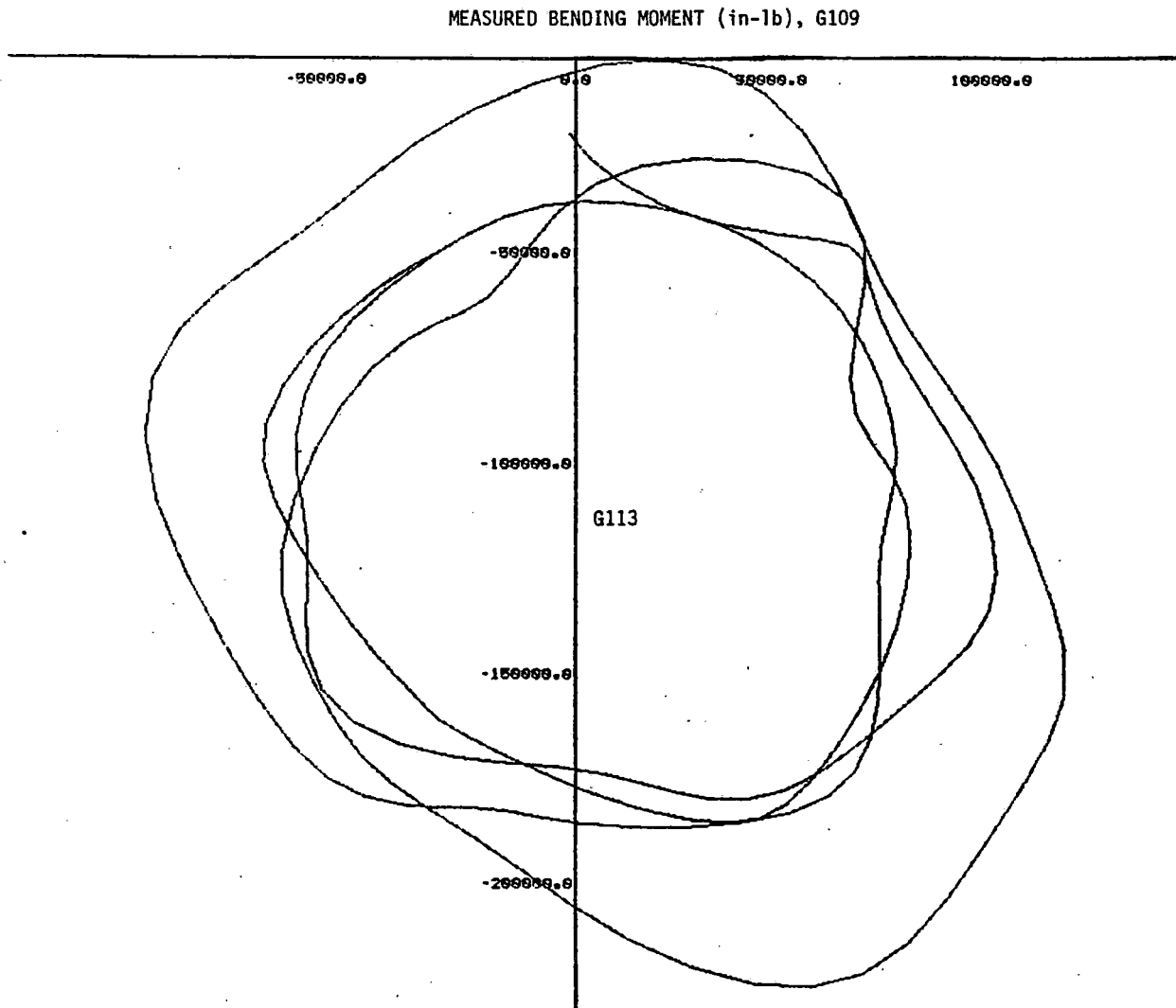


Figure 4.35 - Cross-Plot of Quadrature Pair of Axle Bending Strain Gauges (G109, G113) Filtered at 20Hz, One Second Duration

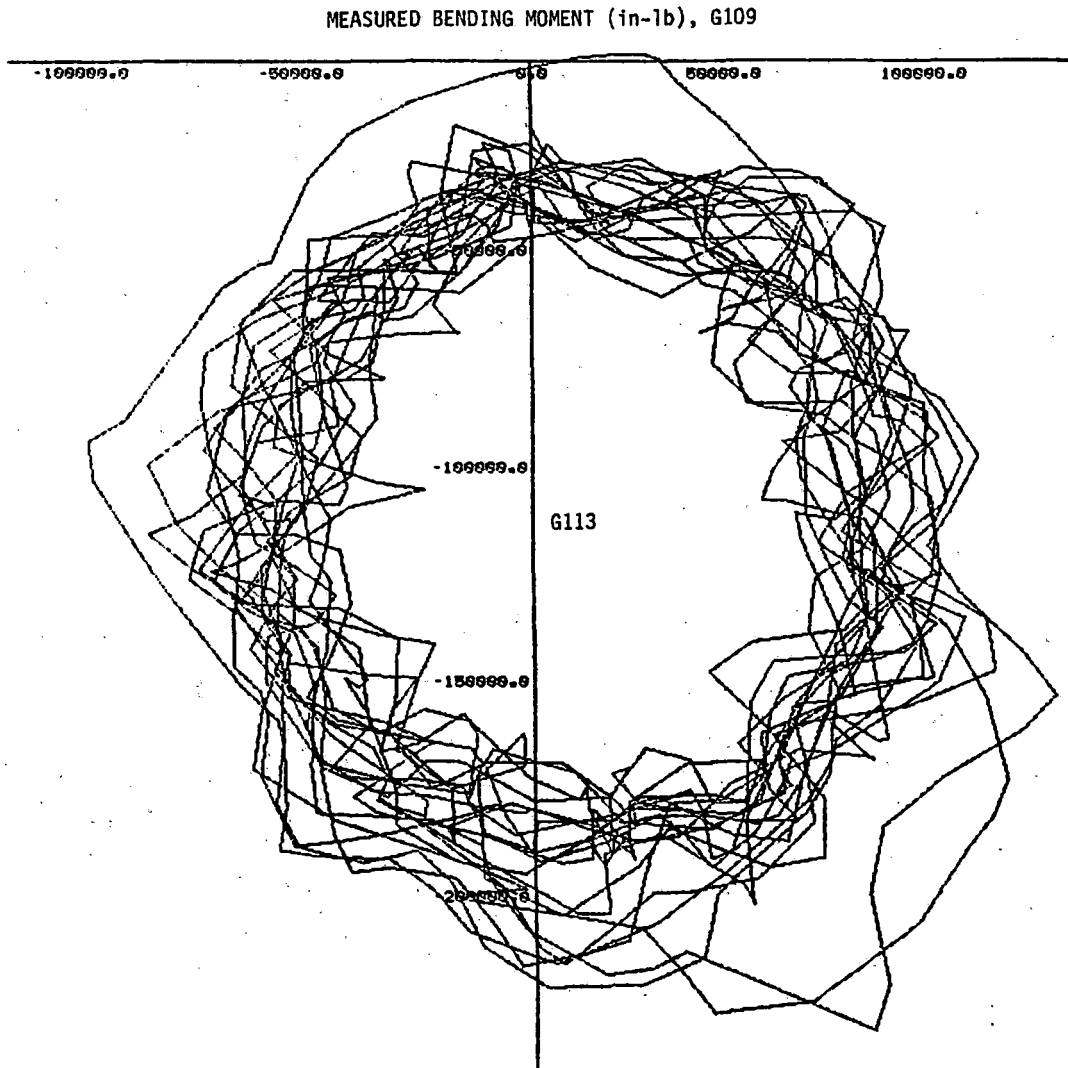


Figure 4.36 - Cross-Plot of Quadrature Pair of Axle Bending Strain Gauges (G109, G113) Filtered at 50Hz, Five Seconds Duration

MEASURED BENDING MOMENT (in-lb), G109

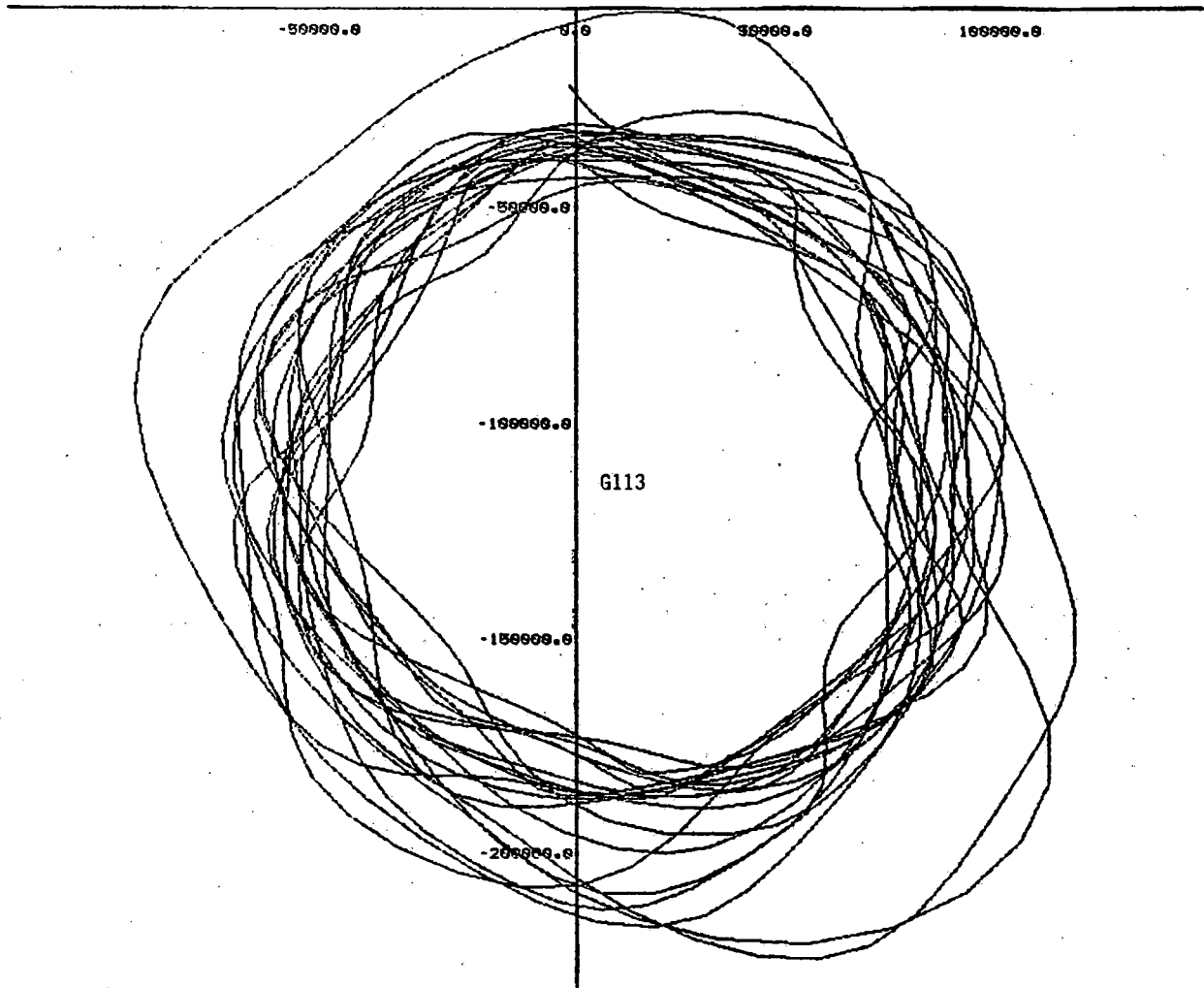


Figure 4.37 - Cross-Plot of Quadrature Pair of Axle Bending Strain Gauges (G109, G113) Filtered at 20Hz, Five Seconds Duration

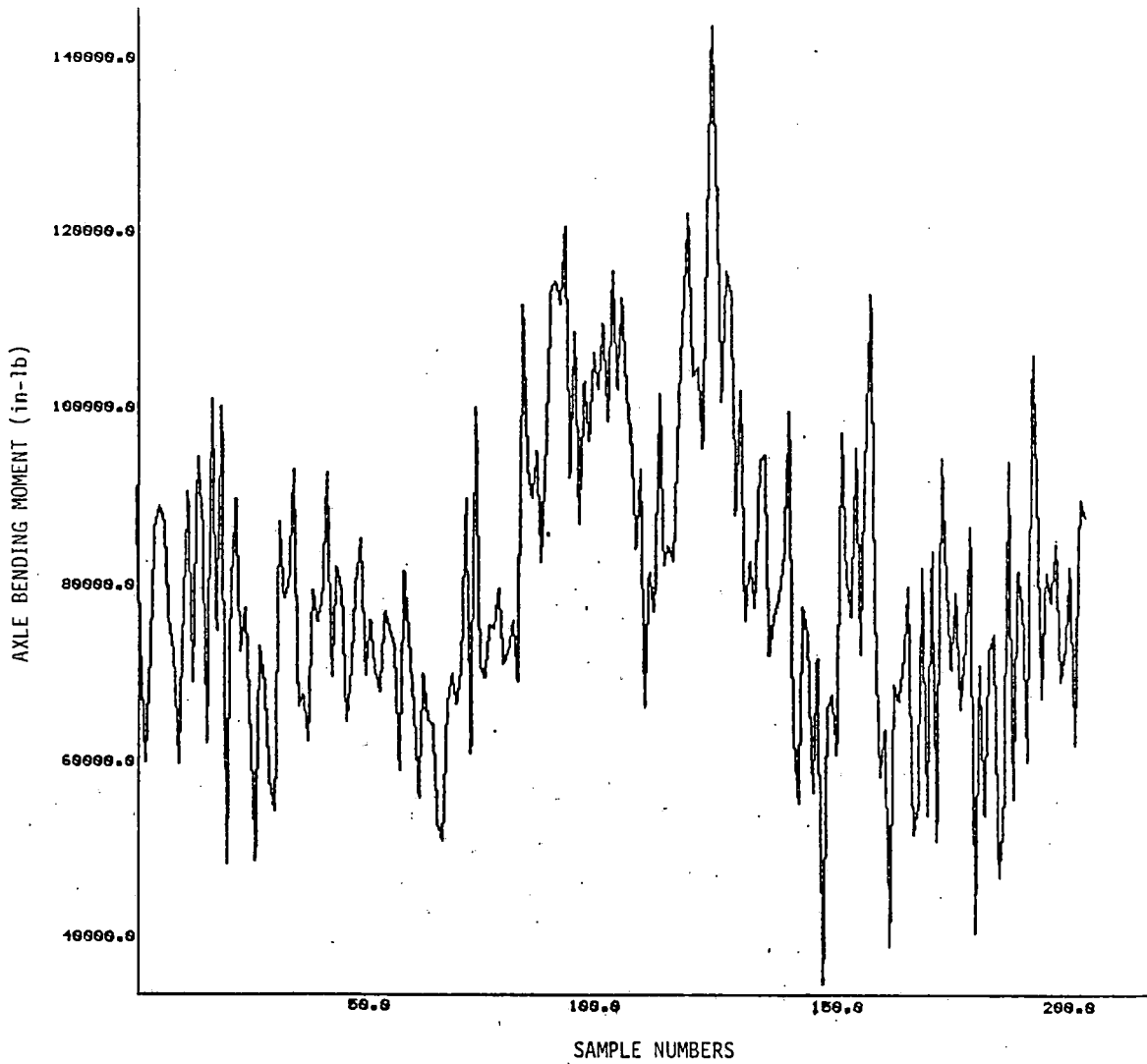


Figure 4.38 - Calculated Axle Bending Moment  
CVR1, Derived from Quadrature Pair  
G109 and G113

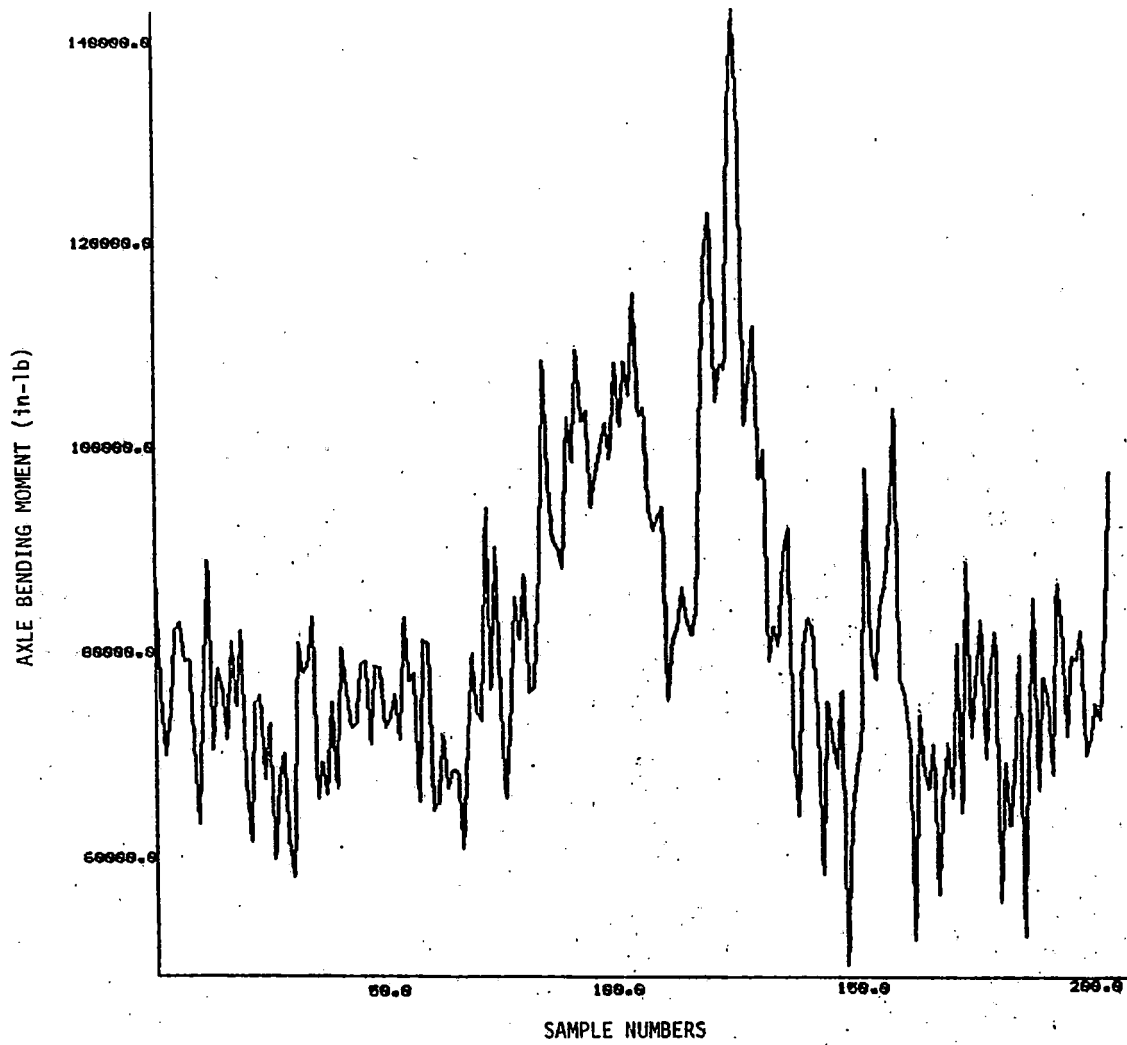


Figure 4.39 - Averaged Axle Bending Moment  
Calculation for Right Side of Front  
Axle (R1V) Unfiltered



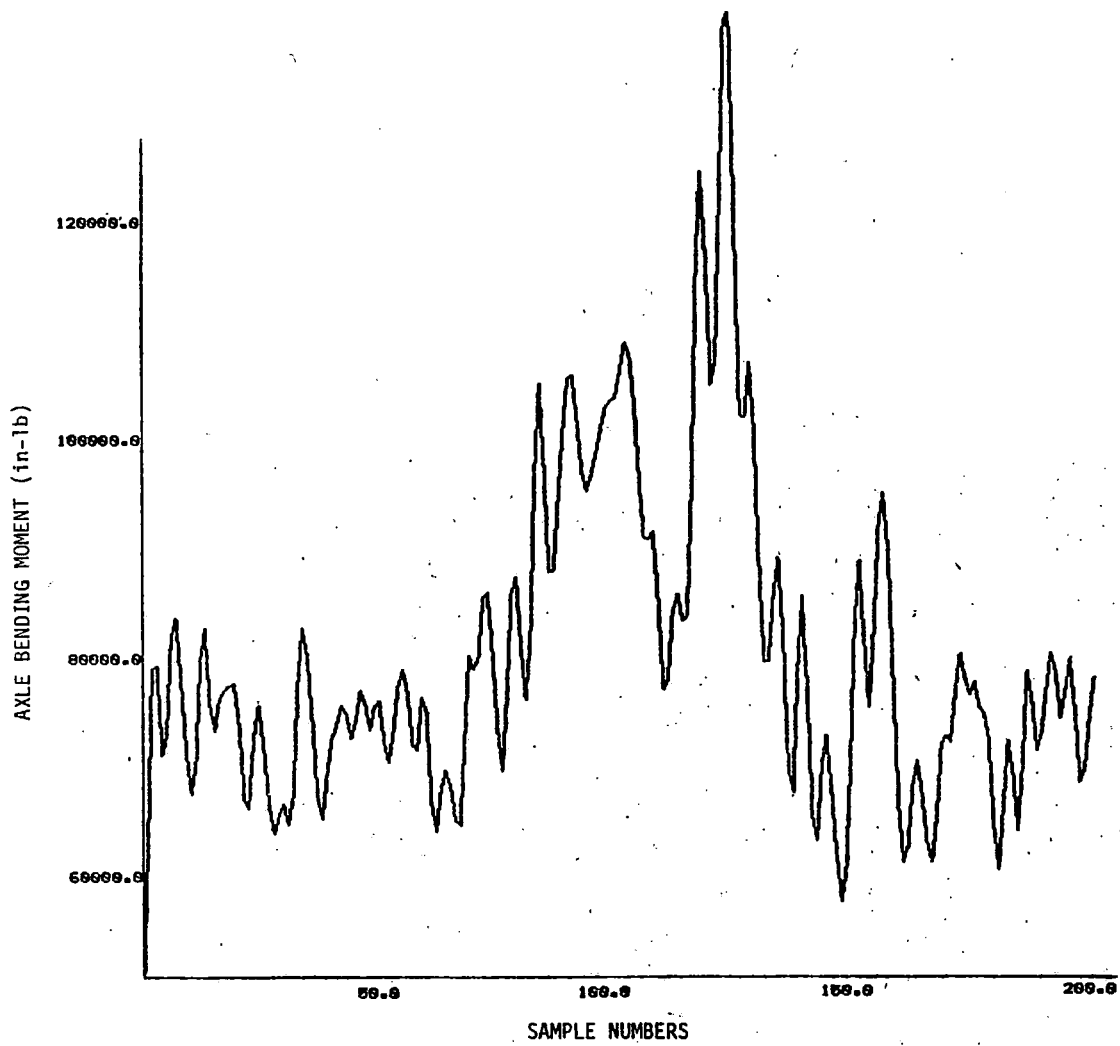


Figure 4.40 - Averaged Axle Bending Moment  
Calculation for Right Side of Front  
Axle (R1V) Using Data Filtered at  
50Hz

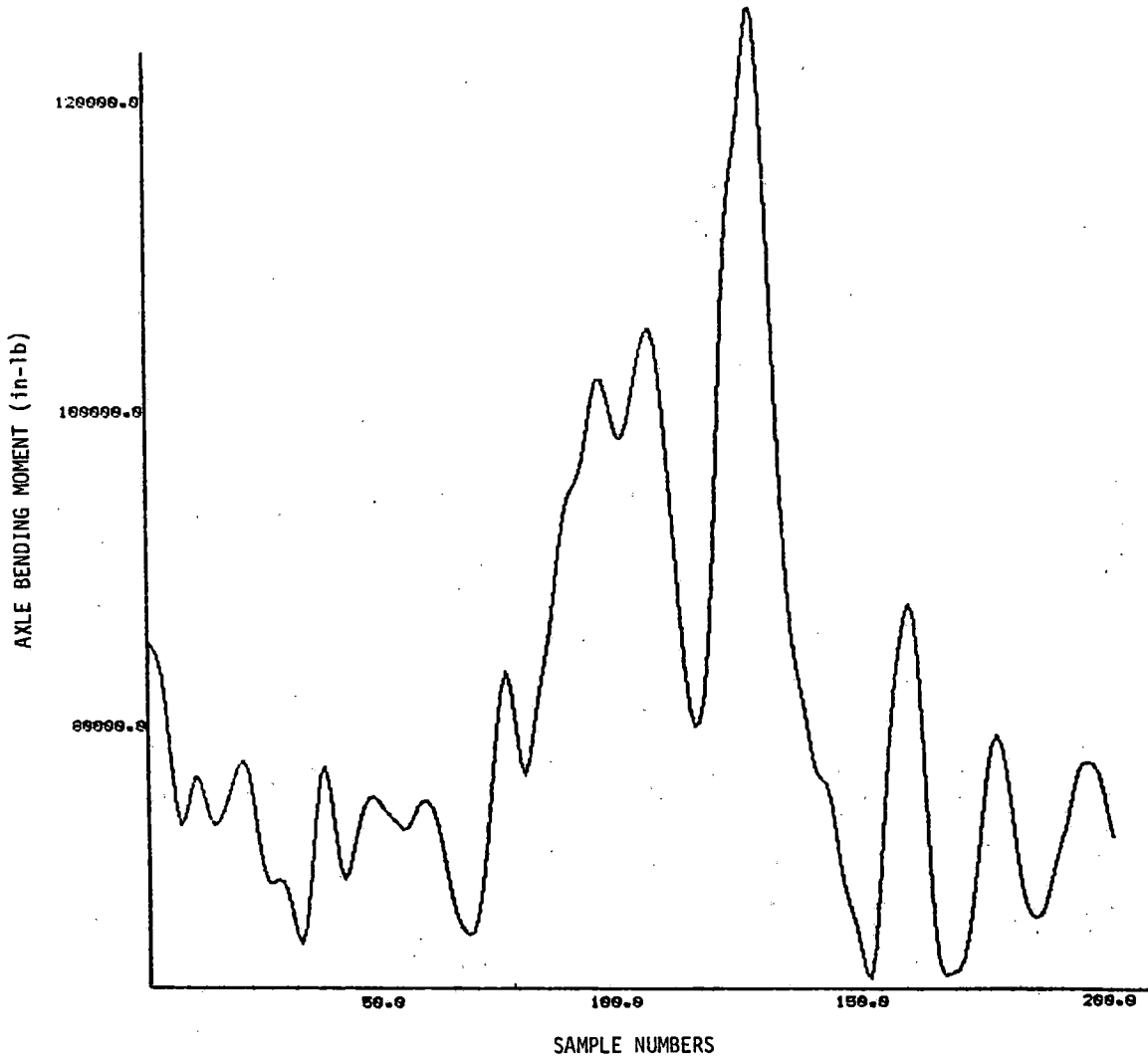


Figure 4.41 - Averaged Axle Bending Moment  
Calculation for Right Side of Front  
Axle (R1V) Using Data Filtered at  
20Hz

G214 gave readings which were only 25% to 35% as large as the readings on the other gauges at the same location in runs BS-002A and BS-010. It should be deleted from the data analysis for these runs, leaving only two quadrature pairs of gauges. Less serious scale factor errors could be compensated for by normalizing the axle bending channels by their standard deviations (analogous to the normalization by RMS which was cited in the TDOP project documentation).

#### 4.6 Bearing Adapter Forces

The vertical bearing adapter forces and their lines of action must be extracted from 12 channels of strain gauge data, four of which are used to estimate vertical force magnitudes and eight of which determine the lines of action and the appropriate calibration factors for the forces. The procedures for reducing these data, using the published calibration information, were explained in Section 3.2. Significant questions have arisen about undocumented differences between the strain gauge excitation voltages and gain factors used in the calibrations and in the vehicle tests. In the absence of positive information about these differences, it is not possible to produce definitive estimates of the magnitudes of the bearing adapter or wheel/rail contact forces.

Bearing adapter strain gauge data from tests of the Barber-Scheffel truck were reduced using the procedures of Section 3.2, assuming no differences between the calibration and test conditions. The calibrations for the DR-1 bearing adapters were used for this exercise on the basis of the statements on page 61 of the Type II Truck Test Results Report. However, some uncertainty about which set of adapters was used on the Barber-Scheffel has been expressed by some TDOP project participants, introducing further doubts into the data analysis. The calculated force levels were much higher than they should

have been (the sum of the vertical forces on the four adapters being about three times the static load on the truck) for the combination of reasons already cited. Although the magnitudes of the calculated forces are incorrect, some sample results are reviewed here to show how they can be used.

Figure 4.42 shows the calculated vertical forces on the four adapters of the instrumented truck. The substantial differences between them could be attributable to the use of the wrong set of calibrations, but the similarities and differences in the waveforms for left and right sides and front and rear axles are still of interest. The bearing adapter force is by far the largest component in the estimate of vertical wheel/rail force, as shown in Figure 4.43. Most of the difference between the bearing adapter force and wheel/rail force appears to be from the 1500 lb. added to represent half the weight of the wheelset, while the axle bending terms only appear to add some noise to the force estimate (probably because of the inadequate filtering of those channels). The estimates of lateral wheel/rail forces were more seriously distorted by the bearing adapter calibration problem, and appeared to be unrealistically high for operations on unperturbed tangent track at 26 mph. It was therefore necessary to disregard the lateral force calculations and the L/V force ratio calculations, which were based on the lateral force estimates.

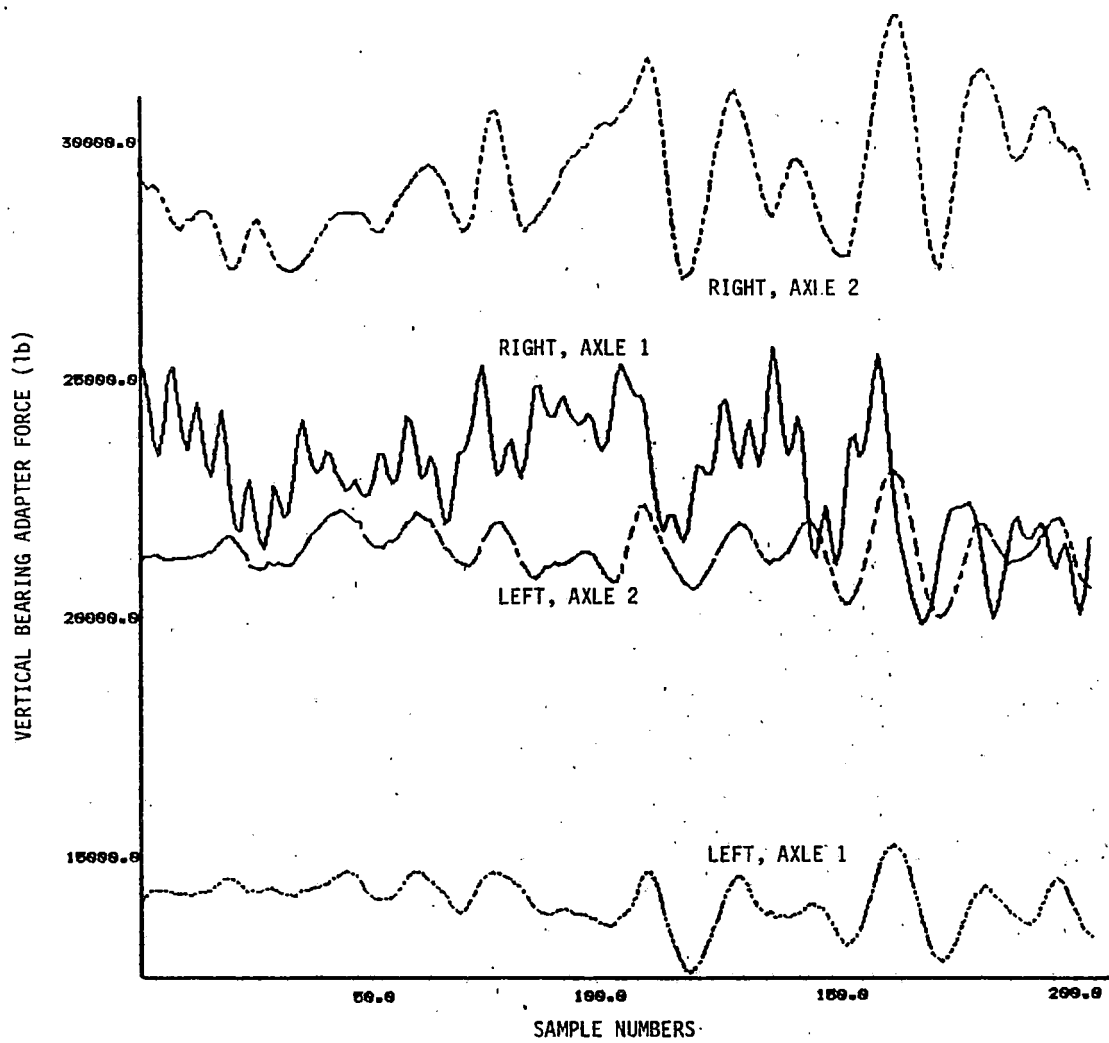


Figure 4.42 - Four Vertical Bearing Adapter Force Estimates Assuming DR-1 Adapters Used on Barber-Scheffel Truck

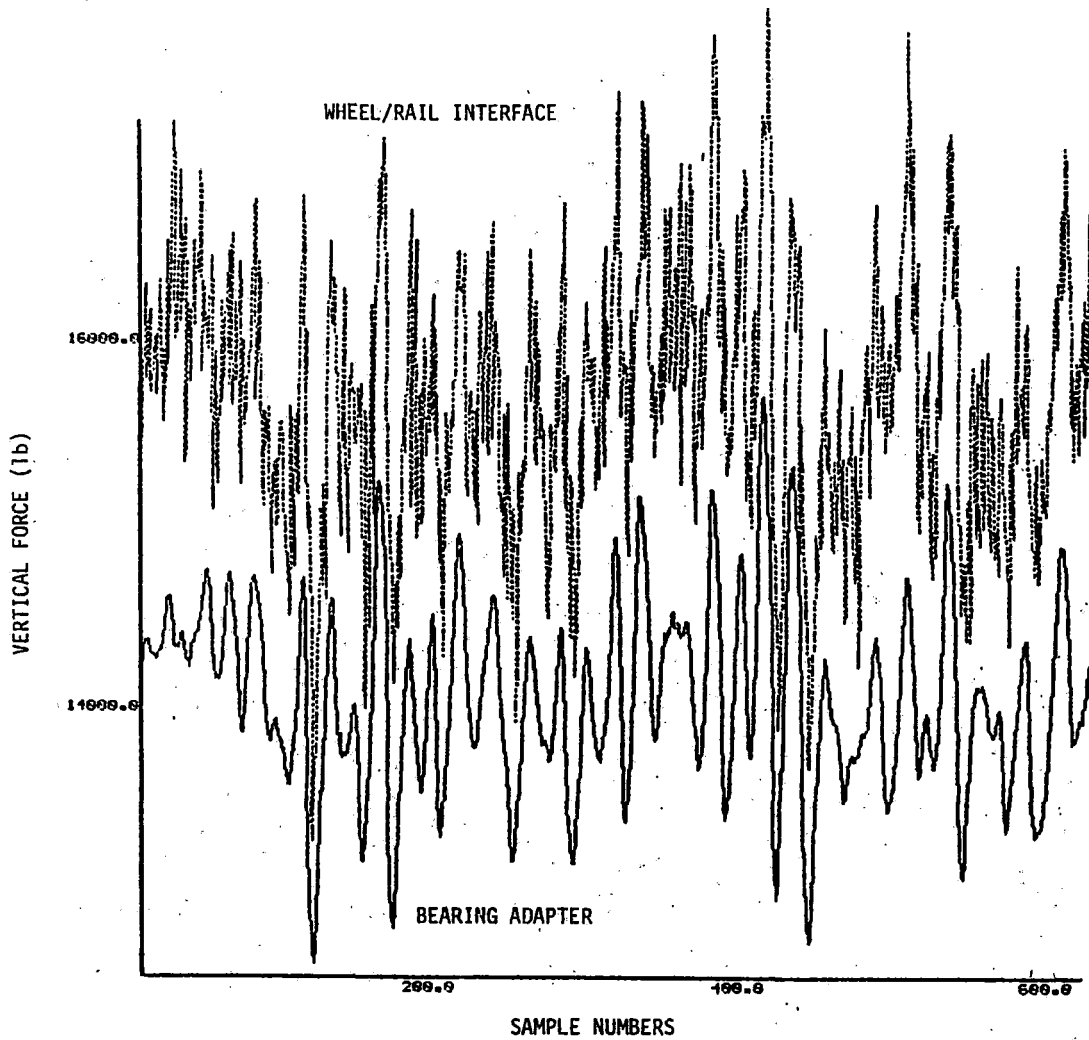


Figure 4.43 - Vertical Bearing Adapter Force and Wheel/Rail Force Estimates on Left Side of Front Axle

## 5. RECOMMENDATIONS FOR FURTHER WORK

The TDOP Phase 2 data should be useful for investigating some aspects of truck performance, but any potential user of these data needs to be aware of their limitations before investing effort in analysis and data reduction. At the same time, new test programs should be designed so as to produce data which will complement the usable data from TDOP. The test cases and measurements should be sufficiently compatible with TDOP that the results can be compared meaningfully, but they should not lead to needless duplication of conditions which were already covered effectively in TDOP.

### 5.1 Applicability of TDOP Phase 2 Data

As part of the current work, it has been necessary to review much of the TDOP Phase 2 data. This review has provided some indications of the suitability of much of these data for more widespread use. The focus has been on truck dynamics data rather than carbody or resistance data, so this review has not considered the carbody accelerometer channels or the instrumented coupler.

Each channel which is to be used should be inspected graphically before extensive data reductions are applied. Undocumented intermittent, dead and biased channels have been found on the TDOP tapes. If these problems are not identified at the outset, very misleading results will be obtained from the data reductions and the sources of error could be quite difficult to identify. The inspections of the channels should be based on a physical insight into the characteristics which should be expected on each channel and a knowledge of the characteristics of these channels on the other data tapes.

### Angle of Attack Measurements

The wheel/rail angle of attack measurements maybe of considerable use with the additional signal processing described in Section 4.1. However, until that processing procedure is implemented and tested, it is not possible to say with any certainty how useful these measurements will be for detailed evaluations of vehicle dynamic response. Straightforward application of the data reduction procedure reported in the TDOP reports leaves these measurements corrupted by irregularities of wheel rims and rail surfaces, although it still permits evidence of some rough trends in steady-state curving to show through.

### Wheel/Rail Lateral Displacements

These measurements are of course derived from the same raw data as the angle-of-attack measurements and are therefore subject to the same recommendations regarding the additional signal processing. On top of that, the available TDOP documentation does not permit the determination of the nominal, unperturbed condition measurements. However, a thorough study of the measurements obtained for steady-state operations in curves and on tangent track may permit a posteriori identification of what the nominal case was.

### Radial Truck Arm and Strut Forces

The Dresser DR-1 truck was fitted with two strain gauge bridges on its steering arm assembly, while the Barber-Scheffel had one each on a cross-arm and a cross-strut. The Barber-Scheffel gauges were never calibrated, and can therefore only be used to show approximate trends or to correlate dynamic variations with other response variables. Although the DR-1 gauges were calibrated, that calibration was derived in terms of



lateral forces imposed on a wheelset and therefore cannot reveal the level of forces or moments transmitted through the steering arm. Consequently, these measurements too can only serve to show rough trends. Detailed studies of radial truck dynamics will require more extensive instrumentation and different calibration procedures.

*What are the bearings?*

### Bearing Adapter Vertical Forces

Two different strain-gauged bearing adapters were used in the TDOP test program, one for the DR-1 and Barber-Scheffel trucks and the other for the remaining trucks. The DR-1 adapters were relatively insensitive to varying vertical loads and apparently very sensitive to the lines of action of those loads. This makes the data reduction process extremely sensitive and prone to error. Indeed, the calibrations are so internally inconsistent about line of action that these measurements cannot be interpreted with any confidence. Therefore, the wheel/rail force measurements for the Dresser truck are best ignored for all further work, and should be assumed to not exist.

The strain gauge measurements from the Type I adapter (used on most of the other trucks) must be translated into force estimates using the calibration information reported in Appendix B of the Type I Test Results report. Although these results did not have as severe a sensitivity problem as the results for the DR-1 adapter, they were still plagued by ambiguities in the line of action calibration. In other words, the combination of the inner and outer strain gauge readings on an adapter can not always reveal the line of action of the force with certainty; some combinations of these readings could represent any of several different lines of action. This ambiguity casts doubt on both the magnitudes of the bearing adapter vertical force estimates and their lines of action. These doubts are reflected in uncertainties about the magnitudes of the vertical and

especially the lateral wheel/rail forces. The results derived from these adapters should be used with caution, based on an understanding of the limitations of the original calibrations. The sensitivity of the results to the specified uncertainties should be quantified in a formal sensitivity study and the data should not be used for purposes which require finer resolution of force information.

### Axle Bending Moments

The axle bending moment measurements are difficult to evaluate because the values found on these channels of the data tapes have already had calibration factors applied (available data are in inch-pounds rather than millivolts). Because these channels were low-pass filtered at 500Hz and sampled at 200Hz, they contain aliased information from frequencies above 100Hz which cannot be eliminated. The seriousness of this aliasing cannot be readily determined because the level of the signals between 100Hz and 500Hz is not known. It is safe to assume that these signals were much lower than the major sinusoidal component of each axle bending channel (corresponding to the axle bending produced by the weight of the entire car, at the wheel rotation frequency). However, it is not clear how significant the aliasing is relative to the variations in the envelopes of the sinusoidal bending signals, which contain the information of interest for wheel/rail force estimates.

The raw axle bending channels are very noisy, probably because of the aliasing and inadequate filtering. Before they are used for calculation of wheel/rail forces they should be low-pass filtered to eliminate as much of the noise as possible without destroying the information of interest. A four-pole Butterworth filter centered at 20Hz was found to be a reasonable choice for the exploratory study reported here. Of course, heavily filtered data will not be usable for investigating

high-frequency wheel/rail force variation. The TDOP data should only be used to investigate lower frequency phenomena (up to 10Hz or at most 20Hz).

Because the wheel/rail force estimates are derived from relatively complicated combinations of the axle bending channels, it is necessary to spot check all of these channels to identify possible problems (dead channels, scale factor errors, etc.). One defective channel could seriously distort an entire set of axle bending data, but could be very difficult to identify only from the processed data.

## 5.2 Instrumentation for New Test Programs

The TDOP Phase 2 test data have yielded some important lessons about truck dynamic test instrumentation systems and test conditions. If these lessons can be applied to future truck test programs, they should make it possible to collect more useful results. The most significant difficulties were associated with the measurements of wheel/rail forces, lateral displacements and angles of attack, which curiously enough were also the sources of the most trouble for the TDOP Phase 1 data.

The combination of instrumented bearing adapters and axle bending strain gauges does not appear to be a desirable way of measuring wheel/rail vertical and lateral forces. The accuracy of this technique appears to be severely limited relative to that of modern plate instrumented wheelsets, which are recommended for use on future truck test programs. Because of the strong influence of wheel profile on vehicle dynamic response, use of instrumented wheelsets with several different profiles must be considered very seriously. This is particularly important for evaluating the influence of component wear on truck dynamics.

The fidelity of the wheel/rail lateral displacements and angle of attack measurements has not been fully established because implementation of the extensive and delicate data

reduction process which must be followed to extract this information from the raw data channels was outside the scope of the present study. Consequently, it has not yet been determined whether the existing raw data are sufficient for deriving usable estimates of lateral displacement and angle of attack. It is recommended that this data reduction process be implemented and tested before drawing further conclusions about these data or about alternate methods for measuring the same quantities.

During the evaluation of the TDOP Phase 2 data it became apparent that some additional measurements would have been very useful to supplement those which were available. It would have been very revealing to have measurements of the friction snubber forces simultaneously with all the other measurements. These forces plus the vertical spring forces (calculated from spring deflections) could serve as cross checks on the bearing adapter force estimates. Because the details of radial truck performance have not been extensively studied in the past, some more thorough instrumentation of the peculiar features of these trucks would have been highly desirable. The rotations of the Barber-Scheffel shear pad housings relative to the side frames should have been measured to give a better indication of the axle alignment. Strain gauges should have been installed at several key locations on the DR-1 steering arms to indicate the stresses present. Similarly, both cross-arms and both cross-struts should have been instrumented on the Barber-Scheffel truck. The strain gauge calibrations should have been performed in bench tests of the arms and struts alone, so that the forces in these members could be identified later under the dynamic test conditions. Calibrations based on forces applied to a complete truck cannot reveal the forces imposed on the individual truck members.

The truck calibration and test configurations should replicate normal truck operating configurations as closely as possible if they are to produce meaningful data about truck performance. Those trucks which are designed to operate with

compliant shear pads should be tested with those pads in place, and supplementary shims and other ad hoc modifications to the trucks should be avoided. These changes would modify truck dynamic performance and obscure the true dynamic characteristics of the truck designs, making the test results unrepresentative of truck performance in revenue service.

### 5.3 Additional Test Cases Needed

It would be very desirable to be able to make maximum use of the truck test data which have already been collected at considerable expense in TDOP Phase 2. The gaps in those data sets cannot be readily filled because the trucks which were tested new have now seen considerable service in the TDOP Wear Data Collection Program. Their performance would be expected to change as wear effects accumulate, and indeed a principal goal of a new test program should be to identify how wear affects truck dynamics. The only way to supplement the existing TDOP Phase 2 data for unworn trucks would be to obtain a new set of trucks and repeat some of the test cases. Indeed, it would appear to be advisable to do this for one of the Type II trucks so that at least one comparison between the new and worn trucks can be conducted on a strictly "ceteris paribus" (all else being equal) basis. The most logical candidate truck to use for this would be the Dresser DR-1, since the bearing adapter force data collected for it in TDOP Phase 2 was seriously deficient. Parallel testing of a new and a worn DR-1 truck also provides the opportunity to collect extensive data about the forces imposed on different portions of the steering arms (after an appropriate calibration).

The remaining trucks need only be tested in their worn condition to provide data which can be compared to the TDOP Phase 2 data for unworn trucks. The level of detail at which these comparisons will be valid will be constrained by the limitations of the TDOP data which have already been discussed.

The test conditions can not be identical to the TDOP test conditions unless the new test program is conducted on the same segments of track, which is not practical. Rather, it should be assumed that these tests will be conducted using the laboratory and track facilities of the Transportation Test Center (TTC) in Pueblo, Colorado. These can to some limited extent be used to replicate the TDOP test conditions, but it would not be wise to expend heroic efforts to force the new tests to conform exactly to those conducted for TDOP Phase 2. Indeed, the preliminary analyses which should be performed in support of test planning may demonstrate some distinct advantages to be gained by deviating from the TDOP test conditions.

The TDOP Phase 2 truck tests were performed in the following five test zones:

1. Mainline Class 4 track, with eleven curves of between 1.1 and 6.2 degrees, both left hand and right hand.
2. Mainline Class 4 tangent track, 5 miles long, made of bolted, jointed rail.
3. Yard track, Class 1 with 12 and 16 degree curves in 0.2 miles.
4. Spur track, Class 2 curved and tangent with substantial cross-level variations.
5. Mainline Class 4 tangent track, 4 miles long, made of continuous welded rail.

These test zones were used to conduct tests in five different test regimes:

1. Harmonic roll and bounce--conducted at speeds between 4 and 30 mph on test zone 4.
2. Curve negotiation--conducted on test zone 1 four times, three times going uphill (above, below and at balance speed) and once going downhill (at balance speed).
3. High Speed Lateral Stability--conducted at speeds between 40 and 79 mph on test zones 2 (and 5 for DR-1 and Maxiride).

4. Fuel Consumption--conducted on test zone 2 in uphill and downhill directions at speeds between 40 and 79 mph.
5. Load Equalization--conducted on test zone 3 at 10 mph forward and reverse.

The new test program should be designed to produce results which can be matched to the five test regimes listed above, even if they are not produced on test zones identical to the five used in TDOP. There are distinct advantages to using the Rail Dynamics Laboratory where possible, since it permits the experiments to be controlled more closely than they could be on track. The harmonic bounce and roll tests (test regime 1) are ideally suited for the Vibration Test Unit (VTU), which can be programmed for idealized cross-level variations or for reproduction of track geometry measured in the field (including any track geometry measurements which may be available for the TDOP test zones).

The curve negotiation tests (test regime 2) pose the most serious problem for reproduction of the TDOP test conditions at TTC, since they cannot be accurately reproduced in the RDL and the existing TTC test tracks have different curvatures and superelevations from the TDOP test zones. The Railroad Test Track (RTT) has curves of only  $0^{\circ}50'$  and the Train Dynamics Track (TDT) and Transit Test Track (TTT) only go up to curves of  $1^{\circ}30'$ . Only the FAST track, with curves of  $3^{\circ}$ ,  $4^{\circ}$  and  $5^{\circ}$  and the balloon loop at  $7^{\circ}30'$  provide substantial curvatures. Because of the heavy utilization of the FAST track for wear related experiments it is not clear whether it would be available for separate truck dynamics testing. Furthermore, its superelevations are markedly different from those of the TDOP test zone 1. Despite these considerations, the FAST track probably remains the most promising candidate among the TTC facilities for further truck curve negotiation testing.

High speed lateral stability and fuel consumption tests (test regimes 3 and 4) are well suited for the Roll Dynamics Unit

(RDU), which can provide very well controlled conditions for these tests. The load equalization tests (test regime 5) could be performed on the VTU, again making use of actual measured track geometry.

#### 5.4 Conclusion

The TDOP Phase 2 test data provide some usable information about freight truck dynamic response. These data must be interpreted very cautiously because of some substantial limitations of the instrumentation and ambiguities in the documentation. The numbers found on the TDOP data tapes cannot be taken at face value, but must be scrutinized carefully to test their physical reasonableness.

The TDOP data can, within certain important limitations, be used to define baseline performance of unworn trucks for later comparison with testing of worn trucks. These limitations specifically refer to the fidelity of the wheel/rail force, displacement and angle of attack data, which may not be adequate for some applications. A new test program for worn trucks can be designed to produce results suitable for comparison with the baseline performance measured in TDOP Phase 2.



APPENDIX

Listing of Data Reduction Programs

This version of the data reduction programs uses the DR-1 bearing adapter calibrations for the DR-1 truck and the Type I adapter for the Barber-Scheffel and Type I trucks. Minor modifications would switch the Barber-Scheffel to the DR-1 adapter calibrations.

*Which one? see P. 87*

```

100 SUBROUTINE REDEQ (IERR)
200 *****
300 REDUCTION EQUATIONS.
400 *****
405 IANS=1-4
410
415 IANT=1-3
420 IANU=1-2
500 *****
600
700 REVISIONS:
800 6-17-82 JJ INITIAL ENTRY
900 *****
1000 C
1100 C
1200 C
1300 C
1400 C
1405 REAL*8 PMIN, PMAX, PMEAN, PMSQ, PRMS, PVAR, PSTD
1410 REAL*8 XMP, XM101, XM102, XM103, XM105, XM106, XM107,
1428 XM109, XM111, XM112, XM113, XM115, XM116,
1446 XM201, XM204, XM205, XM208, XM209, XM210,
1464 XM212, XM213, XM214, XM216
1482 C
1500 REAL*4 LRS1, LWS1, LWR1, LRS2, LWS2, LWR2, LIV, L2V
1600 C
1700 COMMON / SETDAT / ISCHAN(128), JCHAN(128), ICHAN(2,128),
1800 UCHAN(2,128),
1900 XSTART, XSTOP, NAVS, NCHAN
2000 COMMON / SETVAL / JSTART, KSTART, JSTOP, KSTOP,
2100 MMILEP, NMILEP, FMILP
2200 COMMON / LUNS / LUNMSG, LUNNAM, LUNOUT, LUNIN, LUNSCR
2300 C
2400 C
2500 ... COMMONS NEEDED FOR DATA REDUCTION EQUATIONS ...
2600 COMMON / STATS / PMIN(128), PMAX(128),
2700 XMP(46), XM101, XM102, XM103, XM105, XM106, XM107,
2800 XM109,
2900 XM111, XM112, XM113, XM115, XM116,
3000 XM201, XM204, XM205, XM208, XM209, XM210, XM212, XM213,
3100 XM214, XM216,
3200 PMSQ(128), PRMS(128), PVAR(128), PSTD(128)
3300 C
3400 COMMON / OUTDISP / LRS1, LWS1, LWR1, LRS2, LWS2, LWR2,
3500 ARS1, AWS1, AWR1, ARS2, AWS2, AWR2,
3600 XNG1, XNG2, VLSP, VRSP, FSA1, FSA2, SWIV
3700 COMMON / OUTVER / VLA1, VLA2, VLA3, VLA4,
3800 BMA1, BMA2, BMA3, BMA4, AVR1, BVR1, CVR1, RIV,
3900 LIV, R2V, L2V,
4000 FVR1, FVL1, FVR2, FVL2, FLR1, FLL1, FLR2, FLL2,
4100 GUR1, GUL1, GUR2, GUL2, FL1, FL2, FVNT, FLNT,
4200 QLFT, QRG1, FLLT, FNL1, FNL2
4300 C
4400 COMMON / INPSEL / S1, A9, A10, A11, A12, A13, A14, A17,
4500 F1, F11, F12, F2, F21, F22,
4600 F3, F31, F32, F4, F41, F42,
4700 P1, P2, P3, P4, P5, P6, P7, P8,
4800 B1, B2,
4900 D1, D2, D3, D4,
5000 D5, D6, D7, D8, D9, D10,
5100 D13, D14,
D19, D20, D21, D22,

```

```

5200      *          G101, G102, G103, G105, G106, G107, G109,
5300      *          G111, G112, G113, G115, G116,
5400      *          G201, G204, G205,
5500      *          G208, G209, G210,
5600      *          G212, G213, G214, G216
5700      C
5800      C
5900      COMMON / REDCON / IANS, IANT, IANU
6000      COMMON / REDSTAT / LRED, NDISP, NVERT, NSEL, LUN2, LUN3
6100      COMMON / ASCLAB / IADIS(19), IAVER(36), IA(3)
6200      C
6300      DIMENSION PMEAN(128)
6400      EQUIVALENCE (PMEAN(1), XMP(1))
6500      C
6505      DIMENSION XINP(46)
6510      EQUIVALENCE( XINP(1), S1)
6515      C
6600      C*****
6700      C
6800      LRED=. TRUE.
6900      IERR=0
7000      C
7100      C          ... BARBER-SCHEFFEL TYPE TRUCK
7200      IF(IANT.EQ.2) GOTO 10
7205      XKVS=27500.
7206      XC3=2.491
7207      GOTO 15
7300      C          ... DR-1 TYPE TRUCK
7400      10      XKVS=25900.
7405      XC3=2.117
7410      C
7500      C
7600      C*****
7700      C
7705      C          ... REMOVE BIAS FROM THE FOLLOWING CHANNELS :
7710      C          A9-A14; D5-D10. THIS CODE IS
7715      C          ... VERY ORDER DEPENDENT ON THE INPSEL COMMON
7720      C
7725      15      DO 20 I=2,7
7730      XINP(I)=XINP(I)-XMP(I)
7735      XINP(I+33)=XINP(I+33)-XMP(I+33)
7750      20      CONTINUE
7755      C
7800      IF(IANS.EQ.2) GOTO 500
7900      C
8000      C          ... NEED TO CALCULATE THE FOLLOWING VARIABLES
8100      C          ... ACCORDING TO THE CAR TYPE AND LOAD:
8200      C          ... VLA1, VLA2, VLA3, VLA4, BMA1, BMA2, BMA3, BMA4
8300      C          ... THIS IS COMPUTED BY INTRPOLATIONS BASED
8400      C          ... ON THE "F" VALUES.
8500      C
8600      CALL TABLE(IERR)
8700      IF(IERR.NE.0) GOTO 950
8800      C
8900      C*****
9000      C          *
9100      C          V E R T I C A L      F O R C E S          *
9200      C          *
9300      C*****
9400      C
9500      C

```

```

9600 C          ... AXLEBENDING CALCULATIONS...
9700 C
9800     AVR1=(((G116-XM116)**2) + ((G112-XM112)**2))**.5
9900     BVR1=(((G115-XM115)**2) + ((G111-XM111)**2))**.5
10000    CVR1=(((G113-XM113)**2) + ((G109-XM109)**2))**.5
10100    R1V=(AVR1+BVR1+CVR1)/3.
10200 C
10300     AVL1=(((G101-XM101)**2) + ((G105-XM105)**2))**.5
10400     BVL1=(((G102-XM102)**2) + ((G106-XM106)**2))**.5
10500     CVL1=(((G103-XM103)**2) + ((G107-XM107)**2))**.5
10600     L1V=(AVL1+BVL1+CVL1)/3.
10700 C
10800     AVR2=(((G201-XM201)**2) + ((G205-XM205)**2))**.5
10900     BVR2=(((G204-XM204)**2) + ((G208-XM208)**2))**.5
11000     R2V=(AVR2+BVR2)/2.
11100 C
11200     AVL2=(((G209-XM209)**2) + ((G213-XM213)**2))**.5
11300     BVL2=(((G210-XM210)**2) + ((G214-XM214)**2))**.5
11400     CVL2=(((G212-XM212)**2) + ((G216-XM216)**2))**.5
11500     L2V=(AVL2+BVL2+CVL2)/3.
11600 C
11700 C          ... VERTICAL FORCES AT WHEEL/RAIL INTERFACE...
11800 C
11900     FVR1=1500. +(R1V-L1V)/30. +VLA1
12000     FVL1=1500. - ((R1V-L1V)/30.) + VLA2
12100     FVR2=1500. + ((R2V-L2V)/30.) + VLA3
12200     FVL2=1500. - ((R2V-L2V)/30.) + VLA4
12300 C
12400 C          ... LATERAL FORCES AT WHEEL/RAIL INTERFACE...
12500 C
12600     FLR1=156.45 - (.05556*(BMA1-L1V)) + (.081944*(R1V-L1V))
12700     FLL1=156.45 - (.05556*(BMA2-R1V)) - (.081944*(R1V-L1V))
12800     FLR2=156.45 - (.05556*(BMA3-L2V)) + (.081944*(R2V-L2V))
12900     FLL2=156.45 - (.05556*(BMA4-R2V)) - (.081944*(R2V-L2V))
13000 C
13100 C          ... LATERAL/VERTICAL FORCE RATIOS ON INDIVIDUAL WHEELS.
13200 C
13300     QUR1=FLR1/FVR1
13400     QUL1=FLL1/FVL1
13500     QUR2=FLR2/FVR2
13600     QUL2=FLL2/FVL2
13700 C
13800 C          ... WHEELSET NET LATERAL FORCES...
13900 C
14000     FL1=FLR1-FLL1
14100     FL2=FLR2-FLL2
14200 C
14300 C          ... TRUCK NET VERTICAL FORCE...
14400 C
14500     FVNT=FVR1+FVL1+FVR2+FVL2
14600 C          ... TRUCK NET LATERAL FORCE...
14700     FLNT=FLR1+FLR2-FLL1-FLL2
14800 C
14900 C          ... TRUCK SIDE L/V RATIO...
15000 C
15100     QLFT=(FLL1+FLL2)/(FVL1+FVL2)
15200     QRGT=(FLR1+FLR2)/(FVR1+FVR2)
15300 C
15905 C
15915 C          ... ADDED THESE EQUATIONS IN PLACE OF VSBA, VSWR, VSDF
15916 C          ... FLLT TESTS VALIDITY OF EQUATION FOR FLL1

```

```

15920 C
15925 FLLT=0.0556*(44.25*FVL1 - 63560. - VLA1*(ARM1+44.25))
15926 C
15927 C ... EQUATIONS FOR LATERAL FORCES ON BEARING
15928 C ... ADAPTERS. (NET PER WHEEL SET)
15929 C
15930 FNL1=0.0437*(-1.95*(R1V-L1V)-BMA1+BMA2)
15935 FNL2=0.0437*(-1.95*(R2V-L2V)-BMA3+BMA4)
15940 C
16000 C
16005 C
16100 C
16200 C*****
16300 C
16400 C W H E E L / R A I L D I S P L A C E M E N T *
16500 C
16600 C*****
16700 C
16800 500 CONTINUE
16900 IF(IANS.LT.2) GOTO 1000
17000 C
17100 C ... LATERAL TO WHEEL/RAIL CALCULATIONS...
17200 C
17300 LRS1=.5*(P2+P4)
17400 LWS1=.5*(P1+P3)
17500 LWR1=LWS1-LRS1
17600 LRS2=.5*(P6+P8)
17700 LWS2=.5*(P5+P7)
17800 LWR2=LWS2-LRS2
17900 C
18000 C ... ANGLE TO RAIL/WHEEL CALCULATIONS...
18100 C
18200 ARS1=126.17*(P2-P4)
18300 AWS1=171.9*(P1-P3)
18400 AWR1=AWS1-ARS1
18500 ARS2=126.17*(P6-P8)
18600 AWS2=171.9*(P5-P7)
18700 AWR2=AWS2-ARS2
18800 C
18900 C ... AXLE RELATIVE ANGLES (POSITIVE FOR RIGHT CURVE)
19000 C
19100 XNG1=AWR1-AWR2
19200 C ... ANGLE LONGITUDINAL DISPLACEMENT...
19300 XNG2=(D21+D22-D19-D20)*3438./79.
19400 C
19500 C ... SPRING GROUP VERTICAL DISPLACEMENTS TO ESTIMATE
19600 C ... DYNAMIC VERTICAL FORCES
19700 C
19800 C ... LEFT
19900 VLSP=(D3+D4)*XKVS/2.
20000 C ... RIGHT
20100 VRSP=(D1+D2)*XKVS/2.
20200 C
20202 C ... TRUCK SWIVEL TO IDENTIFY CURVED TRACK
20205 SWIV=XC3*(D13-D14)
20300 GOTO 1000
20400 C
20500 C*****
20600 C
20700 950 WRITE(LUNMSG,*) (' ERROR FROM REDEQ ROUTINE. ')
20800 IERR=1

```

```
20900          GOTO 1000
21000          C
21100          C*****
21200          C
21300          1000   CONTINUE
21400          RETURN
21500          END
```

```

10      SUBROUTINE TABLE (IERR)
20      C*****
30      C      REDUCTION EQUATIONS.
40      C      OUTPUT: VLA1-4, BMA1-4
50      C*****
60      C      IANS=1-4      VERT. FORCE, DISPLACEMENT, BOTH,
70      C      STATISTICS ONLY
80      C      IANT=1-3      BARBER-SCHEFFEL, DR-1, TRUCK TYPE1*
90      C      IANU=1-2      LOADED TRUCK OR EMPTY
100     C*****
110     C
120     C      REVISIONS:
130     C      6-17-82 JJ      INITIAL ENTRY
140     C*****
150     C
160     C      D I M E N S I O N S / C O M M O N S
170     C
180     C*****
190     C
200     REAL*8 PMIN, PMAX, PMEAN, PMSG, PRMS, PVAR, PSTD
210     REAL*8 XMP, XM101, XM102, XM103, XM105, XM106, XM107,
220     *      XM109, XM111, XM112, XM113, XM115, XM116,
230     *      XM201, XM204, XM205, XM208, XM209, XM210,
240     *      XM212, XM213, XM214, XM216
250     C
260     REAL*4 LRS1, LWS1, LWR1, LRS2, LWS2, LWR2, L1V, L2V
270     C
280     COMMON / SETDAT / ISCHAN(128), JCHAN(128), ICHAN(2,128),
290     *      UCHAN(2,128),
300     *      XSTART, XSTOP, NAVE, NCHAN
310     COMMON / SETVAL / JSTART, KSTART, JSTOP, KSTOP,
320     *      MMILEP, NMILEP, FMILP
330     COMMON / LUNS / LUNMSG, LUNNAM, LUNOUT, LUNIN, LUNSCR
340     C
350     C      ... COMMONS NEEDED FOR DATA REDUCTION EQUATIONS ...
360     COMMON / STATS / PMIN(128), PMAX(128),
370     *      XMP(46), XM101, XM102, XM103, XM105, XM106, XM107,
380     *      XM109,
390     *      XM111, XM112, XM113, XM115, XM116,
400     *      XM201, XM204, XM205, XM208, XM209, XM210, XM212, XM213,
410     *      XM214, XM216,
420     *      PMSG(128), PRMS(128), PVAR(128), PSTD(128)
430     C
440     COMMON / OUTDISP / LRS1, LWS1, LWR1, LRS2, LWS2, LWR2,
450     *      ARS1, AWS1, AWR1, ARS2, AWS2, AWR2,
460     *      XNG1, XNG2, VLSP, VRSP, FSA1, FSA2, SWIV
470     COMMON / OUTVER / VLA1, VLA2, VLA3, VLA4,
480     *      BMA1, BMA2, BMA3, BMA4, AVR1, BVR1, CVR1, R1V,
490     *      L1V, R2V, L2V,
500     *      FVR1, FVL1, FVR2, FVL2, FLR1, FLL1, FLR2, FLL2,
510     *      QUR1, QUL1, QUR2, QUL2, FL1, FL2, FVNT, FLNT,
520     *      QLFT, QRGT, VSBA, VSWR, VSDF
530     C
540     COMMON / INPSEL / S1, A9, A10, A11, A12, A13, A14, A17,
550     *      F1, F11, F12, F2, F21, F22,
560     *      F3, F31, F32, F4, F41, F42,
570     *      P1, P2, P3, P4, P5, P6, P7, P8,
580     *      B1, B2,
590     *      D1, D2, D3, D4,
600     *      D5, D6, D7, D8, D9, D10,
610     *      D13, D14,

```

```

620          *          D19, D20, D21, D22 ,
630          *          G101, G102, G103, G105, G106, G107, G109,
640          *          G111, G112, G113, G115, G116,
650          *          G201, G204, G205,
660          *          G208, G209, G210,
670          *          G212, G213, G214, G216
680          C
690          C
700          COMMON / REDCON / IANS, IANT, IANU
710          COMMON / REDSTAT / LRED, NDISP, NVERT, NSEL, LUN2, LUN3
720          COMMON / ASCLAB / IADIS(19), IAVR(36), IA(3)
730          C
740          DIMENSION PMEAN(128)
750          EQUIVALENCE (PMEAN(1), XMP(1))
760          C
770          DATA IPBL2 /0/
780          DATA IPBR1 /0/
790          DATA IPBR2 /0/
800          C
810          C*****
820          C
830          ARMN=10.
840          IF((IANT.LT.1).OR.(IANT.GT.3)) GOTD 9950
850          GOTD (900,100,900) IANT
860          C
870          IF(IANU.NE.2) GOTD 500
880          C
890          C*****
900          C
910          C   D R E S S E R   D R - 1   E M P T Y   T R U C K
920          C
930          C*****
940          C
950          C
960          C
970          VLA1=20000.*F1
980          ARMI=ARMN
990          BMA1=VLA1*ARM1
1000          C
1010          C*****
1020          C
1030          C
1040          C
1050          C
1060          IF((F32/F31).LE.-1.0) GOTD 200
1070          IF((-F31.LT.F32).AND.(F32.LE.-0.4*F31)) GOTD 220
1080          IF((-0.4*F31.LT.F32).AND.(F32.LE.-0.1*F31)) GOTD 240
1090          IF(ABS(F32).LT.(0.1*ABS(F31))) GOTD 260
1100          IF(F32/F31.GT.0.0) GOTD 260
1110          C
1120          IF(IPBL2.EQ.0) GOTD 9950
1130          GOTD (200,220,240,260,9950) IPBL2
1140          C
1150          C
1160          C
1170          C
1180          C
1190          C
1200          C
1210          C
1220          C
220          DEL=(F32+(0.4*F31)) / (-0.6*F31)
          VLA3=(DEL*20000. + (1.0-DEL)*25000.)*F3

```



```

1230 ARM3=ARMN-1+DEL
1240 IPBL2=2
1250 GOTD 280
1260
1270 C
1280 DEL=(F32+(0.1*F31)) / (-0.3*F31)
1290 VLA3=(DEL*25000.+(1.0-DEL)*16600.)*F3
1300 ARM3=ARMN-2+DEL
1310 IPBL2=3
1320 GOTD 280
1330 C
1340 VLA3=25000.*F3
1350 ARM3=ARMN+1
1360 IPBL2=4
1370 GOTD 280
1380 C
1390 BMA3=ARM3*VLA3
1400 GOTD 300
1410 C
1420 C*****
1430 C
1440 C
1450 C
1460 C
1470 IF(F22.LE.(0.5*F21)) GOTD 310
1480 IF((0.5*F21).LT.F22).AND.(F22.LE.F21)) GOTD 320
1490 IF((F21.LT.F22).AND.(F22.LE.(1.4*F21))) GOTD 330
1500 IF(((1.4*F21).LT.F22).AND.(F22.LE.(2.0*F21))) GOTD 340
1510 IF(((2.0*F21).LT.F22).AND.(F22.LE.(2.4*F21))) GOTD 350
1520 IF(F22.GT.(2.4*F21)) GOTD 360
1530 C
1540 IF(IPBR1.LT.1) GOTD 9950
1550 GOTD (310,320,330,340,350,360,9950) IPBR1
1560 GOTD 9950
1570 C
1580 C
1590 C
1600 IPBR1=1
1610 VLA2=11100.*F2
1620 ARM2=ARMN-2
1630 GOTD 380
1640 C
1650 IPBR1=2
1660 DEL=(F22-F21) / (0.5*F21)
1670 VLA2=(DEL*11100.+(1.0-DEL)*9100.)*F2
1680 ARM2=ARMN-1-DEL
1690 GOTD 380
1700 C
1710 IPBR1=3
1720 DEL=(F22-(1.4*F21)) / (-0.4*F21)
1730 VLA2=(DEL*9100.+(1.0-DEL)*6700.)*F2
1740 ARM2=ARMN-DEL
1750 GOTD 380
1760 C
1770 IPBR1=4
1780 DEL=(F22-(2.0*F21)) / (-0.6*F21)
1790 VLA2=F2*6700.
1800 ARM2=ARMN+1-DEL
1810 GOTD 380
1820 C
1830 IPBR1=5
      DEL=(F22-(2.4*F21)) / (-0.4*F21)
      VLA2=6700.*F2

```

... ADAPTER BR-1

FELL THRU. IF POSSIBLE INTERPOLATE AS FOR PREVIOUS PASS

```

1840 ARM2=ARMN+2-DEL
1850 GOTD 380
1860 C
1870 360 IPBR1=6
1880 VLA2=6700.*F2
1890 ARM2=ARMN+2
1900 GOTD 380
1910 C
1920 380 BMA2=VLA2*ARM2
1930 GOTD 400
1940 C
1950 C*****
1960 C
1970 C ADAPTER BR-2
1980 C
1990 400 IF(F42.LT.(0.05*F41)) GOTD 410
2000 IF((0.05*F41).LE.F42).AND.(F42.LT.(0.5*F41))) GOTD 420
2010 IF((0.5*F41).LE.F42).AND.(F42.LE.(1.67*F41))) GOTD 430
2020 IF(F42.GT.(1.67*F41)) GOTD 440
2030 C
2040 FELL THRU. TRY TO USE SAME EQUATIONS AS LAST PASS
2050 IF(IPBR2.LT.1) GOTD 9950
2060 GOTD (410,420,430,440,9950) IPBR2
2070 C
2080 410 IPBR2=1
2090 VLA4=25000.*F4
2100 ARM4=ARMN-2
2110 GOTD 480
2120 C
2130 420 IPBR2=2
2140 DEL=(F42-(0.5*F41)) / (-0.45*F41)
2150 VLA4=(25000.*DEL+(1.0-DEL)*14300.)*F4
2160 ARM4=ARMN-2+DEL
2170 GOTD 480
2180 C
2190 430 IPBR2=3
2200 DEL=(F42-(1.67*F41)) / (-1.17*F41)
2210 VLA4=(14300.*DEL + (1.0-DEL)*12500.)*F4
2220 ARM4=ARMN+DEL-1
2230 GOTD 480
2240 C
2250 440 IPBR2=4
2260 VLA4=20000.*F4
2270 ARM4=ARMN
2280 GOTD 480
2290 C
2300 480 BMA4=VLA4*ARM4
2310 GOTD 10000
2320 C
2330 C*****
2340 C
2350 C D R E S S E R D R - 1 L O A D E D T R U C K *
2360 C *
2370 C *****
2380 C
2390 C ADAPTER BL-1
2400 C
2410 500 IF((F11.GE.2.14*F12-0.971).AND.(F11.GT.0.45*F12)) GOTD 510
2420 IF((2.14*F12-.971.GT.F11).AND.(F11.GE.1.25*F12-0.525)) GOTD 520
2430 IF((1.25*F12-.525.GT.F11).AND.(F11.GE.0.741*F12-0.196)) GOTD 530
2440 IF((0.741*F12-0.196.GT.F11).AND.(F11.GE.0.286*F12)) GOTD 540

```

```

2450      IF(F11.LT.0.286*F12) GOTO 550
2460 C      ...FELL THRU. IF POSSIBLE, INTERPOLATE AS FOR PREVIOUS PASS
2470      IF(IPBL1.EQ.0) GOTO 9950
2480      GOTO (510,520,530,540,550) IPBL1
2490      GOTO 9950
2500 C
2510 C
2520 510    VLA1=15625.*F1+7810.
2530      ARM1=ARMN-2.
2540      IPBL1=1
2550      GOTO 560
2560 C
2570 520    CALL TWODIM(2.14, -.971, 1.25, -.525, F12, F11, DEL)
2580      VLA1=(DEL*(15625.*F1 + 7810.)) +
2590 *      ((1.-DEL)*(11500.*F1 + 5750.))
2600      ARM1=ARMN - 1. - DEL
2610      IPBL1=2
2620      GOTO 560
2630 C
2640 530    CALL TWODIM( 1.25, -.525, .741, -.196, F12, F11, DEL)
2650      VLA1=(DEL*(11500.*F1+5750.)) +
2660 *      ((1.-DEL)*(9710.*F1+4850.))
2670      ARM1=ARMN-DEL
2680      IPBL1=3
2690      GOTO 560
2700 C
2710 540    CALL TWODIM( .741, -.196, .286, 0.0, F12, F11, DEL )
2720      VLA1=(DEL*(9710.*F1+4850.)) +
2730 *      ((1.-DEL)*(12990.*F1+3900.))
2740      ARM1=ARMN+1.-DEL
2750      IPBL1=4
2760      GOTO 560
2770 C
2780 550    VLA1=12990.*F1+3900.
2790      ARM1=ARMN+1.
2800      IPBL1=5
2810      GOTO 560
2820 C
2830 560    BMA1=VLA1*ARM1
2840      GOTO 600
2850 C
2860 C*****
2870 C
2880 C      ... ADAPTER BR-1
2890 C
2900 600    IF(F21.GE.3.3*F22+0.69) GOTO 610
2910      IF((3.3*F22+0.69.GT.F21).AND.(F21.GE.1.37*F22+0.311)) GOTO 620
2920      IF((1.37*F22+.311.GT.F21).AND.(F21.GE.0.625*F22+.0625)) GOTO 630
2930      IF((.625*F22+.0625.GT.F21).AND.(F21.GE.0.36*F22-.136)) GOTO 640
2940      IF((0.36*F22-0.136.GT.F21).AND.(F21.GE.0.25*F22-0.2)) GOTO 650
2950      IF(0.25*F22-0.2.GT.F21) GOTO 655
2960 C      ...FELL THRU. IF POSSIBLE INTERPOLATE AS PREVIOUS PASS
2970      IF(IPBR1.EQ.0) GOTO 9950
2980      GOTO (610,620,630,640,650,655) IPBR1
2990      GOTO 9950
3000 C
3010 C
3020 610    VLA2=20000.*F2-10000.
3030      ARM2=ARMN-2.
3040      IPBR1=1
3050      GOTO 660

```

```

3060 C
3070 620 CALL TWODIM( 3.3, 0.69, 1.37, 0.311, F22, F21, DEL )
3080 VLA2=(DEL*(20000.*F2-10000.)) +
3090 * ((1.-DEL)*(11500.*F2-5750.))
3100 ARM2=ARMN-1.-DEL
3110 IPBR1=2
3120 GOTO 660
3130 C
3140 630 CALL TWODIM ( 1.37, 0.311, 0.625, 0.0625, F22, F21, DEL )
3150 VLA2=(DEL*(11500.*F2-5750.)) +
3160 * ((1.-DEL)*(10000.*F2-8000.))
3170 ARM2=ARMN-DEL
3180 IPBR1=3
3190 GOTO 660
3200 C
3210 640 CALL TWODIM (0.625, 0.0625, 0.36, -0.136, F22, F21, DEL )
3220 VLA2=(DEL*(10000.*F2-8000.)) +
3230 * ((1.-DEL)*(8550.*F2-10680.))
3240 ARM2=ARMN-DEL+1.0
3250 IPBR1=4
3260 GOTO 660
3270 C
3280 650 CALL TWODIM (0.36, -0.136, 0.25, -0.2, F22, F21, DEL )
3290 VLA2=(DEL*(8550.*F2-10680.)) +
3300 * ((1.0-DEL)*(20000.*F2-30000.))
3310 ARM2=ARMN-DEL+2.
3320 IPBR1=5
3330 GOTO 660
3340 C
3350 655 VLA2=20000.*F2-30000.
3360 ARM2=ARMN+2.
3370 IPBR1=6
3380 GOTO 660
3390 C
3400 660 BMA2=VLA2*ARM2
3410 GOTO 700
3420 C
3430 C*****
3440 C
3450 C ... ADAPTER BL-2
3460 C
3470 700 IF(F31.GE.3.08*F32-0.31) GOTO 710
3480 IF((3.08*F32-0.31.GE.F31).AND.(F31.GT.2.31*F32-.462)) GOTO 720
3490 IF((2.31*F32-0.462.GE.F31).AND.(F31.GT.1.294*F32-0.159)) GOTO 730
3500 IF((1.294*F32-0.462.GE.F31).AND.(F31.GT.0.567*F32-0.042)) GOTO 740
3510 IF((0.567*F32-0.042.GE.F31).AND.(F31.GT.0.152*F32+0.0045)) GOTO 750
3520 IF(0.152*F32+0.0045.GE.F31) GOTO 760
3530 C ... FELL THRU. IF POSSIBLE, INTERPOLATE AS PREVIOUS PASS.
3540 IF(IPBL2.EQ.0) GOTO 9950
3550 GOTO (710,720,730,740,750,760) IPBL2
3560 GOTO 9950
3570 C
3580 C
3590 710 VLA3=14080.*F3 + 4230.
3600 ARM3=ARMN-2
3610 IPBL2=1
3620 GOTO 770
3630 C
3640 720 CALL TWODIM(3.08,2.31,-0.31,-0.462,F32,F31,DEL)
3650 VLA3=(DEL*(14080.*F3+4230.)) +
3660 * ((1.-DEL)*(12990.*F3+3900.))

```

```

3670      ARM3=ARMN-1. -DEL
3680      IPBL2=2
3690      GOTO 770
3700      C
3710      730      CALL TWODIM(2. 31, -0. 462, 1. 294, -0. 159, F32, F31, DEL)
3720      VLA3=(DEL*(12990. *F3+3900. )) +
3730      *          ((1. -DEL)*(11500. *F3+3450. ))
3740      ARM3=ARMN-DEL
3750      IPBL2=3
3760      GOTO 770
3770      C
3780      740      CALL TWODIM(1. 294, -0. 159, 0. 567, -0. 042, F32, F31, DEL)
3790      VLA3=(DEL*(11500. *F3+3450. )) +
3800      *          ((1. -DEL)*(16670. *F3-1670. ))
3810      ARM3=ARMN-DEL+1.
3820      IPBL2=4
3830      GOTO 770
3840      C
3850      750      CALL TWODIM(0. 567, -0. 042, 0. 152, 0. 0045, F32, F31, DEL)
3860      VLA3=(DEL*(16670. *F3-1670. )) +
3870      *          ((1. -DEL)*(25000. *F3+7500. ))
3880      ARM3=ARMN-DEL+2.
3890      IPBL2=5
3900      GOTO 770
3910      C
3920      760      VLA3=25000. *F3+7500.
3930      ARM3=ARMN+2.
3940      IPBL2=6
3950      GOTO 770
3960      C
3970      770      BMA3=VLA3*ARM3
3980      GOTO 800
3990      C
1000      C*****
1010      C
4020      C          ... ADAPTER BR-2
4030      C
4040      800      IF(F42. GE. 4. 71*F41-0. 37) GOTO 810
4050      IF((4. 71*F41-0. 37. GT. F42). AND. (F42. GE. 3. *F41+0. 1)) GOTO 820
4060      IF((3. *F41+0. 1. GT. F42). AND. (F42. GE. 0. 65*F41+0. 065)) GOTO 830
4070      IF((0. 65*F41+0. 065. GT. F42). AND. (F42. GE. 0. 37*F41+0. 1)) GOTO 840
4080      IF((0. 37*F41+0. 1. GT. F42). AND. (F42. GE. 0. 133*F41+0. 013)) GOTO 850
4090      IF(0. 133*F41+0. 013. GT. F42) GOTO 860
4100      C          ... FELL THRU. IF POSSIBLE, INTERPOLATE AS FOR PREVIOUS PASS.
4110      IF(IPBR2. EQ. 0) GOTO 9950
4120      GOTO (810, 820, 830, 840, 850, 860) IPBR2
4130      GOTO 9950
4140      C
4150      C
4160      810      VLA4=16700. *F4+3330.
4170      ARM4=ARMN-2.
4180      IPBR2=1
4190      GOTO 870
4200      C
4210      820      CALL TWODIM(4. 71, -0. 37, 3. 0, 0. 1, F41, F42, DEL)
4220      VLA4=(DEL*(16700. *F4+3330. )) +
4230      *          ((DEL-1. )*(12500. *F4))
4240      ARM4=ARMN-1. -DEL
4250      IPBR2=2
4260      GOTO 870
4270      C

```

```

4280 830 CALL TWDDIM(3.0,0.1,0.65,0.065,F41,F42,DEL)
4290 VLA4=(DEL*(12500.*F4)) +
4300 * ((1.-DEL)*(10750.*F4+1075.))
4310 ARM4=ARMN-DEL
4320 IPBR2=3
4330 GOTO 870
4340 C
4350 840 CALL TWDDIM(0.65,0.065,0.37,0.1,F41,F42,DEL)
4360 VLA4=(DEL*(10750.*F4+1075.)) +
4370 * ((1.-DEL)*(13700.*F4+2740.))
4380 ARM4=ARMN-DEL+1.
4390 IPBR2=4
4400 GOTO 870
4410 C
4420 850 CALL TWDDIM(0.37,0.1,0.133,0.013,F41,F42,DEL)
4430 VLA4=(DEL*(13700.*F4+2740.)) +
4440 * ((1.-DEL)*(20000.*F4+2000.))
4450 ARM4=ARMN-DEL+2.
4460 IPBR2=5
4470 GOTO 870
4480 C
4490 860 VLA4=20000.*F4+2000.
4500 ARM4=ARMN+2.
4510 IPBR2=6
4520 GOTO 870
4530 C
4540 870 BMA4=VLA4*ARM4
4550 GOTO 10000
4560 C
4570 C*****
4580 C
4590 C
4600 900 CONTINUE
4610 IF(IANU.NE.2) GOTO 1200
4620 C*****
4630 C
4635 C BARBER - SCHEFFEL AND *
4640 C TYPE 1 TRUCK EMPTY *
4650 C *
4660 C*****
4670 C
4680 C ... ADAPTER #1
4690 C
4700 IF(F12.GE.1.15*F11) GOTO 910
4710 IF((1.15*F11.GT.F12).AND.(F12.GT.1.05*F11)) GOTO 920
4720 IF((1.05*F11.GE.F12).AND.(F12.GE.F11)) GOTO 930
4730 IF((F11.GT.F12).AND.(F12.GE.0.886*F11)) GOTO 940
4740 IF((0.886*F11.GT.F12).AND.(F12.GE.0.831*F11)) GOTO 950
4750 IF(0.831*F11.GT.F12) GOTO 960
4760 C ... FELL THRU. IF POSSIBLE, PROCESS AS FOR PREVIOUS PASS
4770 IF(IPBL1.EQ.0) GOTO 9950
4780 GOTO (910,920,930,940,950,960,9950) IPBL1
4790 GOTO 9950
4800 C
4810 C
4820 910 VLA1=1562.5*F1
4830 ARM1=ARMN-2.
4840 IPBL1=1
4850 GOTO 970
4860 C
4870 920 DEL=(F12-1.05*F11) / (0.1*F11)

```

```

4880 VLA1=(DEL*1562.5 + ((1.-DEL)*1450.)) * F1
4890 ARM1=ARMN-1. -DEL
4900 IPBL1=2
4910 GOTO 970
4920
4930 C
4940 DEL=(F12-F11) / (.05 * F11)
4950 VLA1=1450. * F1
4960 ARM1=ARMN-DEL
4970 IPBL1=3
4980 GOTO 970
4990 C
5000 DEL=(F12-(.886 * F11)) / (.114 * F11)
5010 VLA1=1450. * F1
5020 ARM1=ARMN-DEL+1.
5030 IPBL1=4
5040 GOTO 970
5050 C
5060 DEL=(F12-(.831 * F11)) / (.055 * F11)
5070 VLA1=(1450. * DEL + (1-DEL) * 1639. ) * F1
5080 ARM1=ARMN-DEL+2.
5090 IPBL1=5
5100 GOTO 970
5110 C
5120 VLA1=1639. * F1
5130 ARM1=ARMN+2.
5140 IPBL1=6
5150 GOTO 970
5160 C
5170 BMA1=VLA1 * ARM1
5180 GOTO 1000
5190 C
5200 *****
5210 C
5220 .. ADAPTER #2
5230 C
5240 VLA2=1439. * F2
5250 IF (F22. LT. 0.7 * F21) VLA2=1316. * F2
5260 ARM2=ARMN
5270 BMA2=VLA2 * ARM2
5280 C
5290 *****
5300 C
5310 .. ADAPTER #3
5320 C
5330 ARM3=ARMN
5340 VLA3=170. * F3
5350 BMA3=VLA3 * ARM3
5360 C
5370 *****
5380 C
5390 .. ADAPTER #4
5400 C
5410 IF (F41. GE. 0.97 * F42-11.8) GOTO 1110
5420 IF ((F42-12.4. LE. F41). AND. (F41. LT. 0.97 * F42-11.8)) GOTO 1120
5430 IF ((0.82 * F42-12.3. LE. F41). AND. (F41. LT. F42-12.4)) GOTO 1130
5440 IF ((73 * F42-12.3. LE. F41). AND. (F41. LT. 0.82 * F42-12.3)) GOTO 1140
5450 IF (F41. LT. 0.73 * F42-12.3) GOTO 1150
5460 .. FELL THRU. IF POSSIBLE, PROCESS AS FOR PREVIOUS PASS
5470 IF (IPBR2. EQ. 0) GOTO 9950
5480 GOTO (1110, 1120, 1130, 1140, 1150, 9950) IPBR2
GOTO 9950

```

```

5500 1110 VLA4=1220. *F4
5510 ARM4=ARMN
5520 IPBR2=1
5530 GOTO 1160
5540 C
5550 1120 CALL TWODIM(. 97, -11. 8, 1. 0, -12. 4, F42, F41, DEL)
5560 VLA4=(1220. *DEL+(1445. *(1. -DEL)))*F4
5570 ARM4=ARMN-2. +(2. *DEL)
5580 IPBR2=2
5590 GOTO 1160
5600 C
5610 1130 CALL TWODIM(1. 0, -12. 4, 0. 82, -12. 3, F42, F41, DEL)
5620 VLA4=(1445. *DEL + (1230. *(1. -DEL)))*F4
5630 ARM4=ARMN-1. +(2. *DEL)
5640 IPBR2=3
5650 GOTO 1160
5660 C
5670 1140 CALL TWODIM(0. 82, -12. 3, 0. 73, -12. 3, F42, F41, DEL)
5680 VLA4=(1230. *DEL + (1510. *(1. -DEL)))*F4
5690 ARM4=ARMN+1. +DEL
5700 IPBR2=4
5710 GOTO 1160
5720 C
5730 1150 VLA4=1510. *F4
5740 ARM4=ARMN+2.
5750 IPBR2=5
5760 GOTO 1160
5770 C
5780 1160 BMA4=VLA4*ARM4
5790 GOTO 10000
5800 C
5810 C*****
5820 C
5825 C BARBER - SCHEFFEL AND *
5830 C TYPE 1 TRUCK LOADED *
5840 C *
5850 C*****
5860 C
5870 1200 IF(F11. GE. 1. 569*F12-1. 523) GOTO 1210
5880 IF((1. 569*F12-1. 523. LT. F11). AND. (F11. GE. 1. 375*F12-1. 888)) GOTO 1220
5890 IF((1. 375*F12-1. 188. GT. F11). AND. (F11. GE. 1. 124*F12-0. 360)) GOTO 123
5900 IF((1. 124*F12-0. 360. GT. F11). AND. (F11. GE. 0. 774*F12+1. 150)) GOTO 124
5910 IF((0. 774*F12+1. 150. GT. F11). AND. (F11. GE. 0. 697*F12+1. 140)) GOTO 125
5920 IF(F11. LT. 0. 697*F12+1. 14) GOTO 1260
5930 C ... FELL THRU. INTERPOLATE AS FOR PREVIOUS PASS IF POSSIBLE
5940 IF(IPBL1. EQ. 0) GOTO 9950
5950 GOTO (1210, 1220, 1230, 1240, 1250, 1260, 9950) IPBL1
5960 GOTO 9950
5970 C
5980 C
5990 1210 VLA1=7520. *F1-52630.
6000 ARM1=ARMN+2.
6010 IPBL1=1
6020 GOTO 1270
6030 C
6040 1220 CALL TWODIM(1. 569, -1. 523, 1. 375, -1. 188, F12, F11, DEL)
6050 VLA1=(DEL*(7520. *F1-52630. )) + (1. -DEL)*(6000. *F1-49800. )
6060 ARM1=ARMN+1. +DEL
6070 IPBL1=2
6080 GOTO 1270

```



```

6090          C
6100          1230      CALL TWDDIM(1.375,-1.188,1.124,-0.36,F12,F11,DEL)
6110          VLA1=(DEL*(6000.*F1-49800.)) + (1.-DEL)*(5000.*F1-41500.)
6120          ARM1=ARMN+DEL
6130          IPBL1=3
6140          GOTD 1270
6150          C
6160          1240      CALL TWDDIM(1.124,-0.36,0.774,1.15,F12,F11,DEL)
6170          VLA1=(DEL*(5000.*F1-41500.)) + (1.-DEL)*(7140.*F1-55710.)
6180          ARM1=ARMN-1.5+(1.5*DEL)
6190          IPBL1=4
6200          GOTD 1270
6210          C
6220          1250      CALL TWDDIM(0.774,1.15,0.697,1.14,F12,F11,DEL)
6230          VLA1=(DEL*(7140.*F1-55710.)) + (1.-DEL)*(8550.*F1-59830.)
6240          ARM1=ARMN-2.+(0.5*DEL)
6250          IPBL1=5
6260          GOTD 1270
6270          C
6280          1260      VLA1=8550.*F1-59830.
6290          ARM1=ARMN-2.
6300          IPBL1=6
6310          GOTD 1270
6320          C
6330          1270      BMA1=VLA1*ARM1
6340          GOTD 1300
6350          C
6360          C*****
6370          C
6380          C
6390          C
400          1300      IF((F21.GE.1.501*F22-1.305).AND.(F21.GE.5.9)) GOTD 1310
0410          IF((F21.GT.1.166*F22+0.302).AND.(F21.LT.5.9)) GOTD 1320
6420          IF((1.501*F22-1.305.GT.F21).AND.(F21.GE.1.166*F22+0.302).AND.
6430          *
6440          IF((1.166*F22+.302.GT.F21).AND.(F21.GE.91*F22+1.215))GOTD 1340
6450          IF((.91*F22+1.215.GT.F21).AND.(F21.GE.727*F22+1.655))GOTD 1350
6460          IF((727*F22+1.655.GT.F21).AND.(F21.GE.7625*F22+1.036))GOTD 1360
6470          IF(F21.LT.0.7625*F22+1.036) GOTD 1370
0480          C
6490          C
500          500      IF(IPBL2.EQ.0) GOTD 9950
510          GOTD 9950
6520          C
6530          C
6540          1310      VLA2=7690.*F2-61540.
6550          ARM2=ARMN+2.
6560          IPBL2=1
6570          GOTD 1380
6580          C
6590          1320      VLA2=7690.*F2-61540.
6600          ARM2=ARMN+2.
6610          IPBL2=2
6620          GOTD 1380
6630          C
6640          1330      CALL TWDDIM(1.501,-1.305,1.166,0.302,F22,F21,DEL)
0650          VLA2=(DEL*(7690.*F2-61540.)) + ((1.-DEL)*(6250.*F2-54380.))
6660          ARM2=ARMN+1.+DEL
6670          IPBL2=3
6680          GOTD 1380
6690          C

```

7920 10000 CONTINUE  
7930 RETURN  
7940 END

```

100      SUBROUTINE TWODIM( A1, B1, A2, B2, X0, Y0, DEL )
200      C*****
300      C      TWO DIMENSIONAL INTERPOLATION FOR THE TABLE      *
400      C      LOOKUP ROUTINE COMPUTING REDUCTION EQUATIONS      *
500      C      BETWEEN LINES Y1=A1*X+B1 AND Y2=A2*X+B2          *
600      C      FOR POINT (X0, Y0).                                *
700      C                                                         *
800      C      CALLED FROM TABLE. FOR                            *
900      C      INPUT:  A1, A2, B1, B2, X0, Y0                    *
1000     C      OUTPUT: DEL                                        *
1100     C*****
1200     C
1300     C      XD1=(A1*Y0+X0-A1*B1)/(A1*A1+1.)
1400     C      YD1=A1*XD1+B1
1500     C      DIS1=(((XD1-X0)**2) + ((YD1-Y0)**2))**.5
1600     C      XD2=(A2*Y0+X0-A2*B2)/(A2*A2+1.)
1700     C      YD2=A2*XD2+B2
1800     C      DIS2=(((XD2-X0)**2) + ((YD2-Y0)**2))**.5
1900     C      DEL=DIS2/(DIS2+DIS1)
2000     C
2100     C      RETURN
2200     C      END
2300

```

PROPERTY OF FRA  
RESEARCH & DEVELOPMENT  
LIBRARY

Evaluation of Selected TDOP Phase II Test Data,  
Draft Final Report, Systems Control Technology,  
Inc., 1982 -12-Safety

MEMORANDUM FOR THE DIRECTOR